iranchembook.ir/edu

TOPICS IN APPLIED CHEMISTRY

EMULSIFICATION AND POLYMERIZATION OF ALKYD RESINS

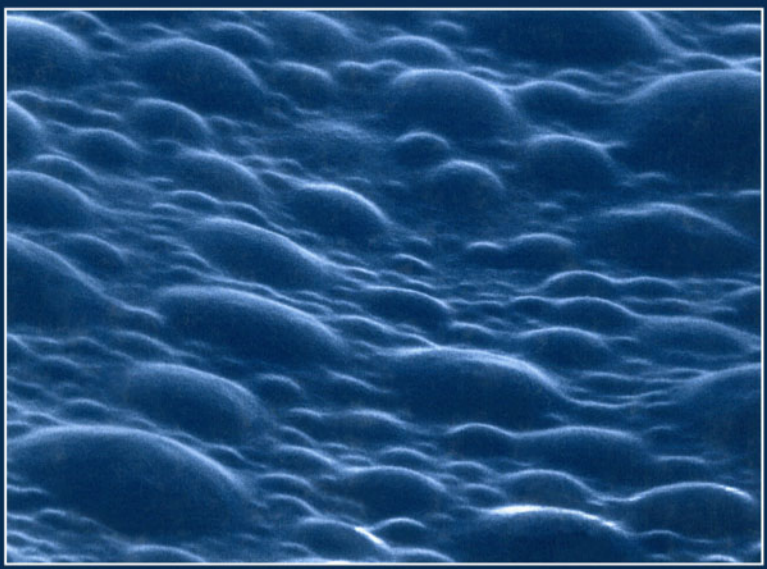

JAN W. GOOCH

iranchembook.ir/edu

Emulsification and Polymerization of Alkyd Resins

iranchembook.ir/edu

TOPICS IN APPLIED CHEMISTRY

Series Editors: Alan R. Katritzky, FRS
University of Florida
Gainesville, Florida

Gebran J. Sabongi
3M Company
St. Paul, Minnesota

Otto Meth-Cohn
Sunderland University
Sunderland, United Kingdom

Current volumes in the series:

ANALYSIS AND DEFORMATION OF POLYMERIC MATERIALS
Paints, Plastics, Adhesives, and Inks
Jan W. Gooch

ELECTRON PARAMAGNETIC RESONANCE IN BIOCHEMISTRY AND MEDICINE
Rafik Galimzyanovich Saifutdinov, Lyudmila Ivanovna Larina, Tamara Il'inichna Vakul'skaya, and Mikhail Grigor'evich Voronkov

EMULSIFICATION AND POLYMERIZATION OF ALKYD RESINS
Jan W. Gooch

FLUOROPOLYMERS 1: Synthesis
FLUOROPOLYMERS 2: Properties
Edited by Gareth Hougham, Patrick E. Cassidy, Ken Johns, and Theodore Davidson

FROM CHEMICAL TOPOLOGY TO THREE-DIMENSIONAL GEOMETRY
Edited by Alexandru T. Balaban

ORGANIC PHOTOCHROMIC AND THERMOCHROMIC COMPOUNDS
Volume 1: Main Photochromic Families
Volume 2: Physicochemical Studies, Biological Applications, and Thermochromism
Edited by John C. Crano and Robert J. Guglielmetti

PHOSPHATE FIBERS
Edward J. Griffith

A Continuation Order Plan is available for this series. A continuation order will bring delivery of each new volume immediately upon publication. Volumes are billed only upon actual shipment. For further information please contact the publisher.

iranchembook.ir/edu

Emulsification and Polymerization of Alkyd Resins

Jan W. Gooch
Georgia Institute of Technology
Atlanta, Georgia

KLUWER ACADEMIC PUBLISHERS
NEW YORK, BOSTON, DORDRECHT, LONDON, MOSCOW

iranchembook.ir/edu

eBook ISBN: 0-306-47554-5
Print ISBN: 0-306-46717-8

©2002 Kluwer Academic Publishers
New York, Boston, Dordrecht, London, Moscow

Print ©2002 Kluwer Academic/Plenum Publishers
New York

All rights reserved

No part of this eBook may be reproduced or transmitted in any form or by any means, electronic, mechanical, recording, or otherwise, without written consent from the Publisher

Created in the United States of America

Visit Kluwer Online at: http://kluweronline.com
and Kluwer's eBookstore at: http://ebooks.kluweronline.com

iranchembook.ir/edu

FOREWORD

Emulsification of vegetable oil-based resins was a daunting task when the author began his research, but the subsequent technology spawned a generation of stable emulsions for waterborne coatings based on vegetable oil-based alkyd resins, oils and fatty acids. Autoxidative polymerization of emulsified alkyd resins is an innovative and original contribution to emulsion technology, because conventional emulsion-polymerization is not applicable to alkyd resins.

Emulsified alkyd particles are polymerized while dispersed in stable aqueous media—an original and patented innovation. Smooth and fast-drying alkyd coatings are generated from non-polymerized emulsions and air-dried with conventional metal driers, and have met with marketing success. The pre-polymerization innovation for emulsified alkyd particles provides very fast air-drying coatings that have potential markets for interior architectural latex coatings and waterborne pressure-sensitive adhesives and inks.

The author demonstrates his knowledge of chemical reaction kinetics by employing a combination of oxygen concentration, internal reactor pressure and other reactor variables to finely control the rate and degree of autoxidative polymerization. He meticulously calculates surfactant chemistry by measuring hydrophile-lipophile balance values, and solubility parameters to emulsify characterized resins. The relationship between hydrophile-lipophile values and solubility parameters is shown in explicit equations.

Homogenization equipment used during the course of this research to generate emulsions is shown in detailed drawings together with concise particle size and distribution data.

The author reports research spawned internationally by his research in the fields of alkyd-acrylic hybrids, polyester and oil-modified urethane resins.

Emulsification and Polymerization of Alkyd Resins contains a wealth of emulsion science, alkyd technology and autoxidative reaction kinetics that will benefit researchers, students and manufacturers studying and working with alkyd emulsions.

F. Joseph Schork
School of Chemical Engineering
Georgia Institute of Technology

iranchembook.ir/edu

PREFACE

The primary goal of this research and development effort was the utilization of renewable (non-petroleum-based) raw materials such as soybean oil in the next generation of waterborne surface coatings. Vegetable oil-based coatings are renewable natural resources, and they are "green technology" materials that are environmentally friendly in the workplace and home. These organic solvent-free coatings are commercially economical from both a manufacturing and a raw materials availability viewpoint, and they reduce the dependency on petroleum products and unpredictable erratic prices. The reader will benefit from the novel treatment of resins, synthesis and techniques of emulsification. The book consists of the following main subjects:

- Alkyd resins and oils and autoxidative polymerization
- Synthesis and polymerization of alkyd resins
- Emulsion and kinetic studies of autoxidative polymerization
- Experimental results, continuing research and applied research

The research and development was successful, and those innovations were patented by Gooch, Bufkin and Wildman (U.S. Patent 4,419,139) and the technology applied to commercial "emulsified alkyd" products, originally by the Cargill Corporation, but later by other resin manufacturers. Individual segments of the above work were applied to products involving the emulsification of alkyd resins, without autoxidative polymerization, and allowed to form a cured hard film on a surface using a metal drier. This has been referred to as a "green" technology because it is an environmentally friendly material and the materials utilized are renewable.

Alkyds, oils and oil-alkyd mixtures have been emulsified and subsequently autoxidatively polymerized (crosslinked) in the emulsion form to a near-gel or gelled state within the polymer particles. During the emulsification, the emulsifier type was carefully selected such that a stable emulsion was generated. The particle size of the emulsion droplets was then reduced to less than 1.0 micron and maintained at this size during the autoxidative process. The autoxidative process was continued until the maximum crosslink density that allowed proper flow, which was a function of the crosslink density, particle size and polymer and polymer type, was achieved. During coalescence, a small amount of further crosslinking, as well as flow, generated a dense uniform film.

iranchembook.ir/edu

This technology produced vegetable oil and alkyd resin-based emulsions which dried to touch rapidly and allowed water clean-up equivalent to that of acrylic and vinyl latex coatings. The many emulsification techniques may be applied to different resins and oils, and they are described in detail within the book. This is a valuable handbook and formulation guide for the coatings manufacturer, a cosmetic product formulator, and anyone interested in emulsifying a material in water.

Paints have been used to improve aesthetic properties and protect almost all surfaces imaginable in the home, office and industry. Paints comprise a pigment (color), a vehicle or binder (resin or polymer) and a solvent (mineral spirits or other). The pigment functions primarily, although not always, for aesthetic purposes such as appearance including color and gloss, but also for practical purposes such as hardness and corrosion protection and, generally, outdoor durability. Indoor durability is important as well, and involves such details as washable surfaces and scuff resistance as well as aesthetic appearance. The polymer (or resin as it used to be called) binder was developed for its properties pertaining to a specific application. The term "paint" is an older, but widely used, term referring to materials made from natural materials such as vegetable oils. A "coating" is a more widely used term (urethanes, vinyls, etc.) since the 1950's pertaining to synthesized materials used in high performance materials not usually formulated from natural sources. Either term refers to a wet applied protective film for a substrate such as wood or metal.

The earliest paints were from Europe and Australia (Boatwright, 2000) and were created 20,000 years ago, when natural pigments (clay, carbon, ochre, and others) were mixed with natural binders such as vegetable oils (soya oil, linseed oils, etc.) and animal fats. The oily binders hardened by reaction with the oxygen in air to autoxidatively polymerize (also called drying) the chains of oil to each other, a process now referred to as crosslinking. The Greeks and Romans designed paints containing drying oils extracted from linseeds, soybeans and sunflower seeds. It was not until the thirteenth century that protective properties of drying oils began to be recognized in Europe. Oils usually consist of three fatty acids connected to a tri-functional alcohol called glycerol. It is the fatty acids that dry and harden. In the first part of the twentieth century, polyester resins were modified with the fatty acids from drying oils to form a resin called an alkyd. The term alkyd comes from the combination of the terms alcohol and acid. Alkyds demonstrate the same drying mechanism as drying oil, but have the advantages of higher molecular weight and harder dried films. However, due to the high viscosities of alkyds, they must be dissolved in solvents such as

iranchembook.ir/edu

mineral spirits. Alkyd paints (or coatings) dominated the decorative and industrial markets for the first half of the twentieth century and continue to enjoy a large share of the total coatings market.

The disadvantages of alkyd-solvent coatings are the objectionable solvents which produce volatile organic compounds (VOC) that are restricted by the Environmental Protection Agency. Everyone wants the objectionable organic solvents out of coatings but also wants the use of the desirable alkyd-type coatings. Acrylic dispersions in ordinary non-toxic water (latex coatings) are widely used, but they do not have the tough, resilient and aesthetic properties of alkyds that outperform acrylics for protecting wood and metal. So, how can alkyds be dispersed in water and wet applied to a substrate without using solvents? This question was answered in two parts, both equally difficult. First, the alkyd resins were dispersed in water by carefully selected surfactants and then mechanically homogenized to form a stable emulsion. Then, the alkyd-water emulsion was oxidatively polymerized to crosslink; this caused it to form gel-like particles that flowed together during evaporation of water forming a continuous film. The aqueous dispersion was practically applied to a substrate, and it dried quickly and formed a continuous alkyd film. Commercialization of this process has been successful at least in part.

iranchembook.ir/edu

ACKNOWLEDGMENTS

I wish to thank B. George Bufkin and Gary C. Wildman for their contributions to this book. I also wish to express my gratitude to those people who provided assistance during the preparation of this book: Sheree Collins, Lisa Detter-Hoskin, Gary Poehlein, and F. Joseph Schork.

iranchembook.ir/edu

CONTENTS

1. ALKYD RESINS, VEGETABLE OILS AND AUTOXIDATIVE POLYMERIZATION 1
   - 1.1. Goals of Research and Development in Alkyd Emulsions 1
   - 1.2. Historical Background of Alkyds, Oils and Emulsions 1
     - 1.2.1. Vegetable Oils and Resins 1
     - 1.2.2. Autoxidative Polymerization of Vegetable Oils and Resins 9
     - 1.2.3. Emulsified Oils and Resins 14
   - 1.3. Theoretical Considerations 16
     - 1.3.1. Intrinsic Viscosity 16
     - 1.3.2. Hydrophile-Lipophile Balance (HLB) 17
     - 1.3.3. Diffusion of Oxygen in an Emulsion 21
     - 1.3.4. Solubility of Air and Oxygen in Aqueous Phase 22
     - 1.3.5. Swelling Ratio 23
   - 1.4. Justification for Research and Development 26
2. SYNTHESIS AND POLYMERIZATION OF ALKYDS 31
   - 2.1. Alkyd Synthesis Procedure 31
   - 2.2. Emulsification Procedure 32
   - 2.3. Autoxidation Procedure 34
   - 2.4. Materials 36
   - 2.5. Characterization 37
     - 2.5.1. Emulsion Particle Size 38
     - 2.5.2. Emulsion Characterization 43
     - 2.5.3. Film Characterization 43
     - 2.5.4. Intrinsic Viscosity Measurement 44
     - 2.5.5. Swell Ratio 44
     - 2.5.6. Turbidimetric Measurement of Swelling Ratio 47
     - 2.5.7. Dissolved Oxygen in Aqueous Phase 49
3. EMULSION AND KINETIC STUDIES OF AUTOXIDATIVE POLYMERIZATION 51
   - 3.1. Emulsifier Studies 51
     - 3.1.1. Emulsifier Sources and Chemical Structures 51
     - 3.1.2. Emulsifiers and Emulsion Stability 52
     - 3.1.3. Emulsifiers and Freeze-Thaw Stability 52
     - 3.1.4. Emulsifiers and Film Characterization 62

iranchembook.ir/edu

3.2. Phase Ratio and Co-Solvent Study 64
3.2.1. Solvent Alkyd Emulsions 64
3.2.2. Co-Solvent Containing Emulsions 65
3.3. Studies on the Autoxidative Crosslinking of Emulsified Soya Oil 67
3.3.1. Autoxidation Reaction of Emulsified Soya Oil 67
3.3.2. Catalysis of Autoxidation Reaction of Soya Oil 70
3.4. Studies of the Autoxidative Crosslinking of Emulsified Alkyd Particles 73
3.4.1. Autoxidation Reaction of Emulsified Alkyd Resins 73
3.4.2. Non-catalyzed Autoxidation Reaction 75
3.4.3. Benzoyl Peroxide Catalysis in the Alkyd Phase 76
3.4.4. Cobalt Naphthenate Catalysis in Aqueous Phase 77
3.4.5. Autoxidized Emulsion Characterization 85
3.4.6. Post pH-Adjustment of Autoxidized Emulsion 90
3.4.7. pH Adjustment Prior to the Autoxidation 91
3.4.8. Cobalt Naphthenate Catalysis in Alkyd Phase 92
3.4.9. Post-Addition of Emulsifier 92
3.4.10. pH Effect on Reaction Rate 95
3.4.11. Increased Oxygen Concentration and Catalysis 96
3.4.12. Scanning Electron Microscopy 97
3.4.13. Water Clean-Up of Emulsion 99
3.4.14. Comparison to Alkyd-Solvent System 100
3.4.15. Effect of Emulsifier Structure on Reaction Rate 101
3.5. Kinetic Study 103
3.5.1. Oxygen Concentration Relationship 103
3.5.2. Correlation of Swell Ratio and Percent Transmittance 104
3.5.3. Catalysis Effect 117
3.5.4. Temperature Effect 120
3.5.5. Agitation Rate Effect 122
3.5.6. Molecular Weight Effect 124
3.6. Studies on Emulsion Particle Size 125
3.6.1. Particle Size with Reaction Time 125
3.6.2. Average Particle Size with Homogenization 129
3.6.3. Particle Size after One Year of Shelf Life 129
3.7. Alkyd Oil Length and Conjugation Study 131
3.7.1. Alkyd Oil Length Study 132
3.7.2. Alkyd Conjugation Study 136

iranchembook.ir/edu

4. EXPERIMENTAL RESULTS, RESEARCH AND COMMERCIALIZATION OF TECHNOLOGY 139
4.1. Autoxidative Crosslinking of Vegetable Oil 139
4.2. Autoxidative Crosslinking of Vegetable Oil Alkyds 140
4.3. Emulsification 141
4.4. Continuing Research and Developments 141
4.5. Commercialization of Alkyd Emulsions 144

APPENDIX – FIGURES 145

APPENDIX – TABLES 179

REFERENCES 215

INDEX 219

iranchembook.ir/edu

LIST OF FIGURES

2.1	Emulsion autoxidation reaction apparatus	35
2.2	Transmittance at two different wavelengths vs. concentration of emulsified alkyd III particles	41
2.3	Light transmittance vs. concentration for varying particle diameter, urethane alkyd III	41
2.4	Light transmittance vs. concentration for particle diameter, urethane alkyd III	42
2.5	Particle pressure of oxygen vs. oxygen concentration at 55°C	49
3.1	Stress-strain curve for alkyd film and alkyd emulsion films	76
3.2	Scanning electron micrograph of non-autoxidized alkyd IV emulsion, with 0.04% cobalt metal post-added to emulsion, 50x magnification	77
3.3	Scanning electron micrograph of air-autoxidized alkyd IV emulsion, non-catalyzed, 50x magnification	78
3.4	Scanning electron micrograph of air-autoxidized alkyd IV emulsion with 0.04% cobalt metal added to emulsion after autoxidation, 50x magnification	79
3.5	Tensile strength vs. reaction time for cobalt catalyzed and noncatalyzed films from alkyd IV emulsion, O – catalyzed and Δ – noncatalyzed	80
3.6	Scanning electron micrograph 80.0 psig oxygen alkyd II emulsion, 7.0 hour sample, 5000x magnification	98
3.7	Scanning electron micrograph 80.0 psig oxygen autoxidized alkyd II emulsion, 7.0 hour sample, 13,000x magnification	99
3.8	Effects of emulsifier structure on reaction rate	102
3.9	Emulsified alkyd particle and oxygen diffusion	104
3.10	Swelling ratio vs. % transmittance	105
3.11	Log swelling ratio vs. % transmittance	106
3.12	Total reaction time vs. oxygen pressure	108
3.13	Induction time vs. oxygen pressure	111
3.14	Crosslinking time vs. oxygen pressure	112
3.15	Intrinsic viscosity vs. induction time	113
3.16	Reaction time vs. % transmittance	119
3.17	Reaction time vs. % transmittance	121
3.18	Zirconium naphthenate concentration vs. reaction rate	123
3.19	Reaction temperature vs. reaction time, reagent grade	124

iranchembook.ir/edu

3.20	Agitation rate vs. reaction time, technical grade	126
3.21	Agitation rate vs. reaction time, reagent grade	127
3.22	Particle size vs. reaction time, technical grade	128
3.23	Particle size vs. homogenization cycles	130
3.24	Oil conjugation vs. reaction time	137
A.1	Bench scale® mini-reactor pressure vessel, cross-sectional view	147
A.2	Bench scale® mini-reactor pressure vessel, top view	148
A.3	Bench scale® mini-reactor pressure vessel, seals and packing cross-sectional view	149
A.4	Viscometer calibration curve	150
A.5	Reaction time vs. % transmittance, 10 psi	151
A.6	Reaction time vs. % transmittance, 20 psi	152
A.7	Reaction time vs. % transmittance, 30 psi	153
A.8	Reaction time vs. % transmittance, 40 psi	154
A.9	Reaction time vs. % transmittance, 50 psi	155
A.10	Reaction time vs. % transmittance, 60 psi	156
A.11	Reaction time vs. % transmittance, 70 psi	157
A.12	Reaction time vs. % transmittance, 80 psi	158
A.13	Particle size distribution, 2.0 hours, by volume	159
A.14	Particle size distribution, 4.0 hours, by volume	160
A.15	Particle size distribution, 6.0 hours, by volume	161
A.16	Particle size distribution, 8.0 hours, by volume	162
A.17	Particle size distribution, 9.0 hours, by volume	163
A.18	Particle size distribution, 2.0 hours, by population	164
A.19	Particle size distribution, 4.0 hours, by population	165
A.20	Particle size distribution, 6.0 hours, by population	166
A.21	Particle size distribution, 8.0 hours, by population	167
A.22	Particle size distribution, 9.0 hours, by population	168
A.23	Particle size distribution, 1 cycle, by volume	169
A.24	Particle size distribution, 2 cycles, by volume	170
A.25	Particle size distribution, 3 cycles, by volume	171
A.26	Particle size distribution, 4 cycles, by volume	172
A.27	Particle size distribution, 1 cycle, by population	173
A.28	Particle size distribution, 2 cycles, by population	174
A.29	Particle size distribution, 3 cycles, by population	175
A.30	Particle size distribution, 4 cycles, by population	176
A.31	Particle size distribution, 1 day, by volume	177
A.32	Particle size distribution, 1 year, by volume	178

iranchembook.ir/edu

LIST OF TABLES

1.1	Use of Fats and Oils in Surface Coatings	2
1.2	Consumption of Synthetic Resins in Paints and Coatings - 1999	3
1.3	U.S. Petroleum Balances, in Million Barrels Per Day	5
1.4	U.S. Land Use for Annual Crops	6
1.5	Oils Used in Coatings Industry 1999	7
1.6	Cost of Solvents: Comparison over 10 Year Span	8
1.7	Cost of Vegetable Oils: Comparison over 10 Year Span	8
1.8	Fatty Acid Composition of Vegetable and Marine Oils	10
1.9	Structure of Fatty Acids	13
2.1	Formulation of AR Soya Oil Emulsion after Optimization	31
2.2	Formulation of Medium Soya/Linseed Alkyd Emulsion after Optimization of Variable Parameters	33
2.3	Material Description and Identification	33
2.4	Formulation for Synthesis of Alkyds for Conjugation Study	36
2.5	Study of Conjugation of Vegetable Oil in Alkyd	37
2.6	Emulsion Particle Size and Homogenization Time	39
2.7	Spectrophotometric Method of Monitoring Particle Size in Emulsion	40
2.8	Turbidimetric Monitoring of Crosslinking Development	48
3.1	Emulsifiers and Structures	53
3.2	Emulsifier Combinations and Emulsion Stabilities	58
3.3	Freeze-Thaw Stability and Emulsifiers	62
3.4	Emulsifiers and Film Characterization	63
3.5	Non-Solvent Alkyd Study for Optimum Stability of Emulsion	64
3.6	Co-Solvent Study for Optimum Stability of Emulsion	65
3.7	Optimum Co-Solvent to Alkyd Ratio for Optimum Emulsion Stability	66
3.8	Optimum Phase Ratio of Alkyd-Solvent to Water	66
3.9	Effect of Agitation Rate on Emulsion Stability with AR Soya Oil	68
3.10	Effect of Reaction Temperature on Emulsion Properties with Alkali Refined Soya Oil	68
3.11	Effect of Air Flow Rate on Emulsion Stability with AR Soya Oil	69
3.12	Reaction Conditions for Processing AR Soya Oil	69
3.13	Effect of Autoxidation Time on AR Soya Emulsion	70

iranchembook.ir/edu

3.14	Intrinsic Viscosity Changes Resulting from Catalyzed Autoxidation of Soya Oil	71
3.15	Ultraviolet Light Catalysis of Soya Oil Autoxidation and Drying	72
3.16	Effect of Air Flow Rate on Emulsion Stability with Alkyd III	73
3.17	Effect of Reaction Temperature on Emulsion Stability with Alkyd III	74
3.18	Effect of Agitation Rate on Emulsion Stability with Alkyd III	74
3.19	Reaction Conditions for Processing Alkyd III	75
3.20	Effect of Autoxidation Time on Alkyd III Emulsion	75
3.21	Effect of Catalysis on Film Dry Time	82
3.22	Effect of Oxygen and Cobalt Naphthenate on Alkyd IV Emulsion	83
3.23	Reaction Time and Film Hardness	84
3.24	Reaction Time and Percent Solids	85
3.25	Emulsion Reaction Characterization	86
3.26	Film Dry Time and Emulsion Reaction Time	88
3.27	Emulsion Reaction Characterization, Alkyd III in Xylene (74.4% w/w, N.V.)	89
3.28	Autoxidized Emulsion Characterization, Alkyd III in Xylene Solvent (74.4% N.V.)	90
3.29	Emulsion Stability with Post-Adjusted pH	90
3.30	Emulsion Reaction Characterization, Alkyd III in Xylene (74.4% N.V.) with pH Adjustment Prior to Processing	91
3.31	Autoxidized Emulsion Characterization, Alkyd III in Xylene (74.4% N.V.) with pH Adjustment Prior to Processing	92
3.32	Emulsion Reaction Characterization, Cobalt Naphthenate (0.04% w/w) Catalysis in Alkyd III	93
3.33	Autoxidation Emulsion Characterization, Alkyd III with Cobalt Naphthenate Catalysis	94
3.34	Post Addition of Emulsifier	94
3.35	Emulsion Particle Crosslinking Development with pH Adjustment Prior to Reaction	95
3.36	Acid Value from Titration of Reacted Emulsion	96
3.37	Reaction Time and Physical Properties	97
3.38	Water Clean-Up of Emulsion	100
3.39	Comparison of Autoxidized Emulsion to Alkyd-Solvent System	101

iranchembook.ir/edu

3.40	Formulation for Oxygen Concentration Dependence on Autoxidation Reaction Study	107
3.41	Functions of Induction Period	109
3.42	Oxygen Concentration, Induction Time, Crosslinking Period, Total Reaction Time and Log Reaction Time	110
3.43	Oxygen Concentration Correlation with Reaction Time	117
3.44	Zirconium Naphthenate Concentration vs. Reaction Rate	120
3.45	Reaction Temperature vs. Log Reaction Time	122
3.46	Emulsion Particle Size after One Year	131
3.47	Characterization of Oxygen Reacted Alkyd Emulsions of Varying Oil Length at Atmospheric Pressure – Part A	133
3.48	Characterization of Oxygen Reacted Alkyd Emulsions of Varying Oil Length at Atmospheric Pressure – Part B	134
3.49	Accelerated Shelf Emulsion Stability	135
3.50	Emulsion Freeze-Thaw Stability	136
4.1	Comparison of Commercial Emulsions to Autoxidized Emulsions	140
A.1	Henry's Law Constants for Oxygen	181
A.2	Henry's Law Constants for Air	182
A.3	Air Dissolved in Water	183
A.4	Oxygen Concentration Expressions	184
A.5	Calibration of Viscometer A627 Viscometer Size 50	185
A.6	Oxygen Concentration and Oxygen Partial Pressure in H_2O at 55°C	186
A.7	Emulsifiers and Manufacturers	187
A.8	Legend for Figures 8-10	188
A.9	Swelling Ratio vs. % Transmittance	190
A.10	Log Swelling Ratio vs. % Transmittance	191
A.11	Particle Size vs. Reaction Time	192
A.12	Particle Size Distribution, 2.0 Hours	193
A.13	Particle Size Distribution, 4.0 Hours	194
A.14	Particle Size Distribution, 6.0 Hours	195
A.15	Particle Size Distribution, 8.0 Hours	196
A.16	Particle Size Distribution, 9.0 Hours	197
A.17	Particle Size Distribution, 2.0 Hours	198
A.18	Particle Size Distribution, 4.0 Hours	199
A.19	Particle Size Distribution, 6.0 Hours	200
A.20	Particle Size Distribution, 8.0 Hours	201

iranchembook.ir/edu

A.21 Particle Size Distribution, 9.0 Hours 202
A.22 Particle Size vs. Homogenization Cycles 203
A.23 Particle Size Distribution as a Function of Homogenization (3500 psi) Cycles, 1 Cycle 204
A.24 Particle Size Distribution as a Function of Homogenization (3500 psi) Cycles, 2 Cycles 205
A.25 Particle Size Distribution as a Function of Homogenization (3500 psi) Cycles, 3 Cycles 206
A.26 Particle Size Distribution as a Function of Homogenization (3500 psi) Cycles, 4 Cycles 207
A.27 Particle Size Distribution as a Function of Homogenization (3500 psi) Cycles, 1 Cycle 208
A.28 Particle Size Distribution as a Function of Homogenization (3500 psi) Cycles, 2 Cycles 209
A.29 Particle Size Distribution as a Function of Homogenization (3500 psi) Cycles, 3 Cycles 210
A.30 Particle Size Distribution as a Function of Homogenization (3500 psi) Cycles, 4 Cycles 211
A.31 Particle Size Distribution of Autoxidized Emulsion, after One Day 212
A.32 Particle Size Distribution of Autoxidized Emulsion, after One Year 213

iranchembook.ir/edu

Chapter 1

ALKYD RESINS, VEGETABLE OILS AND AUTOXIDATIVE POLYMERIZATION

1.1. Goals of Research and Development in Alkyd Emulsions

The primary goal of this research and development effort was the utilization of renewable (non-petroleum based) raw materials such as soybean oil in waterborne emulsion-type surface coatings. These coating are commercially economical from both a manufacturing and raw materials availability viewpoint, and they reduce the dependency on petroleum products and unpredictable erratic prices

Alkyds, oils and oil/alkyd mixtures have been emulsified and subsequently autoxidatively polymerized (crosslinked) in the emulsion form to a near-gel or gelled state within the polymer particles. During the emulsification, the emulsifier type was carefully selected such that a stable emulsion was generated. The particle size of the emulsion droplets was then reduced to less than 1.0 micron and maintained at this size during the autoxidative process. The autoxidative process was continued until the maximum crosslink density that will allow proper flow, which was a function of the crosslink density, particle size and polymer and polymer type, is achieved. During coalescence, a small amount of further crosslinking, as well as flow, generated a dense uniform film.

This technology produced vegetable oil and alkyd resin based emulsions which dried to touch rapidly and allowed water clean-up equivalent to acrylic and vinyl latex coatings.

1.2. Historical Background of Alkyds, Oils and Emulsions

1.2.1. Vegetable Oils and Resins

During the past one hundred years, the coatings industry has employed large quantities of fats and oils. The information in Table 1.1

iranchembook.ir/edu

demonstrates that the coating industry used larger quantities each decade until the 1950's when their use began to decline (Cowan, 1975). The decline in fats and oils has largely been a result of the substitution of petroleum products for the vegetable oils. Alkyd resin contains a large percentage of fatty acids and has been the predominate binder used in the trade-sales and industry for over thirty-five years. Petroleum based product usage increased dramatically over the past decade, but it is evident from information in Table 1.2 that alkyd resins are still employed in large quantities. A large percentage of the trade sales market has switched to water-borne latex coatings based on petroleum- derived materials. The major reason for this is consumer convenience in clean-up, short dry times, and low odor. As coatings based on these products further penetrate the existing market, the usage of vegetable oil-based coatings will continue to decline.

Table 1.1 Use of Fats and Oils in Surface Coatings

Year	Million Pounds
1931-34	474
1940	652
1950	873
1960	716
1972	575
1987	293
1992	302
1997	345
Future projections:	
2002	390
2007	440

Sources: The Kline Guide to the Paint Industry, and Fatty Acids to 2002 Report - The Freedonia Group, Inc., 2001.

iranchembook.ir/edu

Table 1.2 Consumption of Synthetic Resins in Paints and Coatings - 1999

Type of Resin	Millions of Pounds
Alkyd	738
Acrylic	955
Epoxies	275
Other resins	1702
Total Resins	3,670

Source: Paints & Coatings to 2004 Report - The Freedonia Group, Inc.

The demand for fatty acids in paints and coatings is expected to rise 2.5 percent per annum to 390 million pounds in 2002, according to Fatty Acids to 2002. Fatty acids, either in free form or in the form of derivatives, are suited to a wide range of applications due to their versatility, functionality, biodegradability and derivation from renewable resources. New markets include plastics, detergents, paints, cosmetics and toiletries, surfactants, lubricants, food and rubber, among others. Overall growth will be limited by the move toward water-based coatings in a number of applications traditionally reserved for oil-based coatings. Competition from systems based on synthetic resins, urethane polymers, silicones and other synthetic intermediates offering superior drying speed and other performance advantages will further reduce demand. Nevertheless, fatty acids will remain an important constituent of many coatings such as alkyd resins and emulsifiable linseed bodied oils. In addition, the shift to latex will increase demand for fatty acid-based latex paint modifiers, compensating somewhat for the decline in oil-based applications. Suppliers of fatty acids and derivatives to the United States paints and coatings industry include Arizona Chemical (International Paper), Georgia-Pacific, Henkel, Hercules, Twin Rivers Technologies, Unichema North America (ICI), Union Camp, Westvaco and Witco, and distributors such as Ashland.

Environmental factors have contributed to the reduction of the utilization of vegetable oil-based products. The need has been to employ coatings that tend to pollute the environment, i.e., water-borne, higher solids and powder types. Petroleum based products have been acceptable as the solution to the environmental problem, and, consequently, vegetable oil-based materials have lagged behind, still being employed largely in solvent-

iranchembook.ir/edu

borne paints. The major method of every oil-based polymer in non-polluting coatings has been in "exempt" solvent systems as specified by Los Angeles Rule 66. However, the Environmental Protection Agency has stated that all organic solvents pollute the environment even though some are less reactive than are others and thus, began the decline of organic solvents in paints and coatings (McCarthy, 1979).

Most organic solvents are derived from petroleum, and the costs of solvents are linked with the market prices of petroleum. Hannesson (1998) provided a fundamental understanding of how petroleum is priced and a review of the Oil Producing and Exporting Countries (OPEC) regarding their historical influence on the market. Hannesson explained that that the price of petroleum in real terms has followed an unusual pattern over time, a pattern that includes significant price fluctuations. There is not a short answer to why the price of oil cannot be fitted around a trendline, although one reason given is that there are few petroleum companies and the demand for petroleum is elastic (price changes do not substantially affect demand). Petroleum can be stored and resold at a later date, and petroleum prices fluctuate due to speculation regarding future prices. For example, during the Arab oil embargo of 1973-74, crude petroleum prices more than doubled, and the supply was limited to the United States creating rationing lines, but the supply was completely severed in some European countries. In another example, a decision by OPEC countries to limit production in the year 2000 sent oil prices soaring to $37/barrel, a level not seen since the Persian Gulf War (New York Times - 2001 Almanac). The price per barrel is a benchmark indicator of energy costs, and affects everything from the price of a gallon of gasoline (which topped $2.00 in some states) to the cost of delivering natural gas and electricity. These factors are one answer to the question of why petroleum prices may appear unpredictable. The historical markets for petroleum have been in North America, Western Europe and the Western Pacific, whereas most petroleum is produced in the Middle East. However, vegetable oils are abundantly produced domestically in the United States, and their prices are more consistent and predicable than petroleum.

As solvents become more expensive due to petroleum price increases and shortages, the need for water-borne and/or higher solids products will become more acute. This research effort was directed toward the generation of water-borne latex coatings from vegetable oils or vegetable oil derived materials as opposed to the more commonly used water reducible, water dispersible or water soluble products which normally require significant quantities of petroleum derived solvents. The figures in Table 1.3 represent the supply and demand of petroleum for 1965-2000. It is obvious from these data that the U.S.A. is becoming increasingly dependent on imported petroleum. The figures in Table 1.4 represent U.S. land use for annual crops and primary sources of vegetable oils. The total land use of 336.3 million

iranchembook.ir/edu

acres with 470.0 million acres available if needed literally "paints" a more optimistic picture of the future than does continued and accelerated dependence on foreign petroleum. Referenced total land use of 334.3 million acres, there are an additional 133.40 million acres available in needed. This indicates an opportunity for expansion of vegetable oil utilization compared to one of conservation and restriction with imported petroleum expected in the future.

Table 1.3 U.S. Petroleum Balances, in Million Barrels Per Day

Year	Domestic Supply	Demand	Imported To Balance	Imported % Total
1965	9.0	11.5	2.5	21.7
1970	11.3	14.7	3.4	23.1
1975	11.1	18.4	7.3	39.7
1980	11.8	22.5	10.7	47.5
1985	11.2	26.0	14.8	56.9
1990	11.6	33.1	21.5	64.9
1995	11.8	36.9	25.1	68.0
2000	11.9	42.5	30.6	72.0

Source: Energy Industry Review (Hannesson, 1998), The Chemical Marketing Reporter and The Kline Guide to the Paint Industry.

iranchembook.ir/edu

Table 1.4 U.S. Land Use for Annual Crops

Crop	Planted Acres, Millions
Wheat	70.0
Corn	66.9
Hay	61.9
Soybean	53.6
Sorghum	15.5
Oat	13.6
Corn silage	9.7
Cotton	9.1
All other	36.3
Total	336.6
Available if needed	470.0

Source: Princen, 1977.

The oils used in the coatings industry during the year 1999 in all paint systems, i.e., solvent-borne, water-borne and others are represented in Table 1.5. The total figure of 200 million pounds per year for 1999 indicates a continuing major market for vegetable oils and derivative resins in the coatings industry, but at the same time lagging the petroleum products, i.e. acrylics, market significantly (Table 1.2). Petroleum derived solvents have increased in cost over a ten year span as represented in Table 1.6, but vegetable oil product costs increased at a slower rate as represented in Table

iranchembook.ir/edu

1.7 and decreased for soya and linseed. Furthermore, costs of the same solvents in Table 1.6 over the previous twenty years (1969 to 1979) increased by 306, 328, 414, 100, 63, 76, 113 and 323 percent, respectively (American Paint Journal, May 1969 and May 1979). It is obvious that the prices of petroleum-derived solvents have and continue to drastically and unpredictably increase. Observing a twenty-year history, vegetable oil product cost increases are expected to lag significantly behind those of petroleum-derived products, and the source can be expected to be available at far more predictable prices.

A successful and competitive generation of new water-borne coatings based on vegetable oils could shift the usage of coating materials toward vegetable oil products in the future. Resins derived from vegetable oils are renewable-resource materials (Carraher, Jr., and Sperling, 1983) that are grown on farmlands in all agricultural countries and independently of increasing foreign petroleum imports and price fluctuations.

Table 1.5 Oils Used in Coatings Industry 1999

Oil	Millions of Pounds/Year
Linseed	104
Soybean	52
Tung	10
Fish	8
Tall	11
Safflower	2
Other primary oils	13
Total	200

Source: The Chemical Marketing Reporter (1999)

iranchembook.ir/edu

Table 1.6 Cost of Solvents: Comparison over 10 Year Span

Solvent	Cost, May 26, 1989 (¢)	Cost, May 21, 1999 (¢)	% Increase in Cost Over 10 Years
Mineral Spirits	79-160/gallon	155-214/gallon	33.8
Xylene	87/gallon	98/gallon	12.6
Toluene	90/gallon	99/gallon	11.2
Methyle Ethyl Ketone	26.5/lb	46/lb	76.9
N-Butanol	38/lb	55/lb	63
Methanol	25/gal	44/gallon	44.7
Ethanol (190 proof)	110/gallon	135/gallon	22.7
Naphtha	79/gallon	88/gallon	11.4

Note: Total solvents used in the paint & coatings industry for 1989 = 2500 mil. lbs. and 1999 = 2110 mil .lbs.
Source: The Chemical Marketing Reporter (1989-1999)

Table 1.7 Cost of Vegetable Oils: Comparison over 10 Year Span

Vegetable Oil	Cost, May 26, 1989 (¢)	Cost, May 21, 1999 (¢)	% Increase in Cost Over 10 Years
Soya	21.4/lb	15.1/lb	-29.4
Linseed	42.0/lb	36.0/lb	-14.3

Source: The Chemical Marketing Reporter (issues: April 2 1990 and November 20, 2000)

iranchembook.ir/edu

1.2.2. Autoxidative Polymerization of Vegetable Oils and Resins

The autoxidation conditions, mechanism and the reactions involved have been discussed by researchers including Lundberg (1950), Mattiello (1945), Novak (1934), Long (1950), and Taylor (1950). It is generally agreed that there is an induction period that is a function of the type and amount of antioxidants in the oil and the temperature at which the oil is blown. The autoxidation process once initiated is an exothermic reaction and generally requires temperature control in the early stages. As the reaction proceeds, the exotherm diminishes and the system must be heated to maintain the desired temperature.

Auer (1945) discussed preliminary bodying of a fatty oil by heating, blowing or ultra-violet light treatment and then emulsifying the oil. The emulsion absorbs atmospheric oxygen to effect "agglomeration" of the emulsion. Cummings (1966) discussed emulsification of prebodied dying oil and alkyd. Curtis et al. (1965) discussed a method of manufacturing low acid value non-oxidizing alkyd resins in emulsions. Kraft et al. (1965) prepared stable aqueous emulsions from short oil and medium oil alkyd resins by heating the resin with an emulsifying agent and slowly adding the aqueous phase, which also contained an emulsifying agent in order to bring about an inversion of phases.

The autoxidation of oils and alkyds has been employed by Austin and Zetterberg (1963) to "pre-shrink" oils and alkyds and reduce the blistering tendencies of surface coatings prepared from them. Catalysts for the blowing process were discussed by Austin and Zetterberg.

To the author's knowledge, no one has attempted to emulsify an oil or alkyd, autoxidize the emulsion to the particle gel state or near the gel state of the emulsion particle and subsequently prepare surface coatings utilizing the blown emulsion as the binder.

It is expected that the autoxidation reaction proceed via the classic production of peroxides as reported by Farmer et al. (1968). As indicated in Table 1.8 (Martens, 1974), soybean and linseed oils contain lenoleic and oleic fatty acids with their respective percentages in each oil. Martens (1974) described in Table 1.9 each fatty acid with respect to its molecular structure. The number of double bonds in each acid is indicative of reactivity, i.e., lenolenic, lenoleic, and oleic. Therefore, it is expected that oils and alkyds containing a larger percentage unsaturation will autoxidize at a greater rate than oils and alkyds containing a greater percentage of saturated oil.

iranchembook.ir/edu

Table 1.8 Fatty Acid Composition of Vegetable and Marine Oils (Martens, 1974)

	Number of Carbons	Double Bonds	Tung	Oiticica
Oleic	18	1	8	6
Linoleic	18	2	4	
Linolenic	18	3	3	
Eleostearic	18	3	80	
Licanic	18	3		
Ricinoleic	18	1		
Palmitoleic	16	1		
Arachidonic	20	4		
Clupanodinic	22	5		
Stearic	18	0	1	5
Palmitic	16	0	8	7
Myristic	14	0		
Lauric	12	0		
Capric	10	0		
Caprylic	8	0		
Iodine value			160-175	140-160
Viscosity, Gardner-Holdt			I	X
Lb/gal.	7.85		8.10	7.81
Color, Gardner	10 9		5	12
Acid Value	8 8		4	6
Saponification Value			190	190

[a] Distilled <1 1% rosin acids.

iranchembook.ir/edu

Table 1.8 Fatty Acid Composition of Vegetable and Marine Oils (Martens, 1974) (Continued)

	Dehydrated Castor	Fish	Linseed	Safflower
Oleic	9	10	22	13
Linoleic	82	15	16	75
Linolenic			52	1
Eleostearic				
Licanic				
Ricinoleic	9			
Palmitoleic				
Arachidonic		30		
Clupanodinic		25		
Stearic	2	2	4	4
Palmitic		12	6	6
Myristic		6		
Lauric				
Capric				
Caprylic				
Iodine value	125-140	165-195	170-190	140-150
Viscosity,				
Garnder-Holdt G	A	A	A	
Lb/gal. 7.85 7.69	7.76	7.70	7.70	
Color, Gardner 10 9	11	10	10	4
Acid Value 8 8	4	4	3	194
Saponification				
Value	190	190	190	190

[a] Distilled <1 1% rosin acids.

iranchembook.ir/edu

Table 1.8 Fatty Acid Composition of Vegetable and Marine Oils (Martens, 1974) (Continued)

	Soya	Tall Oil Acids	Cottonseed	Coconut
Oleic	25	46	24	
Linoleic	51	41	40	7
Linolenic	9	3		2
Eleostearic				
Licanic				
Ricinoleic				
Palmitoleic				
Arachidonic				
Clupanodinic				
Stearic	4	3	4	6
Palmitic	11	5	29	11
Myristic			1	18
Lauric				44
Capric				6
Caprylic				6
Iodine value	120-140	128-138	99-113	7-10
Viscosity,				
Garnder-Holdt	A	A	A	A
Lb/gal. 7.85 7.53	7.65	7.68		
Color, Gardner 10 9	8	5		
Acid Value 8 8	1	2		
Saponification				
Value	190	196	190	250

[a] Distilled <1 1% rosin acids.

iranchembook.ir/edu

Table 1.9 Structure of Fatty Acids

Example	Formula	Nature of Triglyceride Containing Predominant Amounts of the Acid
Stearic acid	$CH_3(CH_2)_{16}(COOH)$	Nondrying solid fat
Oleic acid	$CH_3(CH_2)_7CH{=}CH(CH_2)_7COOH$	Nondrying oil
Linoleic acid	$CH_3(CH_2)_4CH{=}CH\text{-}CH_2\text{-}CH{=}CH(CH_2)_7COOH$	Semidrying oil
Linolenic acid	$CH_3CH_2\text{-}CH{=}CH\text{-}CH_2\text{-}CH{=}CH\text{-}CH_2\text{-}CH{=}CH(CH_2)_7COOH$	Drying oil
Eleostearic acid	$CH3(CH_2)_3CH{=}CH\text{-}CH{=}CH\text{-}CH{=}CH(CH_2)_7COOH$	Fast drying oil
Ricinoleic acid	$CH_3(CH_2)_5CHCH_2X\text{-}CH{=}CH(CH_2)_7COOH$ (OH)	Nondrying oil
Licanic acid	$CH_3(CH_2)3CH{=}CH\text{-}CH{=}CH\text{-}CH{=}CH(CH_2)_4CO(CH_2)_2COOH$	Fast drying oil
Isamic acid	$CH_2CH(CH_2)_4C{\equiv}C\text{-}C{\equiv}C\ (CH_2)_7COOH$	Drying oil

Muizebelt et al (1998) studied the autoxidative crosslinking of alkyd resins using ethyl linoleate and methyl riconoate as model compounds. The first step in the oxidation is formation of the hydroperoxide via the resonance-stabilized pentadienyl radical, the double bonds becoming conjugated because this product is energetically more stable. No double bonds disappear in this first step. However, double bonds react away in later stages of the oxidation, mainly as a result during formation of epoxides and endoperoxides. Also, addition to double bonds may lead to crosslinking. With quantative carbon -13 nuclear magnetic resonance (^{13}C NMR) it was established that ether-and peroxy-crosslinks were formed in roughly equal amounts. Double bonds reacted to give epoxides, endoperoxides and **β-scission** (cleavage) into aldehydes. With the use of secondary ion mass spectrometry (SIMS), it was established that dimmers through pentamers were formed have included several oxygen atoms. After reduction of peroxide (crosslinks) with stannous chloride, the higher oxygen homologues decreased. In the ^{13}C NMR spectrum of the reduced material, peroxide and epoxide signals completely disappeared. High-resolution electrospray ionization mass spectra (ESI-MS) yielded evidence regarding the mechanisms of crosslinking. The non-conjugated linoleic acid was found to crosslink by combination of radicals: dimmers were detected in masses of

iranchembook.ir/edu

2(M-1). The conjugated linoleic acid crosslinked by addition of radicals to the double bond and disproportionation, yielding masses 2M as well. The results of the work on the model compound indicated that drying of alkyds proceeds by ether-and peroxy-crosslink formation. A hydrogen atom of the methylene group separating the double bonds of linoleate was abstracted. The resulting radical after reaction with oxygen yielded a hydroperoxide with conjugated double bonds. Using quantitative ^{13}C NMR it was established that the conjugated double bonds decreased owing to epoxide formation and **β -scission** (cleavage) into aldehydes and acids. The double bond concentration could be followed independently with iodine monochloride titration. Epoxide and acids may react to form esters compensating for the loss of crosslink density due to cleavage. However, this could not be seen with ^{13}C NMR. Mass spectroscopy (SIMS, ESI-MS) indicated the homologous oxygen derivatives comprising the various oligomers. ESI-MS gives high-resolution spectrum enabling mechanistic interpretation. Generally, it appeared that a combination of radicals occurred in linoleate crosslinking and addition to double bonds with recinoate. However, the formation of higher oligomers took place via addition in both systems presumably because the double bonds have become conjugated in the dimers.

1.2.3. Emulsified Oils and Resins

Bufkin and Grawe (1978) discussed most of the principal concepts that have been employed to develop thermosetting or crosslinking emulsions based upon different chemistries including a discussion of drying oils and alkyd resins in emulsions. This six-part review was designed to serve as an introduction to a series of publications describing research and development of crosslinking emulsions.

El-Aasser, et al. (1974) was able to successfully emulsify polyurethanes and epoxies by using a surfactant combination of sodium lauryl sulfate and cetyl alcohol. They were able to reduce these systems by mechanical sheaf to about 2-3 microns and further reduce the particle diameter to about 0.5-micron by utilization of ultrasonic vibration or homogenization.

Crews, Wildman, and Bufkin (1974) conducted an in-depth study of the swelling ratio of crosslinked latex particles. Bourne (1978) conducted a study of crosslinked thermosetting emulsions containing various silicon moieties. These studies by Crews, Wildman, Bufkin, and Bourne have focused on the swelling ratio theories as a concept useful in emulsion science together with an analytical tool to measure crosslinking density within emulsified particles. Leggett et al (1977) applied the swelling ratio technique

iranchembook.ir/edu

for measuring the relative crosslinking density of polymer particles to three commercially available thermosetting acrylic emulsions: Arolon X801 (Ashland Chemical Company); Rhoplex AC-604 (Rohm and Haas Company); and Ucar 4510 (Union Carbide Corporation). The crosslinking agent was Cymel 303 (American Cyanamide Company).

Dong et al (1999) and Gooch et al (2000) developed novel products by grafting oil modified polyurethane resins onto acrylic polymeric moieties, via hydrogen abstraction mechanisms, in miniemulsions. Draw-down films on glass demonstrated acceptable hardnesses and adhesion. Wang et al (1996) prepared miniemulsions by grafting alkyds resins onto acrylic polymeric moieties. Miniemulsion polymerization offers some advantages over conventional emulsion (macroemulsion) polymerization systems. Among the advantages are a process that is more tolerant of contaminants, and a product with more uniform copolymer composition, narrow particle size distribution, and high shear-stability. The miniemulsion polymerization is a "batch" reaction compared to emulsion polymerization which is a continuous feed operation and subsequently, continuous. More specifically, each emulsified particle in a miniemulsion is an individual reaction separate from all other particles and with no continuous feed of monomers.

In some ways, the preparation of autoxidative polymerization of alkyd resins and vegetable oils was one of the first miniemulsions, possibly with the exception that the average particle size of the typical miniemulsion particle is significantly smaller. Miniemulsion polymerization involves the use of a more effective emulsifying system to produce very small monomer droplets (<500 nm). Particle nucleation occurs primary via radical entry into the small monomer droplets. These must be stabilized against coalescence and diffusional degradation. Coalescence may be precluded by the addition of an appropriate surfactant. Diffusional degradation, or Ostwald ripening can be eliminated by the addition of a small amount of a water-insoluble (hydrophobe), monomer-soluble stabilizer. Polymers, comonomers, and chain transfer agents have been reviewed as hydrophobes. Miniemulsions have some unique and desirable properties: They are far more robust to variations in the recipe or to contaminant levels than conventional emulsions. Particle number is less sensitive by at least an order of magnitude to changes in initiator, water-phase retarder, and oil-phase inhibitor concentrations than macroemulsion polymerizations from which typical latex paint dispersions are derived. Perhaps because of this robustness, it was possible to produce latex with a narrow polydispersity. Hydrophobic comonomers have been used successfully as hydrophobes. It has been found that such systems will give a more uniform copolymer composition since the supply of hydrophobic comonomer is not mass-transfer limited than in macroemlsion polymerization. Miniemulsion polymerization also can be used to produce copolymers in which one of the comonomers (i.e. macromers) is almost

iranchembook.ir/edu

completely insoluble in water. Such copolymers are often not possible with macroemulsion polymerization. Finally, graft copolymers with alkyds, polyesters, urethanes, etc., can be made by hybrid miniemulsion polymerization, and may be the basis for a new generation of low volatile organic compound (VOC) alkyd coatings. A major effort in the development of miniemulsion technology is the Reaction Engineering Group directed by Dr. F. Joseph Schork in the School of Chemical Engineering at the Georgia Institute of Technology.

1.3. Theoretical Considerations

1.3.1. Intrinsic Viscosity

Staudinger (Billmeyer, 1973) was the first to report that the viscosity of polymer solutions was related to polymer molecular weight. Later work by Mark-Houwink and Sakurods (Billmeyer, 1973) modified Staudinger's equation to

$$[\eta] = k\ M_v^{\ a}$$

where: $[\eta]$ = intrinsic viscosity
k = a constant, 0.5 to 5 x 10^{-4} nominally
a = a constant (branching), 0.6 to 0.5 nominally
M = viscosity-average molecular weight.

The k and a constants are determined from a plot of $\log [\eta]$ vs. $\log M_V$ is the curve intercept and a is the slope of the curve, usually an expression for the degree of branching along a polymer chain.

Measurements of solution viscosity are usually made by comparing the efflux times for a specified volume of polymer solution to flow through a capillary tube with the corresponding solution and the solvent is the relative viscosity (η_r). The specific (η_{sp}), reduced (η_{red}), and inherent (η_{inh}), viscosities are derived as follows, where c is the concentration of polymer in solvent:

$$\eta_{sp} = \eta_r - 1$$

$$\eta_{red} = \eta_{sp}/C$$

iranchembook.ir/edu

$$\eta_{inh} = 1n\ \eta_r/C$$

The intrinsic viscosity vs. concentration and the viscosities are extrapolated to zero concentration, which is the intrinsic viscosity.

1.3.2. Hydrophile-Lipophile Balance (HLB)

The numerical, but non-theoretical Griffin (Beerbower, 1971) hydrophile-lipophile concept is based on an experimental method assigning numbers to emulsifiers by observation of emulsion stability. The resulting HLB numbers reduce a vast amount of experimental work to a single numerical scale and express a hydrophile-lipophile balance in an emulsion system.

The following procedure is used: A specified test oil and pure water are to be emulsified. Oleic acid and Potassium oleate are the primary reference emulsifiers. The oleic acid is assigned the arbitrary HLB number of 1.0 as the lipophile component and potassium oleate is assigned the arbitrary HLB number of 20 as the hydrophilic component. All subsequent HLB numbers are derived from these primary standards, even if determined from secondary reference emulsifiers. It is then assumed that the two primary reference emulsifiers and all subsequent emulsifiers, can be blended in various ratios on a weight fraction basis in a linear and additive manner to give a continuous series of HLB numbers according to the following equation:

$$\frac{W_A \times HLB_A + W_B \times HLB_B}{W_A + W_B} = HLB_{AB}$$

where:

W_A = weight of emulsifiers A (oleic acid)

W_B = weight of emulsifiers B (potassium oleate)

HLB_A = HLB number of emulsifier A (oleic acid = 1)

HLB_B = HLB number of emulsifier B (potassium oleate = 20)

HLB_{AB} = calculated HLB number for any given weight ratio of A to B.

Finally, it is observed that the HLB number of the ratio of reference emulsifiers that gives the most stable emulsion with a given oil, as

iranchembook.ir/edu

determined by experiment, may be designated as the "HLB requirement" for that oil when used with any combination of emulsifiers (McCutheon's Detergents & Emulsifiers, 1977).

There is a continuous range of liquid phase mixture types, from true solutions which are fully dispersed at a molecular level, through clusters or aggregates of relatively small numbers of solute molecules in miscelles, and translucent colloidal dispersions (10^{-9} to 10^{-6} m) up to opaque solid-liquid suspensions, liquid-liquid emulsions, and liquid-vapor foams. All can be discussed in terms of cohesion parameters (Barton, 1983).

The dispersal efficiency of surfactant or emulsifier molecules is a function of the relative interactions of their polar, hydrophilic "heads" with the aqueous phase and nonpolar, lipophilic "tails" in the hydrocarbon phase. Surfactants may be nonionic or ionic, but high polarity is achieved only in the ionic surfactants. The original HLB value was a concept by Griffin (1949) to devise a quantitative, but empirical hydrophile-lipophile (HLB) scale, on which oleic acid has $HLB = 1$ and potassium oleate has $HLB = 20$, to describe this behavior.

The emulsion stability of hydrocarbons in water may be correlated with the cohesion parameters of the hydrocarbons, while the solubility and aggregation characteristics of surfactants may be related to the cohesion parameters of the surfactants and of the solvents on which they are dispersed (Atwood et al, 1974). This localized segregation or structuring is not confined to aqueous systems or to liquids: microdomains occur in block and graft copolymer (Hefland, 1975; Hefland and Wasserman 1977).

Little and Singleterry (1964, 1970 and 1975) used Hildebrand parameters, pointing out that the aggregation number (the number of surfactant molecules per micelle) of dinonylnaphthalene sulfonate surfactants is an approximately linear function of the Hildebrand parameter of the oil. Also, there is a clear correlation between HLB data for surfactants and their δ values (Barton, 1983). These data conform to the relationships:

$$HLB = \left(\frac{\delta\ /\mathrm{MPa}^{1/2} - 16.8}{\delta\ /\mathrm{MPa}^{1/2} - 12.3} \right) 54$$

$$\delta/\mathrm{MPa}^{1/2} = \frac{243}{54 - HLB} + 12.3$$

A related hydrophile-lipophile balance function,

iranchembook.ir/edu

$$D(\delta) = (\delta - {}^{aq}\delta)^2/(\delta - {}^{o}\delta)^2$$

has been used in assessing the efficiency of phase transfer catalysts in the benzene-water system in terms of Hilderbrand parameters (Fukunaga, Shirai and Kimura, 1980). Such expressions obviously suffer from using only single-cohesion parameters, and progress has been made with multicomponent parameters.

Beerbower (1972) and co-workers were among those who discussed the dispersing tendencies on the oil and water interfaces of the surfactant or emulsifier region in terms of the ration of the cohesive energies of the mixtures of oil with the lipophilic portion of the surfactant and of water with the hydrophilic portion. They used Hansen parameters (Hansen and Skaarup, 1967), and for situations where δ_d, δ_p, and δ_h match for oil/lipophile and for water/hydrophile, their expression takes a simplified form. This can be related to the hydrophile-lipophile balance (HLB), for which Beerbower's definition is:

$$HLB = \frac{20\,H_M}{L_M + H_M} = \frac{20\,H_V H_\rho}{L_V L_\rho + H_V H_\rho}$$

H_V = volume, hydrophile
H_ρ = density, hydrophile
L_v = volume, lipophile
L_ρ = density, lipophile

where H_M is the molecular weight of the hydrophilic portion of the emulsifier (including the CO group if an acid is involved) and L_M is the molecular weight of the lipophile starting with the first carbon not attached to oxygen. It is possible to relate this to the cohesive energy ratio (Winsor, 1954) in the form

$$R_o = L_V L_{\delta *}^{2} / H_V H_{\delta *}^{2}$$

where

$$\delta_*^2 = \delta_d^2 + 0.25\ \delta_p^2 + 0.25\ \delta_h^2$$

$$R_o = (L_{\delta *}^{2} / H_{\delta *}^{2})\,(20/HLB - 1)\,(H\rho/L\rho)$$

iranchembook.ir/edu

Correlation of literature data for the optimum value of R_O for oil (o) in water emulsifier yields the optimum HLB value for the emulsifier:

$$HLB_O = \frac{20^o \delta_*^2/MPa}{o\delta_*^2/MPa + 161}$$

Other criteria for the selection of the emulsifier are

$$L_{\delta_*} \approx o_*, L_V \approx o_V$$

A plot of log R_O against HLB was found to be approximately linear, and it proved convenient to define and extended hydrophile-lipophile balance scale, HLB_E,

$$\log R_O = 0.925 - 0.0963 HBL_E$$

This allows the estimation of R_O and subsequent correlation with the cohesion parameters of emulsifiers with HBL_E values covering a wider range than the original definition. The method of Section 6.5 is used to determine ^LV and ^HV.

Marszall (1976) has proposed an alternative to the cohesive energy ratio, called the cohesive energy balance,

$$H_V(aq_\delta - H_\delta)^2 / L_V(aq_\delta - L_\delta)^2$$

Relative advantages and disadvantages of these approaches are not clear.

Cohesion parameters have been applied to various other commercial emulsions, dispersions and suspensions.

- Water-based paints
- Aqueous emulsions of cellulose nitrate/acrylic polyblends
- Suspensions of drug compounds
- Hansen parameter maps of commercial pastes
- Extraction of organic colloids from soil
- Correlation with δ_h of the sedimentation of the inorganic pigment ultramarine blue from organic liquids
- Pigmented polymer compositions

iranchembook.ir/edu

- Degree of aggregation of Tween ® (polyoxyethylene sorbitan aliphatic ester) and Span ® (sorbitan aliphatic acid ester) commercial detergents
- Properties of alkyl polyglycol monoethers
- State of aggregation of poly-(-benzyl-L-glutamute

Foaming behavior may also be correlated by means of cohesion parameters. At the beginning of this chapter it was pointed out that there could be an abrupt transition from defoaming (foam inhibiting behavior) to profoaming (foam stabilizing behavior) in a series of surfactants, associated with an insolubility-solubility transition. The same effect occurs with a single surfactant if its solubility is strongly temperature dependent, illustrated by sodium stearate which is much more soluble in hot water than cold, and which foams only at higher temperature. Block copolymers containing polyethylene oxide act in a similar way. It follows that the spherical Hansen solubility surfaces for polymers and others materials represent polymer-solvent combinations, which are likely to exhibit foaming. Solvents that readily dissolve polymers do not form foaming solutions, solvents that dissolve no polymer do not foam, but solvents that exhibit limited solvent action exhibit a maximum in foaming ability. This has been illustrated by plotting foam stability as a function of the distance between the solvent and solute points in Hansen three-dimensional solubility space for polymethylmethacrylate, the chlorinated polypropylene Parlon® P10 (Hercules, Inc.) and the epoxy-resin Epikote 1001 (Shell Chemicals). Foaming behavior appears to be a more sensitive indicator of the limits of polymer-solvent interaction than solubility or swelling.

The optimal selection of surfactants for emulsification of materials (with or without solvent) involves an understanding of HLB values and solubility parameters with respect to chemical relationships between each resin and/or monomer and the chemistry and conditions (pH, conductivity, etc.) of the continuous phase, usually an aqueous phase. Arbitrary selection of surfactants (soaps, detergents, etc.) for emulsification of monomers and resins will usually produce unacceptable results.

1.3.3. Diffusion of Oxygen in an Emulsion

Fick's Law (Barrow, 1973) describes the relationship between dissolved oxygen or air diffusing through the aqueous phase of an emulsion. Fick's Law is expressed as follows:

$$\frac{dw}{dt} = -DA\ \frac{dc}{dx}$$

iranchembook.ir/edu

where: w = mass of diffusing oxygen
t = time
D = diffusion coefficient
A = area of aqueous boundary
C = concentration of oxygen
X = distance in aqueous phase.

Experimentally, the rate of diffusion is proportional to the concentration difference across the boundary of aqueous phase, dc/dx concentration gradient. The diffusion rate is also proportional to the cross-section area, A, of the aqueous phase. If the diffusion rate is written dw/dt, mass of oxygen transferred across the aqueous boundary per second, then the expression becomes equation (6). The proportionality constant, D is called the diffusion coefficient and the negative sign is introduce so that D will have a positive value. The diffusion coefficient can be recognized as the amount at the amount of oxygen that diffuses across a unit area in one second under the influence of a unit concentration gradient. The diffusion coefficient is characteristic for a fluid at a given temperature.

The diffusion constant, D, is described as follows:

$$D = RT/C \pi r \eta$$

where: D = diffusion constant, per mole
R = ideal gas constant
T = absolute temperature
R = radius of diffusing molecule (oxygen)
0 = viscosity of solvent (water).

1.3.4. Solubility of Air and Oxygen in Aqueous Phase

Oxygen gas concentration in the aqueous phase of an emulsion increases with oxygen pressure. This statement is based upon Henry's Law (Barrow, 1973), which states that the concentration of a slightly soluble gas increases with increasing partial pressure of that gas. Therefore, in order to increase the concentration of oxygen in the aqueous phase of the emulsion, it is necessary to increase the oxygen partial pressure. If the oxygen concentration, in grams of oxygen per liter of aqueous phase, can be correlated with oxygen pressure, then controlling the oxygen pressure can control the oxygen concentration. It is necessary to draw a correlation curve from which oxygen concentration can be derived by knowing the oxygen partial pressure under various conditions of temperature and pressure.

iranchembook.ir/edu

Henry's Law expresses the partial pressure and concentration of oxygen as follows:

$$X_{O_2} = \frac{P_{O_2}}{H}$$

$$X_{O_2} = \frac{P_{O2}}{P_{O_2} + H_2O}$$

where: H = Henry's Law Constant, atmospheres/ mole

X_{O_2} = mole fraction O_2

P_{O_2} = partial pressure O_2, atmospheres

Henry's Law constants (in the Appendix) represent constants for oxygen at temperatures of 0°C to 100°C. Since the autoxidation reaction proceeds at 55°C, the Henry's law constant is 6.085×10^4. Table A.2 represents Henry's Law Constants for air. At 55°C the Henry's Law constant is 9.78×10^4. Since the last figure indicates that 3.695×10^4 atmospheres per mole greater partial pressure is necessary to dissolve one mole of air in one liter of water relative to elemental oxygen, it is apparent that elemental oxygen is more soluble than air. Air is 20.946% oxygen by weight. Therefore, the concentration of oxygen from air (Table A.3) at the same partial pressure is not equal to the equivalent partial pressure of elemental oxygen in water as described in Table A.4 in the Appendix.

1.3.5. Swelling Ratio

The solubility behavior of polymers has been interpreted by Cragg and Manson (1951) in terms of two different phases of different structures. The sol phase is the portion completely soluble in solvents of similar solubility parameter. The gel phase is insoluble in all solvents, although the gel-phase is capable of swelling in some solvents to a degree.

A three-dimensional network polymer such as a vulcanized rubber will not become completely dissolved but may absorb a large quantity of an appropriate solvent. Flory (1953) stated that swelling occurs under these conditions for the same reason that the solvent mixes with the same linear polymer to form a polymer solution. If the polymer swells with solvent, then

iranchembook.ir/edu

it is described as a swollen gel solution, elastic rather than a viscous one. An increase in entropy accompanies the swelling phenomenon due to the added volume of the polymer throughout which the volume may spread. As the network is swollen by adsorption of solvent, the chains between networks are required to assume elongated configurations and a force similar to the elastic retractive force in rubber develops in opposition to the swelling processes. As swelling proceeds, this force increases and the diluting forces decrease. A state of equilibrium swelling is ultimately reached in which the two forces are in balance similar to osmotic equilibrium.

There are numerous techniques for studying the network structure in crosslinked polymers. An excellent technique involves the swelling of polymer in solvent. If a crosslinked polymer is added to a solvent for the uncrosslinked polymer, then the crosslinked polymer will swell, but it will not dissolve, the total volume will increase. The soluble fraction of the polymer material will dissolve and diffuse out of the swollen polymer. The uncrosslinked matter is the sol fraction of the total polymer matter. The crosslinked material will swell in the three-dimensional polymer gel phases until the solution of osmotic forces are balanced by the forces due to the stretched segments of polymer chains. These elastic retractive forces are inversely proportional to the molecular weight of polymer between crosslinks. A highlinked polymer will not swell as much as a lightly crosslinked polymer.

Flory (1953) has discussed the theory of crosslinked polymers. The equation relation the extent of swelling to the molecular weight between crosslinks is as follows:

$$-[\ln(1 - V_{2m}) + V_{2m} + \chi_1 V_{2m}^2] = \frac{(V_1)}{\bar{v} M_c}\left(1 - \frac{2M_c}{M}\right)\left(V_{2m}^{1/3} - \frac{V_{2m}}{2}\right)$$

where: m = equilibrium swelling
V_{2m} = volume fraction of polymer in swollen gel
V_1 = molar volume of solvent
$\bar{v}$ = specific volume of polymer
χ_1 = a solvent-polymer interaction term
M = molecular weight of polymer before crosslinking
Mc = molecular weight of polymer chain between points of crosslinking.

iranchembook.ir/edu

Swelling is expressed as the swelling ratio, q_m, which is equal to the ratio of the volumes of the swollen to unswollen gel. The swelling ratio q_m, is the reciprocal of V_{2m} in the equation above, $q_m = 1/V_{2m}$. Substituting q_m for $1/V_{2m}$, in the following equation , it becomes

$$-[1n\,(1 - 1/q_m) + 1/q_m + \chi/q_m^2] = [V_1/\bar{v}\,M_c)]\,(1 - 2M_c/2M)\,(1/q_m)^{1/3} - 1/(2/q_m)$$

Albert Einstein derived a relationship (Crews et al, 1977) between the viscosity of a suspension, η, the viscosity of the fluid phase, η_o and the volume fraction of the particles in suspension $\emptyset$. This relationship is expressed in the equation

$$\eta = \eta_o\,(1 + 2.5\phi)$$

If the unswollen volume fraction of the polymer is known, the above equation can be used to determine the swelling ratio of the latex particles providing a solvent would be employed for the external phase that is capable of swelling the polymer gel. However, a problem exists, because volume fraction, N, is limited to a maximum of 0.02 due to particle interaction at higher concentrations. Therefore, at corresponding concentrations of polymer particles, the viscosity change of the solvent upon addition of particles would be very small and inaccurate to measure. In order to circumvent this problem, researchers including Guth, Simha and Gold (1936) have expanded Einstein's equation into a power series to linearize the function of volume fraction and the hydrodynamic measurements. The general form of this equation is

$$\eta = \eta_o\,(1 + a_o\phi + a_1\phi^2 + a_2\phi^3 \ldots)$$

Guth calculated the value of a on theoretical grounds and arrived at the equation

$$\eta = \eta_o\,(1 + 2.5\,\phi + 14.1\,\phi^2)$$

which increases the validity of the equation to lower values on η down to approximately 0.06. This equation can be solved for the internal phase volume fraction, swelled polymer, $\emptyset$, by equating it to zero and applying the quadratic formula.

iranchembook.ir/edu

Equate to zero.

$$(14.1\ \eta_o)\ \phi^2 + (2.5\ \eta_o)\ \phi + (\eta_o - \eta) = 0$$

Apply quadratic formula.

$$\phi = \frac{-2.5 \pm \sqrt{6.25\eta_o^2 - 56.4\ (\eta_o - \eta)}}{28.2\eta_o}$$

Cancel η_o terms.

$$\phi = \frac{-2.5 \pm \sqrt{6.25 \quad - 56.4\ (\eta_o \eta - \eta)}}{28.2}$$

Rearrange the equation.

$$\phi = \frac{\sqrt{6.25 \quad + 56.4\ (\eta_o \quad - \eta/\eta_o)}}{28.2} - 2.5$$

1.4. Justification for Research and Development

The major justifications for water-borne coatings based on vegetable oils are

1. Economics
   a. Continual increase in cost of petroleum
   b. Continual increase in costs of processing, e.g., heating
2. Energy
   a. Water-borne resins processed at temperatures below 60 °C
   b. Solvent system resins processed at temperatures above 300°C
3. Pollution
   a. Solvent vapor from drying coatings are pollutants
   b. Malodorous solvent vapors
   c. Water vapor evaporated from water-borne coatings during drying.

iranchembook.ir/edu

Because of the above advantages attributed to water-borne coatings systems, research on water-borne coatings based on vegetable oil was initiated.

The emulsification of an oil or alkyd in water by mechanical shear usually gives an average particle size of 2.0 to 3.0 microns. Under the best conditions, the average particle size is still above 1.0 micron and the distribution is typically broad. In contrast, emulsions generated via emulsion polymerization usually have more narrow particle sizes distributions and average particle sizes of 0.1 micron to 0.3 micron. The three to five fold difference in particle size between the systems generated by emulsion polymerization and emulsion polymerization and emulsification is critical. For example, Vanderhoff (1970) and Vanderhoff, Vanderhul, Tausk, and Overbeek (1970) reported that a monodisperse polystyrene latex of 0.2 micron diameter will never settle.

The tendency of colloidal particles to settle upon standing is offset by their Brownian motion and the convection currents arising from small temperatures gradients in the sample. The motion, which results from the unbalanced collisions of liquid molecules with colloidal particles, is more intensive the smaller the particle size. The convection currents depend on the sample size and storage conditions such as temperature. The rate of sedimentation of spherical particles according to Stoke's Law is

$$\text{Rate of Sedimentation} = (D^2/18\eta)(\rho_p - \rho_m)\, g$$

where: D = particle diameter
η = viscosity of the medium
ρ_p = density of particle
ρ_m = density of medium
g = gravitational constant.

One criterion proposed for settling is that a sedimentation rate of 1.0 mm per 24 hours will be offset by the thermal convection and Brownian motion in a sample (Overbeek, 1952). Substituting this sedimentation rate into the equation for a typical alkyd (density = 1.1 g/cm^3) in a water medium (density = 1.00g/c m^3), it is found that the largest particle size that will not settle is 0.46 micron in diameter, assuming the viscosity of the medium is 1.0 centipoise. The resins in this project will range in density from 0.9 to 1.2 g/c m^3 and thus, particle size can be critical.

Particle size is also an important consideration for coalescence and film formation of an emulsion. The forces exerted on the emulsion or latex particles during drying are those arising from the water-air and polymer-

iranchembook.ir/edu

water interfacial tension (Vanderhoff, 1966 and 1970) that bring the particles into close contact and initiate the coalescence. The maximum shear modulus of a polymer particle then that can coalesce upon drying of its aqueous dispersion is calculated to be about 112.5 kg/cm^2 for a particle diameter of 0.1 micron at 30-dynes/cm surface tension (Vanderhoff, 1973). This maximum shear modulus decreases inversely with increasing particle size, i.e., the maximum shear modulus for coalescence for a particle diameter of 1.0 micron and 10.0 microns are 11.2 kg/cm^2 and 1.1 kg/cm^2, respectively. Thus, the larger the particle size of the dispersion, the softer the polymer must be in order for the particles to coalesce upon drying. If the shear modulus of the polymer is too high for the emulsion particle, the particle coalescence will be incomplete and the film properties will be diminished.

From the above discussion, it is clear that the particle size and the crosslink density within the latex particle are critical. In this research the emulsification technique and the selection of proper emulsifying agents have controlled the particle size of the alkyd, oil or oil/alkyd mixture. The crosslink density was developed by autoxidation (oxygen blowing) of the emulsion.

Particle size of the emulsions was measured with optical microscopy and spectrophotometric methods. Scanning electron microscopy and spectrophotometric methods. Scanning electron microscopy was used to examine the films formed from the reacted emulsion in order to examine the films formed from the reacted emulsion in order to examine coalescence of the particles.

Although there are numerous procedures for autoxidation of oils available, none of them involve the utilization of emulsions, i.e., aspiration a flow of air or oxygen into an emulsion. Thus, a range of temperature between 40° C and 95 ° C was employed with no catalyst added. From these data, the need for catalysis was concentrations to choose the best one(s). Since both particle size and crosslink density are critical in these systems, an optimum temperature and catalyst combination was established by minimizing particle size increases due to agglomeration and maximizing the crosslink density within the particles.

The agglomeration of particles during the autoxidation process was observed via optical microscopy in the early stages of polymerization and by scanning electron microscopy in the latter stages.

The following parameters have been involved during the autoxidation reaction on the emulsion particles.

1. Rate of flow of air or oxygen
2. Temperature of the emulsion
3. pH of the emulsion
4. Rate of agitation (emulsion/oxygen).

iranchembook.ir/edu

An independent study was conducted on each parameter to obtain optimum set of conditions for reaction of the emulsion.

iranchembook.ir/edu

Chapter 2

SYNTHESIS AND POLYMERIZATION OF ALKYDS

2.1. Alkyd Synthesis Procedure

Alkyd polymers used for experimentation were short, medium, long and extra-long. In addition, an oil modified urethane alkyd was used. These alkyds were synthesized from dibasic acids, polyols and vegetable oils. The short, medium, long and extra-long alkyds contained 30, 52, 60, and 75 percent vegetable oil by weight, respectively. The urethane alkyd was synthesized from toluene diisocyanate, polyol, dibasic acid and 62 percent vegetable oil. The percent composition of each component is listed in Table 2.1.

Table 2.1 Formulation of AR Soya Oil Emulsion after Optimization

AR Soya Oil	50.0%, w/w
Distilled Water	49.0%, w/w
Dupanol (sodium lauryl sulfate)	2.0%, w/w of oil

Note: Procedure for preparing emulsion

(1) Dissolve surfactant in water.
(2) Pre-emulsify AR Soya in water with ultrasonic generator for five (5) minutes.
(3) Emulsify pre-emulsion in homogenizer for one (1) cycle.

The alkyds mentioned above were synthesized by charging the polyol and dibasic acid into a 200 milliliter four-neck resin kettle equipped

iranchembook.ir/edu

with a mechanical stirrer, nitrogen inlet, 0-250°C thermometer and a steam jacketed condenser, barrett trap, water cooled condenser assembly. Xylene was added as solvent and the temperature was raised to 100°C, at which time the polyol was added. Upon continued heating, the temperature reached 160°C and water began to be evolved as the esterification proceeded. The reaction temperature was held below 180°C until the appropriate acid value (See Table 2.1) was reached. The acid value is related to the molecular weight of the alkyd as described by Patton (1962). The acid value is calculated by titrating the alkyd with an aqueous solution of base and calculating as follows:

$$\text{Acid Value} = \frac{(\text{milliliters, base})(\text{normality, base})(\text{M.W. KOH})}{\text{grams, alkyd sample}}$$

2.2. Emulsification Procedure

The oils and alkyd materials were emulsified by the following procedure:

1. The emulsifying agent was dissolved in distilled water at 25.0°C.
2. The oil (or alkyd) was mixed with the emulsifier solution while being dispersed with the **Bransonic**^{R} Ultrasonic Vibrator that formed a pre-emulsion.
3. The pre-emulsion was stable enough to remain intact during transfer to the **Gaulin**^{R} Sub-micron Disperser and Homogenizer. The emulsion was recycled until the desired particle size reduction was achieved. The **Gaulin**^{R} Homogenizer was operated at a normal 3500 pounds per square inch of shear force.

Table 2.2 lists the components of the formulation that was found to be suitable for the emulsification of alkali refined soya oil emulsion. Table 2.3 lists the components for the formulation of the medium soya/linseed emulsion. The emulsifier for emulsification of medium soya/linseed was a combination of emulsifiers as observed in Table 2.3.

iranchembook.ir/edu

Table 2.2 Formulation of Medium Soya/Linseed Alkyd Emulsion after Optimization of Variable Parameters

Alkyd IV (50% alkyd and 50% mineral spirits)	50.0%, w/w [a]
Distilled water	48.0%, w/w
Emulsifier 75% Nonylphenoxypoly (ethyeneneoxy)$_4$ alcohol of Alkyd 25% Dodecyl sodium sulfate	4.0%, w/w

[a] Weight/weight basis.

Note: Procedure for preparing emulsion:

(1) Dissolve dodecyl sodium sulfate in distilled water, 25 ^{o} C.

(2) Dissolve nonylphenoxypoly (ethyeneneoxy)$_4$ alcohol in (1).

(3) Pre-emulsify alkyd in surfactant-water solution for fifteen (15) minutes. Emulsify pre-emulsion in homogenizer for one (1) cycle

Table 2.3 Material Description and Identification

Number	Material Description	Cargill^{R} Code	Solventa	% Non-Volatile
I	Alkali refined soya oil	AR Soya	---	100
II	Short oil soya alkyd	5216	Xylol	50
III	Medium oil soya alkyd	5184	Mineral Spirts	50
IV	Medium soya/linseed alkyd	5150	Mineral Spirts	50
V	Long oil soya alkyd	5500	---	100
VI	Extra-long oil soya alkyd	5070	Mineral Spirits	70
VII	Urethane soya alkyd[b]	4355	Mineral Spirits	55
VIII	Tall oil fatty acid alkyd	5020	Mineral Spirits	50

iranchembook.ir/edu

Table 2.3 Material Description and Identification (Continued)

Number	% Polyol	% Phthalic Anhydride	Acid Value	% Oil (Oil Length)
I	---	---	---	100
II	28	42	12	30
III	18	35	10	52
IV	18	30	10	52
V	8	17	12	60
VI	17	23	8	75
VII	11	9	10	62
VIII	41	23	12	36

[a]Solvent in commercially available alkyd product

[b]Urethane soya alkyd contains 11% polyol and 18% toluene disocyanayte with 62% soya oil and 9% phthalic anhydride, weight by weight basis.

2.3. Autoxidation Procedure

The autoxidation of oil and alkyd emulsions were conducted in the Bench Scale[R] pressure vessel illustrated in Figure 2.1. The vessel was pressure, temperature and agitation controlled. The cross-section view of the pressure vessel is illustrated in Figure A.1 in the Appendix. It can be seen that the turbine agitator controlled by a tachometer is capable of thoroughly circulating the emulsion within the vessel. The temperature sensor rests within the liquid adjacent to the turbine agitator that produces a continuous signal to the proportional temperature controller. The proportional temperature controller pulses heat to the vessel proportional to the difference between the desired temperature setting in the controller and the actual vessel temperature. The oxygen (or air) pressure is controlled by a pressure regulator connected to a delivery tube beneath the surface of the emulsion as shown in Figure A.1 in the Appendix. The autoxidation is thus controlled while periodic samples are taken from the interior of the vessel, beneath the surface of the liquid and through a sample valve.

iranchembook.ir/edu

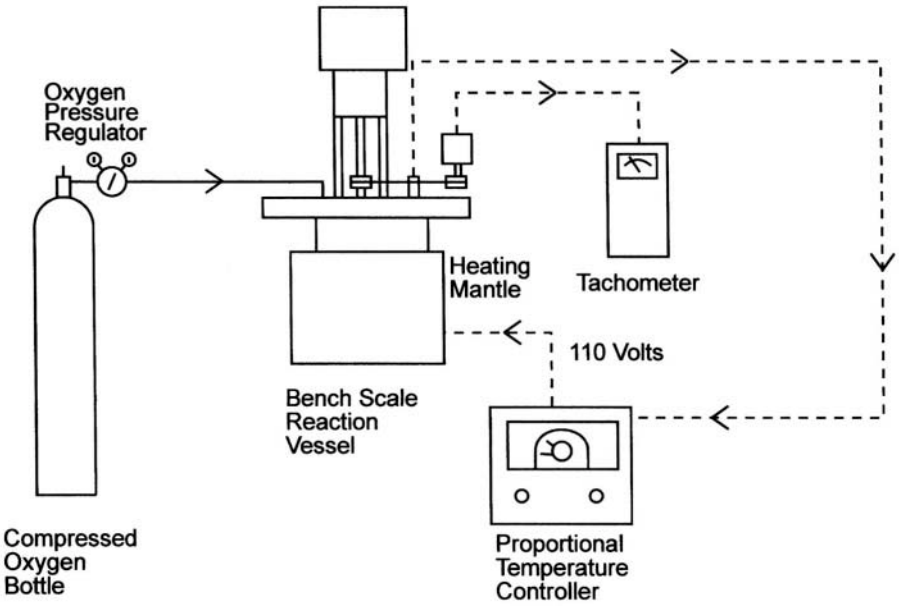

Figure 2.1. Emulsion autoxidation reaction apparatus.

The apparatus shown in Figure 2.1 was suitable for studying the effects of parameter variances during autoxidative crosslinking of emulsified particles.

The autoxidation reaction was conducted by the following procedure:

1. The emulsion was charged into the pressure vessel under atmospheric conditions.
2. The oxygen (or air) pressure regulator was adjusted to the predetermined vessel pressure.
3. The temperature controller was adjusted to the predetermined vessel temperature.
4. The turbine agitator was engaged to the predetermined revolutions per minute.
5. Samples were taken on a periodic time basis in order to monitor the progress of the reaction.

iranchembook.ir/edu

2.4. Materials

Vegetable oil derived materials used for experimentation are listed in Table 2.3. These oils and alkyds were originally provided by the Research Center, Cargill Corporation, Minneapolis, Minnesota, but presently supplied by Eastman Corporation in year 2000 acquired the McWhorter Technologies plants in Chicago Heights, Illinois. Alkyds were prepared by esterification of vegetable oils with phthalic anhydride and multifunctional alcohols to obtain the correct oil length within the structure of the alkyd molecule (Patton). The raw soya oil was refined with sodium hydroxide to remove free fatty acids and purify the oil.

The conjugated oils used for varying the percent conjugation of alkyds for autoxidizable emulsions were synthesized by the formulation described in Table 2.4. The vegetable oil derived fatty acids with varying percent conjugation were provided by the Hercules Corporation and the Sylvachem Corporation. The percent conjugation of the oils (for synthesizing alkyds of varying percent conjugation) are contained in Table 2.5. These alkyds were emulsified, autoxidized and results are reported in section 3.6.

Solvents used for dissolving alkyd III are listed as follows: 2-butoxyethanol, mineral spirits, and xylene. The 2-butoxyethanol and mineral spirits were of technical grade quality and xylene was of reagent grade quality.

Table 2.4 Formulation for Synthesis of Alkyds for Conjugation Study

Component	Percent, (w/w)
Trimethylol	31.90
Fatty acid oil, Vegetable	41.12
Phthlaic anhydride	33.10
Less water	6.10
	Total 100.00

Note: Final Acid Value = 15.0 ± 0.2

iranchembook.ir/edu

Table 2.5 Study of Conjugation of Vegetable Oil in Alkyd

Fatty Acid Oil, vegetable	Conjugated Lenoleic Acid Percent
Pamolyn 200	10
Pamolyn 327B	26
Pamolyn 300	38
Pamolyn 380	68
Sylfat 11%	11
Sylfat 21%	21
Sylfat 32%	32
Sylfat 42%	42

Note: Pamolyn[R] conjugated fatty acids acquired from Hercules Corporation, Wilmington, Delaware; Sylvachem[R] conjugated fatty acid acquired from Sylvachem Corporation, Panama City, Florida.

2.5. Characterization

The emulsification of vegetable oil and vegetable oil derived alkyds was characterized by determining the particle size of the emulsified material which is indicative of shelf stability of the emulsion together with the freeze-thaw stability of the emulsion. The progress of the autoxidation reaction was followed in order to ascertain the kinetic nature of the reaction.

The polymer can be characterized by solution techniques when soluble, but a different technique must be employed when the polymer has become crosslinked to the point of insolubility. The autoxidation reaction increases in rate and therefore the method of determining crosslinking must be faster in order to control the reaction. Film properties are directly related to the crosslinking of the emulsified oils and alkyds.

iranchembook.ir/edu

2.5.1. Emulsion Particle Size

The stability of an emulsion has been related to the particle size or diameter. Thus, it is necessary to know the particle size and particle distribution in order to assure emulsion stability. The change of particle size during autoxidation of the emulsion has also been measured in order to determine the stability of the processed emulsion.

2.5.1.1. Microscopic Measurement

The microscopy method consisted of diluting a one-milliliter emulsion sample to one hundred milliliter's with distilled water at 25°C and placing approximately 0.1 milliliter (one drop) sample of the dilution on a glass microscope slide with cover slide. The microscope possessed a grating positioned in the ocular component of the microscope. The grating was calibrated with a 1.0 micron American Optical Company micrometer. An oil immersion lens increased the magnification power to 2000 x. The basic advantage of the microscopy technique is a fast inspection of the sample and an approximation of the average particle size and distribution. Table 2.6 represents the homogenizationi of emulsion samples and an average particle size approximated with the microscopy method. It is obvious that this method suffers from an inability to accurately measure particle size below 1.0 micron and to detect small differences in particle size distribution.

2.5.1.2. Spectrophotometric Measurement

Referring to Table 2.7, an emulsion sample of alkyd III was diluted with distilled water to a concentration of 0.2 grams per liter of water. The percent transmittance varies from 49.1 to 46.7, which gave an undistinguishable change under microscopic analysis. This change in transmittance was studied further in Figure 2.2 where concentration is expressed on dry weight alkyd basis. It can be seen from Figure 2.2 and Figure 2.3 that percent transmittance decreases with increasing alkyd concentration. It can be seen from Figure 2.3 that increasing average particle size decreases percent transmittance.

A second alkyd, VII, was employed to determine a correlation between different types of alkyd materials and percent transmittance with concentration. Figure 2.4 is a percent transmittance and concentration curve for the alkyd VII. The curve has a greater slope than the alkyd III, but the curve is as linear, which indicates consistency. Both of these curves were reproduced and the same correlation was obtained.

iranchembook.ir/edu

Table 2.6 Emulsion[a] Particle Size and Homogenization Time

Homogenization Time, hours [b]	Cycles	Particle size, microns [c]
0.0	0	10.0-20.0
0.1	1	1.0-10
0.5	5	1.0-10
1.0	10	1.0
2.0	10	1.0
3.0	30	1.0
4.0	40	1.0
5.0	50	1.0

[a] Alkyd III emulsion in xylene solvent, nonvolatile solids of 74.4%, 50% water/50% alkyd and xylene.

[b] Emulsion flow rate: 57 liters/hour, 15 gallons/hour; Operating pressure: 246 Kg/cm^2, 3500 psi, utilizing Laboratory Homogenizer and Sub-Micron Disperser, Model 15M-8TA, Gaulin Corp.

[c] Microscopic examination.

iranchembook.ir/edu

Table 2.7 Spectrophotometric Method of Monitoring Particle Size in Emulsion

Reaction Time Hours	% Solids	Average Particle Size, Microns	% Transmittance[a]
0	39.57	1.0	49.1
5	---	---	---
10	40.57	1.0	47.6
15	40.63	1.0	49.2
20	40.79	1.0	47.1
25 (insoluble)[b]	40.78	1.0	46.1
30 (insoluble)	---	---	---
35 (insoluble)	41.77	1.0	46.6
40 (unstable)	41.25	1.0	46.7

[a]% transmittance was measured at 509 nm and 0.2 grams alkyd III per liter of distilled water.

[b]Insoluble at a reaction time indicates the alkyd particle was not totally soluble in acetone at 20oC and exhibited turbidity.

iranchembook.ir/edu

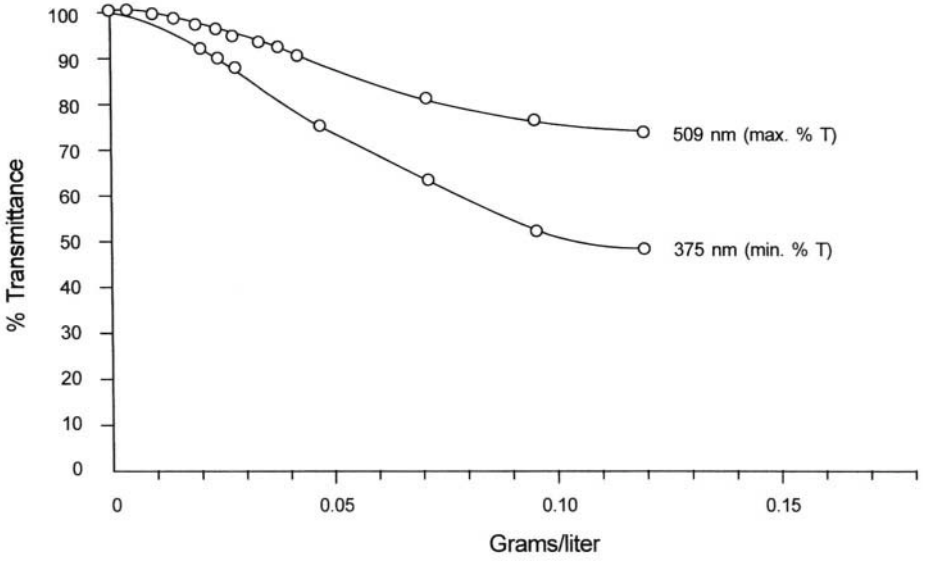

Figure 2.2. Transmittance at two different wavelengths vs. concentration of emulsified alkyd III particles.

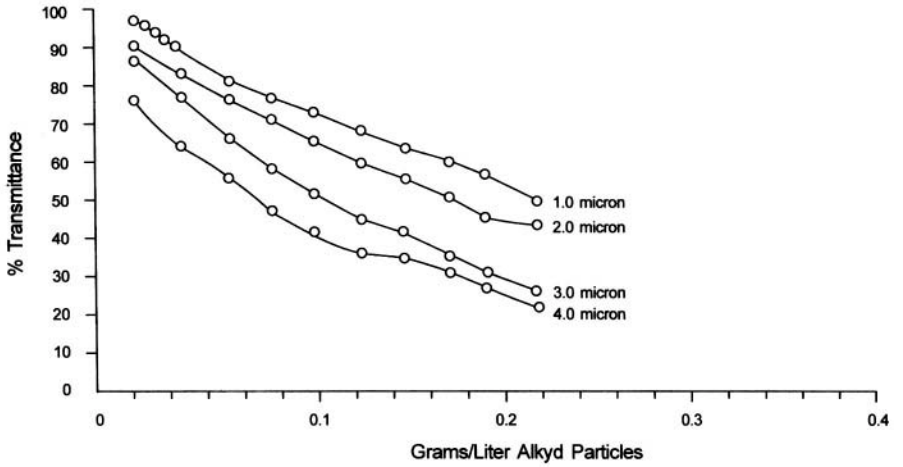

Note: 509 nm was used for this experiment.

Figure 2.3. Light transmittance vs. concentration for varying particle diameter, urethane alkyd III.

iranchembook.ir/edu

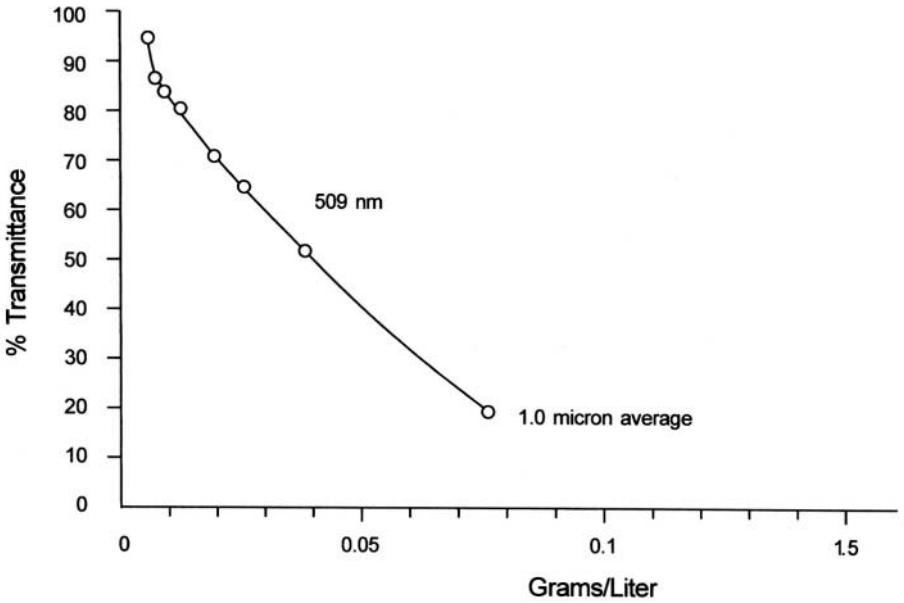

Figure 2.4. Light transmittance vs. concentration for particle diameter, urethane alkyd III.

Tables 2.6 and 2.7 and Figures 2.2 - 2.4 were constructed utilizing a Bausch and Lomb Spectronic 710 Spectrophotometer for transmittance measurements. The average particle size of each emulsion sample was approximated with a Bausch and Lomb Polarizing Microscope. The accuracy of the average particle size specified in Table 2.4, Figures 2.2 – 2.4, was checked with a Coulter-Counter^{R} and found to be accurate within about 1.0 micron for average particle size measurements.

2.5.1.3. Coulter-Counter^{R} measurements

A Coulter-Counter^{R} model TAII was used with a M3 Data Converter (43) and a 15-micron aperature to measure particle size diameter. The limiting particle diameter for this instrument is 0.20% NaCl electrolyte before measurement. The data were reported in particle diameter distribution by volume and population. Cumulative and differential curves were constructed from the data points for emulsion particle percent by volume vs. diameter.

iranchembook.ir/edu

2.5.2. Emulsion Characterization

The emulsions were tested for shelf stability with the accelerated shelf stability method described in ASTM D 1849-1987. The stabilities of the emulsions were reported in days.

The emulsion mechanical stability was determined by agitation in a Waring Blender and is reported in minutes that the emulsion withstood being agitated at a rate of 1800 revolutions per minute before demulsification began.

The emulsions were tested for freeze-thaw stability by freezing the emulsion samples at -9.4°C and thawing at 25.0°C as described in ASTM D 2243-90.

The emulsion viscosity, in centipoise (cps), was determined with a Brookfield Viscometer, model LVI. Relative viscosities of the emulsions were determined using a capillary Cannon-Fenske Viscometer, size 100. The relative viscosity was determined by flowing the emulsion through the viscometer and obtaining a ration between the efflux times for the emulsion and distilled water, which represents the aqueous phase of the emulsion.

2.5.3. Film Characterization

The films were prepared by drawing down a two-milliliter sample for the emulsion on a smooth glass panel with a doctor blade with 3.0 to 6.0 mil openings. The thickness of the dried film was measured with a micrometer after the film was freed from the glass panel.

The hardness of the film was determined with a Sward Hardness Rocker Tester, Model C, (Paint Testing Manual, 1972) by the procedure described in the Paint Testing Manual.

The tensile strength and percent elongation of the free films were determined with an Instron 1130 Tensile Tester. The specimens possessed a width of 1.0 centimeter, a thickness of 1.0 to 3.0 millimeters and gauge length of 2.0 centimeters. The crosshead speed was 2.0 centimeters per minute.

The scanning electron microscopy (SEM) samples were prepared by adhering thin samples of dried film to the aluminum sample pedestal with double-stick tape. A layer of carbon was deposited on the samples and they were shadowed with gold-paladium alloy in a vacuum evaporator. The micrographs were taken directly from these samples with an AMR scanning electron microscope at a magnification of fifty to fifty thousand times.

iranchembook.ir/edu

2.5.4. Intrinsic Viscosity Measurement

Determination of intrinsic viscosity is directly related to the determination of viscosity average molecular weight. Therefore, monitoring intrinsic viscosity is directly indicative of viscosity molecular weight development. The intrinsic viscosity for the polymers that will be discussed in following chapters was determined using the theory for dilute solution viscosity and procedure for the Cannon-Fenske viscometer as described by Collins, Bares, and Billmeyer (1973) in section 1.3.

2.5.5. Swell Ratio

The swelling ration is the volume ration of the swollen to unswollen polymer. The volume of a polymer in water, hydrodynamic volume, may be obtained by density measurements. This may be expressed as mass-density quotient, m/p_ρ, where m is the weight of particle solids per cubic centimeter of suspension and p_ρ is the dry polymer density.

$$S = \frac{\phi}{m/\rho_p} = \rho_\rho \frac{\phi}{m}$$

When φ is substituted in the above equation in terms of η and η_o, then

$$S = \frac{\rho_p \sqrt{6.25 + 56.4\ (\eta - \eta_o)/-\eta_o} - 2.5}{28.2\, m}$$

The variables in the equation are measurable by viscometric and gravimetric methods. About 0.2 grams of solids were added to a deciliter of acetone to dissolve the aqueous phase and swell the polymer. Acetone was selected because it is a water and alkyd miscible solvent which is useful for diluting a water borne soya alkyd latex. A suspension will appear as a very dilute latex and will exhibit a Tyndal effect. It is necessary to keep this sample covered to prevent evaporation, which would change the concentration.

Accuracy is essential in the viscometric measurements of the suspension and the fluid phase of the suspension. A Cannon-Fenske #50 viscometer in a water bath is controlled at $\pm 0.01°C$. Densities are required of both the suspension and the fluid phase. These densities are determined

iranchembook.ir/edu

by use of a 25-milliliter pyconometer. Temperature control is essential during these measurements, there being one temperature held constant throughout the experiments. After viscosity and density measurements have been completed on the initial suspension, a 5-10 milliliter aliquot must be utilized for a percent solids determination.

The remaining suspension sample is then centrifuged (14,500 rpm at 10°C). The supernatant (fluid phase) is then decanted, thermally stabilized and density, viscosity and percent solids measurements are performed. With these measurements completed, the equation for the swollen volume fraction, *N*, can be applied in the following equation:

$$\phi = \frac{\sqrt{6.25 + 56.4\ (\eta - \eta_o/\eta_o)} - 2.5}{28.2}$$

The viscosities of the suspension and fluid phase are determined by

$$\eta = (At_s - B/t_s)(\rho_s - \rho_a)$$

$$\eta_o = (At_o - B/t_o)(\rho_o - \rho_a)$$

In the above equations, A and B are calibration constants of the #50 Cannon-Fenske viscometer. The constants A and B are the intercept and slope of the curve resulting from ploting η/pt vs. $1/f^2$ from Figure A.4 and Table A.5 in the Appendix. The flow times for the suspension and fluid phase are t_s to t_o. The densities of suspension and fluid phase are represented by ρ_s and ρ_o. The correction factor for buoyancy in air is added by the expression containing the air density, ρ_a, as follows:

$$\rho_s = \frac{k(P_G - P_T) + \rho_a}{V}$$

$$\rho_o = \frac{k(P_G - P_T) + \rho_a}{V}$$

iranchembook.ir/edu

The pycnometer tare weight is represented by P_T and pycnometer gross weight by P_G. Measurements P_G and P_T are utilized to determine the weights of the samples. The weight is divided by the pycnometer volume, V. A correction factor, k, is used for buoyancy factors and is defined in the following equation.

$$K = 1 - (\rho_a/8.4)$$

It is then necessary to determine the unswollen volume fraction of the polymer by the following equation:

$$\text{Unswollen polymer density} = m/\rho_p$$

And polymer density, ρ_p, can be determined directly or the undiluted latex density can be measured and by applying the percent solids, the unswollen polymer (dry) density can be calculated. The mass, m, of the particles in suspension is calculated by

$$M = \rho_S\ (W_s - W_o)$$

Where W_s is the solids content of the suspension (grams of solids per ram of suspension) and W_o is the solids content of the fluid phase (grams of solids per gram of fluid phase). The swelling ratio is calculated by

$$S = \phi\ \rho_P/m$$

A summary of the above calculations,

$$S = \frac{\rho_p\ (\sqrt{6.25 + 56.4\,(\eta_s - \eta_o\ /\eta_o}) - 2.5}{28.2\,m}$$

Where: $\eta_s = (\rho_s - \rho_a) \cdot (At_s - B/t_s)$; centipoise viscosity latex dilution

iranchembook.ir/edu

η_o = $(\rho_o - \rho_a) \cdot (At_o - B/t_o)$; centipoise viscosity latex liquor

ρ_s = $k\,(P_G - P_T)/V + \rho_a$; latex dilution density

ρ_o = $k\left(P_{liquor} - P_T\right)/V + \rho_a$; latex liquor density

m = $k\,\rho_s\,(W_s - W_o)$; calculated gram particle solids per cubic centimeter suspension

ρ_p = dry polymer density

ρ_a = density of air (25°C) = 0.001169 g/cm^3

V = pycnometer volume

K = $1 - \rho_a/8.4 = 0.99986$ at 25°C

P_G = pycnometer volume

P_T = pycnometer tare weight

B = viscometer calibration constant

A = viscometer kinetic energy constant

t_o = flow time of clear liquor in seconds

t_s = flow time of latex dilution in seconds

W_o = grams solids per gram of clear liquor

W_s = grams solids per gram of latex dilution

2.5.6. Turbidimetric Measurement of Swelling Ratio

Due to a two-hour analysis time to obtain the swelling ratio of crosslinked emulsion particles, it was necessary to utilize a faster method of determining degree of crosslinking during the progress of the reaction. The autoxidation reaction under 80 pounds per square inch (p.s.i.g.) of oxygen pressure required less than ten hours. Thus, it is necessary to measure the swelling ratio with the aid of a technique, which requires less than fifteen minutes.

An emulsion sample will increase in crosslink density with decreasing swelling ratio and will decrease in swelling ratio with decreasing solubility in solvent as shown in Table 2.8.

iranchembook.ir/edu

Table 2.8 Turbidimetric Monitoring of Crosslinking Development

Reaction Time, Hours	% Solids	Average Particle Size, microns[a]	% Transmittance[b]
0	39.57	1.0	98.0
5	39.91	1.0	98.0
10	40.57	1.0	97.9
15	40.63	1.0	97.3
20	40.79	1.0	96.4
25	40.78	1.0	95.3
30	41.10	1.0	80.2
35	41.77	1.0	6.4
40	41.25	1.0	3.6

[a]Microscopic examination
[b]Spectrophotometer

The critical period of the reaction occurs while the swelling ratio is decreasing rapidly, and the solubility of the emulsion particles is decreasing as rapidly. The autoxidized emulsion with crosslinked particles was dissolved in a series of solvents to determine the most preferable media for measuring turbidity of the emulsion particles. Naturally, the best solvent would create the greatest solubility of the polymer due to maximum polymer-solvent interactions. In a good solvent, the particles would exhibit turbidity due only to significant crosslinking and not due to a lack of polymer-solvent interactions.

Acetone was found to be the best solvent for the emulsion sample. The polymer particles and aqueous phase dissolved easily and quickly in reagent grade acetone. Turbidity developed in the form of reduced percent transmittance in a spectrophotometer. The emulsion sample was dissolved directly in acetone as taken from the pressure reactor.

iranchembook.ir/edu

2.5.7. Dissolved Oxygen in Aqueous Phase

Table A.6 in the Appendix represents a tabular correlation of oxygen partial pressure in convenient and useful terms with oxygen concentration, grams per liter of water. Figure 2.5 represents a calculated graphical correlation curve between oxygen in water, grams per liter. The pressure regulator actually used in these experiments was calibrated in pounds per square inch, psig (pounds per square inch, gravity).

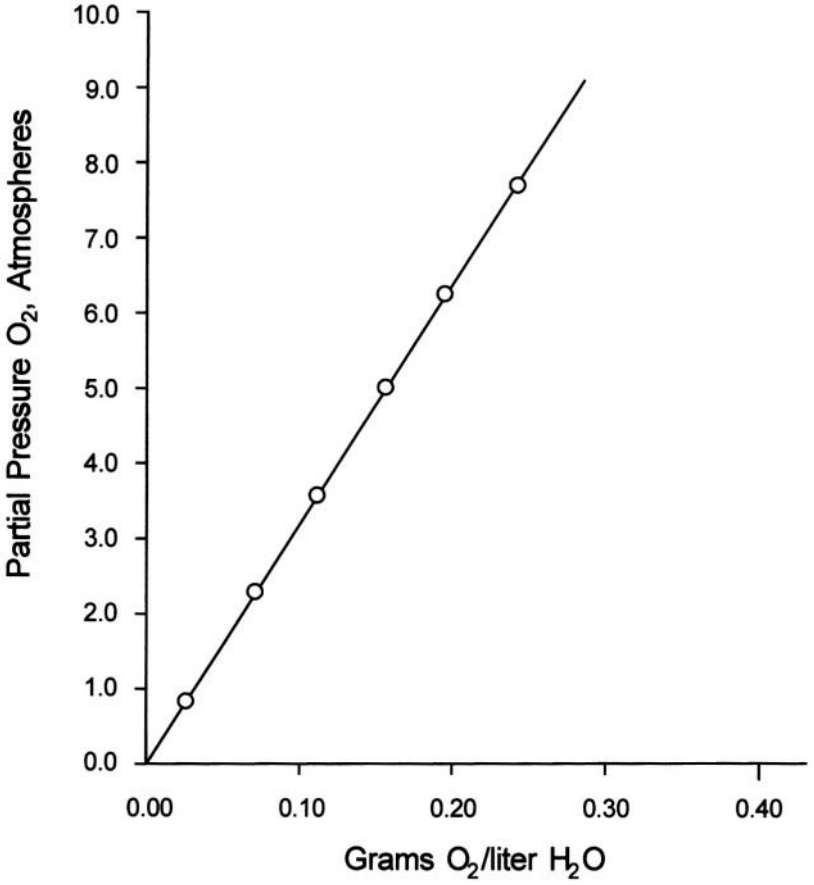

Figure 2.5. Particle pressure of oxygen vs. oxygen concentration at 55°C.

iranchembook.ir/edu

Table A.4 in the Appendix represents convenient and useful tabular correlation between psig and oxygen concentration, oxygen grams per liter and moles per liter of water. These correlations were useful for interpreting the influence of oxygen concentration of the autoxidation reaction.

iranchembook.ir/edu

Chapter 3

EMULSION AND KINETIC STUDIES OF AUTOXIDATIVE POLYMERIZATION

3.1. Emulsifier Studies

The emulsification of vegetable oils and vegetable oil derived alkyd polymers requires suitable emulsifying agents. The selection of an emulsifier for stabilization of vegetable oil material will not necessarily be the most favorable emulsifier for a vegetable oil derived alkyd. Emulsification experiments must be conducted after determining solubility parameters of the emulsifier in the aqueous and polymer phases such that the hydrophile-lipophile balance (HLB), which is related to the solubility parameter (McCutheon's Detergent, & Emulsifiers, 1977), may be obtained.

Properties of films prepared from emulsions with a standard drying agent will be examined in the following pages in order to demonstrate the influence of emulsifiers on film formation.

3.1.1. Emulsifier Sources and Chemical Structures

Emulsifiers were selected on the basis of the general characteristics that appeared to be necessary for emulsification of vegetable oils and vegetable oil derived alkyds. McCutcheon's Detergents and Emulsifiers (1999) was reviewed for this general purpose and the emulsifiers and manufacturers for selected compounds are specified in Table A.7 in the Appendix. Table A.7 in the appendix contains only nonionic and anionic emulsifiers. Cationic emulsifiers do not appear (from experimentation) to be as useful for emulsification of vegetable oils and derived alkyds.

The chemical structures of the emulsifiers from Table A.7 are described in Table 3.1. The chemical structures were obtained from the manufacturers and are presumed to be correct.

iranchembook.ir/edu

3.1.2. Emulsifiers and Emulsion Stability

An initial study was conducted to determine the emulsifying capability of the general types of emulsifiers contained in Table 3.1. The emulsions were prepared by pre-emulsifying alkyd IV, a medium soya/linseed product. The emulsifier was dissolved in distilled water and in concentration of 4.0 percent by weight of the dry alkyd. It was predetermined that 4.0 percent emulsifier was adequate for emulsification. The concentration of the emulsifier is important since emulsifier for stabilization must adequately surround each alkyd particle surface. The alkyd, in mineral spirits solution at 50.0 percent by weight was pre-emulsified with 48.0 percent distilled water. The emulsifier concentration by weight was 4.0 percent dry weight of alkyd. Table 3.2 represents preliminary screening emulsifier and emulsion studies. The accelerated stability test was employed to evaluate the performance of the emulsifiers.

The pH term in Table 3.2 represents the pH of the pure emulsifier. The hydrophile-lipophile balance (HLB) is indicative of the pure emulsifier only. It can be seen from inspection of Table 3.2 that the maximum stability for emulsifiers employed in the pure state was only about four days. It was observed that when Dupanol C (dodecyl sodium sulfate) was combined with a nonionic emulsifier that the average HLB value was greater than any of the nonionic emulsifiers. Therefore a combination of selected nonionic emulsifiers was studied for emulsion stability. The lower portion of Table 3.2 represents an emulsifier combination study and it can be seen that the stability of emulsions was improved significantly. A combination of 75.0% Igepal CO-430 and 25.0% Dupanol C dramatically increased the emulsion stability to fourteen days of heat accelerated stability.

3.1.3. Emulsifiers and Freeze-Thaw Stability

Freeze –thaw stability is representative of the ability of the emulsion to withstand repeated freezing and thawing cycles. Practically, the shipment of emulsions to cold areas of the nation could result in freezing of the emulsion. Therefore the emulsion must withstand freezing and thawing, preferably five cycles.

Table 3.3 represents the freeze-thaw stability of selected emulsifiers from Table 3.1 and demonstrates that Gafac RE-960 stabilized emulsions possess superior stability for freeze-thaw cycling.

iranchembook.ir/edu

Table 3.1
Emulsifiers and Structures

Oxyethylated straight chain alcohol CH_3-$(CH_2)_x$-CH_2-$(O$-CH_2-$CH_2)_y$-OH	Plurafac A-24
Oxyethylated straight chain alcohol CH_3-$(CH_2)_x$-CH_2-$(O$-CH_2-$CH_2)_y$-OH	Plurafac B-26
Oxyethylated straight chain alcohol CH_3-$(CH_2)_x$-CH_2-$(O$-CH_2-$CH_2)_y$-OH	Plurafac D-25
Oxyethylated straight chain alcohol CH_3-$(CH_2)_x$-CH_2-$(O$-CH_2-$CH_2)_y$-OH	Plurafac RA20
Oxyethylated straight chain alcohol CH_3-$(CH_2)_x$-CH_2-$(O$-CH_2-$CH_2)_y$-OH	Plurafac RA30

iranchembook.ir/edu

Table 3.1
Emulsifiers and Structures (cont.)

Oxyethylated straight chain alcohol $CH_3\text{-}(CH_2)_x\text{-}CH_2\text{-}(O\text{-}CH_2\text{-}CH_2)_y\text{-}OH$	Plurafac RA40
Condensation of propylene oxide with propylene glycol $HO\text{-}(CH(CH_3)\text{-}CH_2\text{-}O)_x\text{-}CH_2\text{-}CH(CH_3)\text{-}OH$	Pluronic L61
Dodecyl sodium sulfate, sodium lauryl sulfate $CH_3\text{-}(CH_2)_{11}\text{-}OSO_3\text{-}Na$	Dupanol C
Oxyethylated alkylphenol ester of phosphoric acid 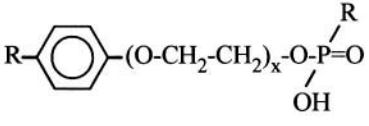	Gafac RA-960

iranchembook.ir/edu

Table 3.1
Emulsifiers and Structures (cont.)

Nonylphenoxypoly(ethyleneoxy) alcohol 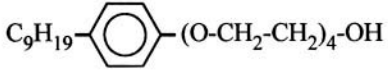	Igepal CO-430
Nonylphenoxypoly(ethyleneoxy) alcohol 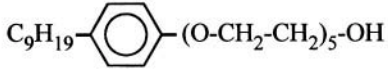	Igepal CO-520
Nonylphenoxypoly(ethyleneoxy) alcohol 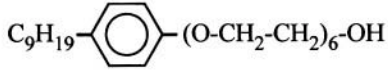	Igepal CO-530
Nonylphenoxypoly(ethyleneoxy) alcohol 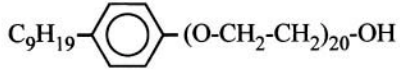	Igepal CO-850
Alkylaryl polyether alcohol 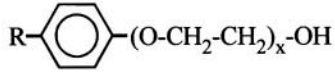	Triton X-207

R = alkyl group

iranchembook.ir/edu

Table 3.1
Emulsifiers and Structures (cont.)

Alkylaryl polyether alcohol 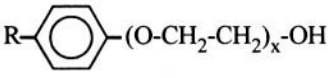 R = alkyl group	Triton X-363M
Dodecyl alcohol with ethylene oxide adduct	
CH_3-$(CH_2)_{10}$-CH_2-$(O$-CH_2-$CH_2)_{60\%}$-OH	T-DET AO26
CH_3-$(CH_2)_{10}$-CH_2-$(O$-CH_2-$CH_2)_{65\%}$-OH	T-DET TDA 65
Castor oil with 40 moles of ethylene oxide	T-DET C-40
Oxyethylated alkylphenol ester of phosphoric acid 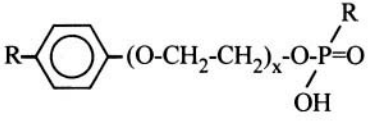 R = alkyl group	T-Mulz 565

iranchembook.ir/edu

Table 3.1
Emulsifiers and Structures (cont.)

Oxyethylated alkylphenol of phosphoric acid	T-Mulz 596

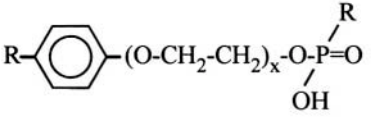

R = alkyl group

Oxyethylated alkylphenol of phosphoric acid	T-Mulz 776

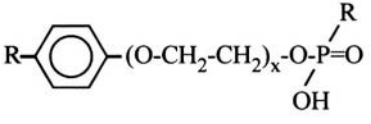

R = alkyl group

iranchembook.ir/edu

Table 3.2 Emulsifier Combinations and Emulsion Stabilities

Formula	Trade Name	Type	Emulsifier HLB [a]
1. Nonylphenoxypoly (ethyleneoxy) $_4$ ethanol	Igepal CO-430	Nonionic	8.8
1. Nonylphenoxypoly (ethyleneoxy) $_5$ ethanol	Igepal CO-520	Nonionic	10.0
2. Nonylphenoxypoly (ethyleneoxy) $_6$ ethanol	Igepal CO-530	Nonionic	10.8
3. Nonylphenoxypoly (thyleneoxy) $_{20}$ ethanol	Igepal CO-850	Nonionic	16.0
5. Modified oxyethylated straight chain alcohol	Plurafac D-25	Nonionic	11.0
6. Modified oxyethylated straight Chain alcohol	Plurafac B-26	Nonionic	15.0
7. Modified oxyethylated straight Chain alcohol	Plurafac RA-40	Nonionic	7
8. Modified oxyethylated straight Chain alcohol	Plurafac RA-30	Nonionic	9
9. Modified oxyethylated straight Chain alcohol	Plurafac RA-20	Nonionic	10
10. Alkylaryl polyether alcohol (plus a nonionic solubilizer)	Triton X-207	Nonionic	10.7
11. Alkylaryl polyether ethanol	Triton x-363M	Nonionic	
12. Dodecyl Sodium Sulfate	Dupanol C	Anionic	40
50% (1) + 50% (12)			
50%(2) + 50% (12)			
50%(3) + 50%(12)			
50%(4) + 50%(12)			

iranchembook.ir/edu

Formula	Trade Name	Type	Emulsifier HLB [a]
50%(5) + 50%(12)			
50%(6) + 50%(12)			
50%(7) + 50%(12)			
50%(8) + 50%(12)			
50%(9) + 50%(12)			
75%(1) + 25%(12)			
75%(2) + 25%(12)			
75%(3) + 25%(12)			
75%(4) + 25%(12)			
75%(5) + 25%(12)			
75%(6) + 25%(12)			
75%(7) + 25%(12)			
75%(8) + 25%(12)			
75%(9) + 25%(12)			
75%(10) + 25%(12)			
75%(11) + 25%(12)			
75%(12) + 25%(12)			

iranchembook.ir/edu

Table 3.2 Emulsifier Combinations and Emulsion Stabilities (Continued)

Formula	Emulsifier pH	Satability, Days, 62.8°C
(1) Nonylphenoxypoly (ethyleneoxy) $_4$ ethanol	6.8	4
(2) Nonylphenoxypoly (ethyleneoxy) $_5$ ethanol	6.8	3
(3) Nonylphenoxypoly (ethyleneoxy) $_6$ ethanol	6.8	2
(4) Nonylphenoxypoly (thyleneoxy) $_{20}$ ethanol	6.8	3
(5) Modified oxyethylated straight chain alcohol	7.3	4
(5) Modified oxyethylated straight Chain alcohol	7.3	4
(7) Modified oxyethylated straight Chain alcohol	7.3	4
(8) Modified oxyethylated straight Chain alcohol	7.3	4
(9) Modified oxyethylated straight Chain alcohol	7.3	4
(10) Alkylaryl polyether alcohol (plus a nonionic solubilizer)	7.2	3
(11) Alkylaryl polyether ethanol	7.2	4
(12) Dodecyl Sodium Sulfate	11.0	2
50% (1) + 50% (12)		12
50%(2) + 50% (12)		4
50%(3) + 50%(12)		5
50%(4) + 50%(12)		5

iranchembook.ir/edu

Formula	Emulsifier pH	Satability, Days, 62.8°C
50%(5) + 50%(12)		6
50%(6) + 50%(12)		6
50%(7) + 50%(12)		6
50%(8) + 50%(12)		7
50%(9) + 50%(12)		7
75%(1) + 25%(12)		14
75%(2) + 25%(12)		5
75%(3) + 25%(12)		4
75%(4) + 25%(12)		3
75%(5) + 25%(12)		6
75%(6) + 25%(12)		6
75%(7) + 25%(12)		6
75%(8) + 25%(12)		7
75%(9) + 25%(12)		8

[a]Hydrophile-lipophile balance

Note: Emulsions were prepared by a standard 50.0% medium soya/linseed alkyd (weight/weight) in 50% mineral spirits, 48.0% water and 4.0% emulsifier weight/weight of standard alkyd plus mineral spirits.

iranchembook.ir/edu

Table 3.3 Freeze-Thaw Stability and Emulsifiers

Emulsifier[a]		Freeze-Thaw Cycles (-5°C to 20°C)
Plurafac	RA20	1
T-Det	A026	1
T-Mulz	596	1
Igepal	CO - 430	<1
	CO - 520	<1
	CO - 850	<1
Pluronic	L44	<1
Pluronic	L61	<1
Gafac	RE - 960	7
T-Det	565	6
Dodecyl Sodium Sulfate		<1

[a]4.0% weight/weight of alkyd basis

Mechanical stability: All samples unaffected by 5 minutes of agitation, Waring blender (laboratory model)

3.1.4. Emulsifiers and Film Characterization

In subsequent emulsifier selection study, films were formed on glass panels from emulsions that contained 0.04% cobalt naphthenate. Cobalt naphthenate is a preferred catalyst for curing an alkyd in mineral spirits. The catalyst was added to the aqueous phase of the emulsion prior to film formation. The tensile strength and percent elongation properties of the free film were determined. Table 3.4 presents the emulsifiers, film tensile strength, elongation and stability of the emulsion when no catalyst was employed. Referring to the hydrophile-lipophile balance (HLB) of the emulsifiers in the pure state, together with their pH in water, it can be seen in Table 3.4 that Gafac RE-960, T-Det A026 and T-Mulz 596 engender superior tensile strength properties to films of alkyd III compared to the remaining emulsifiers. Gafac RE-960 and T-Mulz 596b are oxyethylated

iranchembook.ir/edu

alkylphenol esters of phosphoric acid. T-Det A026 is dodecyl alcohol with sixty percent by weight ethylene oxide adduct. The Igepal class of emulsifiers is nonylphenoxypoly (ethyleneoxy) alcohols. Apparently, the chemical structure of emulsifiers plays a significant role in the film drying process of autoxidation. Also, it is observed from Table 3.4 that emulsifiers such as T-Mulz 565 may enhance emulsion stability but give poor film formation.

Table 3.4 Emulsifiers and Film Characterization

Emulsifier,[a] Trade Name	Tensile Strength[b] Kg/cm^2	% Elonga-tion	Stability Days, 62.8°C	Emulsifier HLB	Emulsifier Ph	Emulsifier Type
Gafac RE-960	12.72	73	14	----	2.0	anionic
Igepal CO-430	3.11	80	7	8.8	----	non-ionic
Igepal CO-520	2.02	70	8	10	----	non-ionic
Igepal CO-850	3.52	90	8	16	----	non-ionic
Plurafac A-24	-----	-------	4	----	----	non-ionic
Plurafac B26	5.05	120	6	15	----	non-ionic
Plurafac D-25	-----	-------	4	11	----	non-ionic
Plurafac RA20	3.79	133	6	----	----	non-ionic
Pluronic L61	6.73	140	7	3	----	non-ionic
Dupanol C	3.61	82	7	18	11.0	anionic
T-Det A026	9.86	138	7	13.5	6.0	non-ionic
T-Det C-	----	----	6	----	----	non-ionic
T-Det TDA-65	----	----	4	----	5.0	non-ionic
T-Mulz 565	----	----	14	----	2-3	anionic
T-Mulz 596	9.74	133	11	----	2-3	anionic
T-Mulz 776	----	----	10	----	----	anionic

[a] Emulsion: Alkyd III emulsion with 0.04% cobalt naphthenate (weight/weight alkyd).

[b] Films dried seven (7) days at ambient conditions.

[c] Concentration of emulsifier in each emulsion was 4.0% weight/weight alkyd.

iranchembook.ir/edu

3.2. Phase Ratio and Co-Solvent Study

The optimization of the polymer phase is important because a maximum amount of polymer phase is desired within the emulsion. The polymer phase is the film forming component within the emulsion and the greater the polymer phase fraction, the less total emulsion is required to form an identical thickness film. The economic factor would dictate that the percent solids or polymer fraction be as great as possible in order to reduce freight costs of shipping water.

Co-solvent utilization within the polymer phase has been a stabilizing factor (Becher, 1965). Thus, the optimization of co-solvent type and amount needed with the polymer phase of the emulsion for optimal stability and lowest pollution was sought. The selection of a co-solvent for the alkyd polymers was studied with respect to stabilizing effects.

3.2.1. Solvent Alkyd Emulsions

Emulsions were prepared by homogenizing medium soya alkyd without any co-solvent present in an attempt to avoid hydrocarbons or other petroleum derived material in the preparation of the emulsion. Table 3.5 lists the emulsifiers and their concentrations expressed in emulsifier weight per weight of alkyd. The emulsifier combination of dodecyl sodium sulfate and T-Det A026 was unsuccessful for stabilizing the homogenized particles for even one day. The Gafac RE-960 emulsifier successfully stabilized the emulsion for a period of more than four days, but the emulsion sample did not autoxidize when reacted with oxygen at one atmosphere of pressure. This emulsifier is an oxyethylated alkyl phenol ester of phosphoric acid and is suspected of retarding autoxidation of scavenging oxygen effectively as it diffuses into the emulsified particles.

Table 3.5 Non-Solvent Alkyd Study for Optimum Stability of Emulsion

Emulsion System [a]	Emulsifier, w/w alkyd	Stability, days 62.8°C (145°F)
Alkyd II	T-Det A026, 2% w/w	
Alkyd II	Dodecyl Sodium Sulfate, 2% w/w	<1, Settling
	Gafac RE-960, 4%	<5, Does not react

[a] Pre-emulsion prepared with 2.0 hours of ultrasonic vibration at 300 watts; homogenization of pre-emulsion was conducted at 3500 psi.

iranchembook.ir/edu

3.2.2. Co-Solvent Containing Emulsions

Based upon the results when non co-solvent was added, it was obvious that a co-solvent compatible with the medium soya alkyd would be needed. Xylene, ethylene glycol monobutyl ether (butyl cellosolve) and mineral spirits were selected as co-solvent candidates for the medium soya alkyd. The co-solvent and amounts present in each alkyd solution are specified in Table 3.6. The emulsions were prepared as reported in Chapter II utilizing T-Det A026 and dodecyl sodium sulfate in concentrations of 4.0 percent, weight per weight of alkyd. The non-volatile (N.V.) represents alkyd weight percent in the solvent solution prior to emulsification. Table 3.7 represents the co-solvent combinations with subsequent accelerated shelf stability. These data clearly show that xylene co-solvent is the only candidate worthy of further study. Increasing co-solvent concentration did increase the emulsion stability for mineral spirits, but a co-solvent concentration of fifty percent was necessary. The stability of the emulsion with increasing alkyd and xylene solution concentration is represented in Table 3.8. Such a high co-solvent concentration is undesirable due to pollution and percent non-volatile considerations.

Table 3.6 Co-Solvent Study for Optimum Stability of Emulsion

Alkyd	Solvent	Alkyd % N.V. [a] In Organic Medium Prior to Emulsification	Emulsion Stability, days, 62.8°C
III	Xylene	74.7	13
III	Butyl Cellosolve	72.8	0
III	Mineral Spirits	74.0	0
III	Mineral Spirits	88.8	0
III	None	100.0	0

[a] N.V. is equivalent to non-volatile matter or dry alkyd, weight basis.

Note: Emulsion components, weight per 1000 grams emulsion

Alkyd + Co-solvent	500.0 grams	T-Det A026	10.0 grams
Water, distilled	490.0 grams	dodecyl sodium sulfate	10.0 grams

iranchembook.ir/edu

Table 3.7 Optimum Co-Solvent to Alkyd Ratio for Optimum Emulsion[a] Stability

% Xylene	% III	Density, g/cm^3	Stability, days
5	95	1.08	<1
10	90	1.07	<1
15	85	1.05	<1
20	80	1.04	5
25	75	1.03	6
30	70	1.01	7
*30.2	*69.8	*1.00	8
40	60	0.96	7
50	50	0.95	6

[a] Emulsion formula: emulsifier, 2.0%; distilled water, 48.0%; medium soya alkyd plus xylene, 50%; on a weight/weight basis.

Note: This emulsion was unreacted.

Table 3.8 Optimum Phase Ratio of Alkyd-Solvent to Water

III (w/w basis)	Water % (w/w)	Emulsifier % (w/w alkyd)	Stability[a] days 62.8°C
30	66	4.0	8
40	56	4.0	8
50	48	4.0	8
60	36	4.0	5
70	26	4.0	4

[a] Stability Study: 62.8°C constant in constant temperature oven.
Note: Emulsifier concentration based on alkyd I in xylene.

iranchembook.ir/edu

In summary, preparation of emulsions of one hundred percent by weight medium soya alkyd does not produce acceptable emulsion stability and utilization of xylene as a co-solvent enhances the stability. Alkyd III adjusted to the density of the aqueous phase does enhance the stability. A phase ration of fifty percent alkyd/xylene solution to forty-eight percent distilled water containing two percent emulsifier is the maximum achievable weight acceptable. The homogenization of the co-solvent emulsions must be temperature controlled in order to prevent co-solvent loss. Throughout the rest of this paper, the emulsion will be cooled to utilize higher rates of homogenization, above three thousand pounds per square inch of shearing force.

3.3. Studies on the Autoxidative Crosslinking of Emulsified Soya Oil

A study of autoxidative crosslinking of soya oil was initiated with the expectation that films could be formed from an emulsion of the processed soya oil. The primary advantage of emulsifying pure soya oil is the elimination of pre-emulsification, processing and co-solvent requirements, because the soya oil is a vegetable product and requires less energy to industrially produce than the more complex materials such as alkyd resins synthesized by co-esterification of soya oil fatty acids with anhydrides and alcohols. Obviously, elimination of additional processing steps and raw materials would improve the economics of emulsion preparation.

The emulsification of soya oil was accomplished by reaction with air at atmospheric pressure.

3.3.1. Autoxidation Reaction of Emulsified Soya Oil

The data in Table 3.9 describe a study for selecting an agitation rate suitable for emulsion processing without foam and with acceptable emulsion stability. It was found that a rate of sixty revolutions per minute gave the best results. Table 3.10 presents a study for determining the optimal temperature for autoxidation while retaining acceptable emulsion stability. Fifty-five degrees Celsius (55°C) was selected as the reaction temperature as adjudged by an accelerated shelf stability test. Table 3.11 represents a study for optimizing the flow rate of air through the emulsion. The maximum flow rate of air before undesirable levels of foaming appeared was 708 cubic centimeters of air per minute. The process conditions selected for autoxidation of the soya oil emulsion are summarized in Table 3.12.

iranchembook.ir/edu

Table 3.9 Effect of Agitation Rate on Emulsion Stability with AR Soya Oil

Agitation Rate, Rpm	Effect on Emulsion Stability days
60	16
180	10
540	1 (foam)
1620	0 (foam)

Note: Emulsion stability study taken during autoxidation reaction and at 55°C, 6.25 cm paddle stirrer in 1.0-liter resin kettle.

Table 3.10 Effect of Reaction Temperature on Emulsion Properties with Alkali Refined Soya Oil

Temperature, °C	Effect on Emulsion Stability [a]
54.0	16 days
65.0	15 days
75.0	8 days
80.0	2 days
95.0	0 days

[a] Emulsion stability measured after reaction operation by Shelf Stability ASTM Method, 62.8°C.

iranchembook.ir/edu

Table 3.11 Effect of Air Flow Rate on Emulsion Stability with AR Soya Oil

Air Flow Rate, cm^3/min.	Effect on Emulsion Stability, days
236.0	16
472.0	16
708.0	16
944.0 (foam)	14
1180.0 (foam)	8

Note: Emulsion stability study conducted at 55.0°C, 60 rpm and during autoxidation operation. Samples were transferred to container for Shelf Stability ASTM study.

Table 3.12 Reaction Conditions for Processing AR Soya Oil

Temperature	55.0°C
Air Flow Rate [a]	708 cm^3/min.
Agitation (6.25 cm paddle stirrer)	60 rpm [b]
Vessel (resin kettle)	1.0 liter

[a] Airflow source is from dry cylinder compressed air, pre-humidified before entering vessel and aspirated through emulsion.

Utilizing the autoxidation reaction conditions contained in Table 3.12, an emulsion prepared by the formulation in Table 1.10 was processed in a one-liter resin vessel with dry air from a compressed air cylinder. The reaction continued for seven days and the intrinsic viscosity was determined for the alkali refined (AR) soya at various intervals of time. The dry time was determined experimentally. The dry time was long as can be seen upon

iranchembook.ir/edu

inspection of Table 3.13, and in fact, the film was not totally dry after one week at ambient conditions. Table 3.14 represents the change of intrinsic viscosity with respect to time.

3.3.2. Catalysis of Autoxidation Reaction of Soya Oil

Due to the very slow autoxidation time of the AR soya oil emulsion, it seemed appropriate to employ a catalyst to enhance the rate of reaction and dry time. Table 3.14 represents catalysts that have been successful for heat and air bodying of vegetable oils (Martens, 1974). A hydroperoxide catalyst was chosen as a primary candidate for autoxidation catalysis and mixed into the oil phase of the emulsion prior to processing. It can be seen from Table 3.14 that none of the catalysts were effective relative to uncatalyzed autoxidation.

Table 3.13 Effect of Autoxidation Time on AR Soya Emulsion

Autoxidation Time, days	Intrinsic Viscosity	Dry Time, Tack-Free hours
0	0.0096	--
1	--------	--
2	--------	--
3	--------	--
4	--------	--
5	0.038	96
7	0.046	48

Note: This study was conducted under the conditions of 708 cm^3/min. air flow, 55.0°C and 60 rpm in 1.0 liter resin kettle.

iranchembook.ir/edu

Table 3.14 Intrinsic Viscosity Changes Resulting from Catalyzed Autoxidation of Soya Oil

Catalyst (% by wt/wt oil)	Reaction Conditions (Days/°C)	Intrinsic Viscosity
None	7/55	0.0461
Methyl Ethyl Ketone	7/55	0.0466
Hydroperoxide	7/55	0.0459
2-Methyl Anthraquinone	7/55	0.0450
AR [a] Soya Oil	None	0.0096

Note: Catalysts were in concentration of 0.2% weight/weight oil

[a] AR' = Alkali refined soya oil

In another attempt to utilize catalysis to increase the rate of reaction and intrinsic viscosity build up, the emulsion was exposed to ultra-violet (UV) light (4 bulbs of 100 watts intensity each) during autoxidation. The ultraviolet light theoretically should produce free radicals for autoxidizing soya oil molecules and thus increase the intrinsic viscosity, which would be reflective of increased viscosity average molecular weight and crosslinking between soya oil molecules. Table 3.15 represents the results of ultra violet radiation catalysis of the soya oil emulsion while under the constant conditions contained in Table 3.12. The dry time is not significantly reduced as the films of the UV catalyzed materials require as long to dry, as do uncatalized autoxidation products. Increasing the reaction temperature was attempted in an effort to increase the rate of autoxidation during processing, but temperatures below 80°C degraded the emulsion. Catalysis by 2-methylanthraquinone (0.1% weight/weight soya oil) decreased the time

iranchembook.ir/edu

significantly, but the film was very soft and possessed a very low tensile strength. The results from Table 3.14 reveal that autoxidation of alkali refined soya oil does increase the intrinsic viscosity which increases the viscosity-average molecular weight.

Table 3.15 Ultraviolet Light Catalysis of Soya Oil Autoxidation and Drying

Emulsion	Catalyst	Reaction Time	Drying Time (7 mil film)
2% sodium lauryl sulfate 48% water (distilled) 50% soya oil (AR') [a] (weight/weight)	None	7 days	120 hours (dry) 48 hours (tacky)
2% sodium lauryl sulfate 48% water (distilled) 50% soya oil (AR') [a] (weight/weight)	4 watt UV light	7 days	120 hours (dry) 48 hours (tacky)
2% sodium lauryl sulfate 48% water (distilled) 50% soya oil (AR') [a] (weight/weight)	UV light, 100 watt	7 days	160 hours (tacky)
2% sodium lauryl sulfate 48% water (distilled) 50% soya oil (AR') [a] (weight/weight)	Heat, 80°C	6 days Emulsion broke	160 hours (tacky)

[a] AR = Alkali refined soya

In summary, the air autoxidation of emulsified alkali refined (AR) soya oil increases intrinsic viscosity, but not to the degree that is necessary to form a film processing acceptable tensile strength and a drying time of less than seven days. Films that were formed from these autoxidized emulsions were rubbery and of insufficient quality to test for tensile strength and percent elongation.

iranchembook.ir/edu

3.4. Studies of the Autoxidative Crosslinking of Emulsified Alkyd Particles

Utilizing the results of autoxidative crosslinking of soya oil as a guideline for processing, the autoxidative crosslinking of emulsified alkyd polymer was initiated. The progress of crosslinking was followed and the degree of crosslinking was compared to that accomplished using soya oil.

3.4.1. Autoxidation Reaction of Emulsified Alkyd Resins

Alkyd III, after emulsification, was used to conduct an airflow rate, temperature, and agitation rate study similar to those described for AR soya oil. The results of these studies are presented in Tables 3.16, 3.17, and 3.18. Airflow rate was found to be optimal at 708.0 cubic centimeters per minute as is demonstrated by the data in Table 3.16. This flow of dry compressed cylinder air was the maximum flow rate attainable without producing foam within the emulsion. A processing temperature of 55.0°C for 48 hours produced the best overall emulsion stability and sixty revolutions per minute produced the best emulsion stability for processing the emulsion at atmospheric pressure.

Table 3.16 Effect of Air Flow Rate on Emulsion Stability with Alkyd III

Air Flow Rate cm^3/min.	Effect on Emulsion Stability [a] In Reaction Vessel
236.0	14 Days
412.0	14 Days
708.0	14 Days
944.0	13 Days (foam)
1180.0	9 Days (foam)

[a] Emulsion stability study conducted at 55.0°C, 60 rpm and during reaction operation. Samples were transferred to oven container for Shelf Stability ASTM Method (145°F or 62.8°C) Study.

iranchembook.ir/edu

Table 3.17 Effect of Reaction Temperature on Emulsion Stability with Alkyd III

Temperature, °C	Effect on Emulsion Stability,[a] 62.8°C
55.0	14
65.0	13
75.0	7
85.0	0
95.0	0

[a] Emulsion stability measured after autoxidation (48 hours) reaction by Shelf Stability ASTM Method.

Table 3.18 Effect of Agitation Rate on Emulsion Stability with Alkyd III

Agitation Rate, Rpmin Reaction Vessel	Effect on Emulsion Stability[a]
60	14 days
180	8 days (foam)
540	1 days (foam)
1620	0 days (foam)

[a] Emulsion stability study taken during blowing operation and at 55°C/. 6.25 cm paddle stirrer in 1.0-liter resin kettle. Samples were transferred to container for Shelf Stability ASTM study (145°F).

Table 3.19 summarizes the results from the processing studies mentioned. The conditions listed will be utilized in all following autoxidation reaction of alkyd emulsions at atmospheric pressure.

iranchembook.ir/edu

Table 3.19 Reaction Conditions for Processing Alkyd III

Temperature	55.0°C
Air Flow Rate	708 cm^3/min.
Agitation	60 rpm
Vessel	1.0 liter

Air autoxidation of the alkyd emulsion produced significant improvements relative to air-autoxidized soya oil emulsions. Intrinsic viscosity was increased beyond the highest intrinsic viscosity obtained with air autoxidation of the soya oil emulsions and the drying time was dramatically reduced. The improved properties were expected because alkyd III possessed a higher viscosity-average molecular weight before autoxidation and higher functionality available for reaction.

3.4.2. Non-catalyzed Autoxidation Reaction

This emulsion was air autoxidized under a variety of conditions (Table 3.22). Initially, the intrinsic viscosity of the alkyd polymer phase of the emulsion was determined in order to detect viscosity-average molecular weight increases during autoxidative crosslinking. Table 3.20 represents the autoxidation reaction time as related to intrinsic viscosity and dry time of the films formed from the emulsion. It can be seen from these data that intrinsic viscosity increases to a significant degree and the drying time of films formed from the emulsion decreases rapidly with increasing autoxidation.

Table 3.20 Effect of Autoxidation Time on Alkyd III Emulsion

Autoxidation Time, hours	Intrinsic Viscosity	Dry Time, Tack-Free hours
0	0.025	-
38	0.027	3.0
52	0.030	2.5
70	0.058	1.0

Note: Airflow rate of 708.0 cm^3/sec.

iranchembook.ir/edu

3.4.3. Benzoyl Peroxide Catalysis in the Alkyd Phase

In subsequent air autoxidation experiments, benzoyl peroxide was dissolved in alkyd III in concentrations of 0.5 and 1.0 percent of weight of polymer and emulsified. The emulsions were autoxidized under the standard conditions and samples were taken at hour intervals during the blowing process. As indicated in Figure 3.1, the results of benzoyl peroxide catalysis with regard to intrinsic viscosity and reaction time, is that as the benzoyl peroxide concentration increases, the intrinsic viscosity increases more rapidly. Benzoyl peroxide was chosen as the catalyst for this experiment because of its "temperature of decomposition value" and half-life to produce radicals being near the temperature of represents processing. The improvement in rate of reaction definitely indicates that benzoyl peroxide does catalyze the reaction.

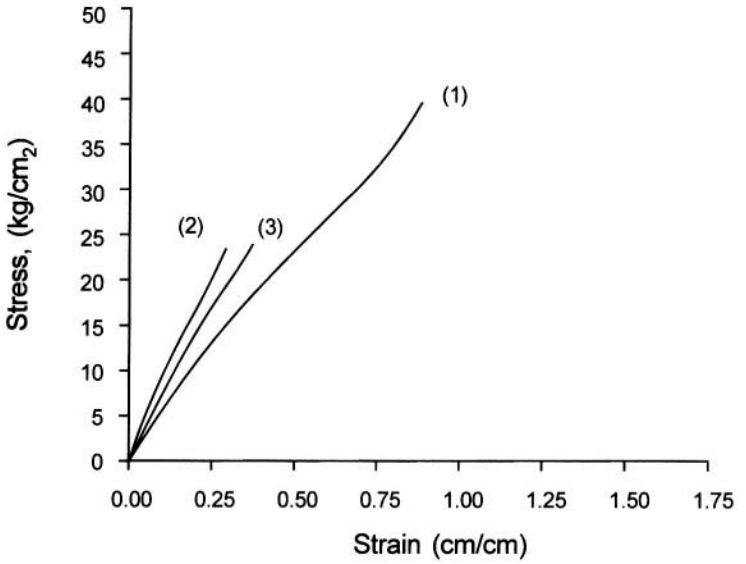

(1) Alkyd IV with 0.04% cobalt naphthenate and no autoxidation
(2) Alkyd IV emulsion (autoxidized 39 hours) with 0.4% Cobalt naphthenate added after autoxidation operation
(3) Alkyd IV emulsion (autoxidized 39 hours)

Note: Films were oven dried for 5.0 hours at 60°C.

Figure 3.1. Stress-strain curve for alkyd film and alkyd emulsion films.

iranchembook.ir/edu

3.4.4. Cobalt Naphthenate Catalysis in Aqueous Phase

Cobalt naphthenate, a commonly used autoxidation catalyst, was utilized to catalyze, was utilized to catalyze the autoxidation of an alkyd IV emulsion. Figure 3.2 represents stress-strain relationships for catalyzed and uncatalyzed alkyd IV emulsions. The unreacted emulsion, catalyzed with 0.04% by weight cobalt metal, possessed a greater tensile strength than autoxidized emulsions, catalyzed and non-catalyzed, although the air autoxidation reaction was expected to increase the tensile strength of the films to a value comparable to that of the catalyzed alkyd/mineral spirits system.

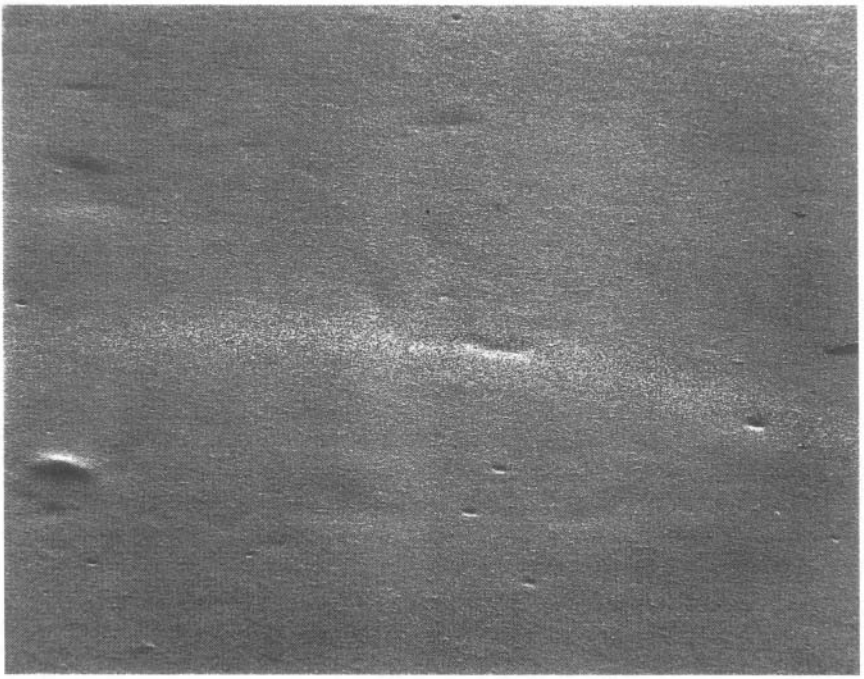

Figure 3.2. Scanning electron micrograph of non-autoxidized alkyd IV emulsion, with 0.04% cobalt metal post-added to emulsion, 50x magnification.

The films of the cobalt-catalyzed systems were examined with the scanning electron microscope. Figure 3.3 shows an SEM photomicrograph of the alkyd IV emulsion system catalyzed with cobalt naphtehnate after 168 hours dry time. Sparsely distributed air inclusions can be seen within this film. However, upon inspection of Figure 3.4, air autoxidized and

iranchembook.ir/edu

uncatalyzed, a large degree of air entrapment can be observed. The large amount of void space within this film contributes to the decrease in tensile strength compared to the film formed from the non-autoxidized emulsion. Figure 3.5 represents the air autoxidized, but non-catalyzed, emulsion film, which contains voids of air inclusions, but less than Figure 3.4. The tensile strength of the film in Figure 3.4 is also greater than the film illustrated in Figure 3.5. The only difference between the two films is that the last film was non-catalyzed. It is obvious from inspection of the micrographs why the tensile strengths of the films differ considering the significant voids contained within the films. The films discussed were oven-cured for 5.0 hours at 80°C. Oven drying was a fast method of curing the films and observing results, but air-drying at 20.0°C allows more air inclusions to escape from the film and form a more consistent film. In addition, the tensile strength of an oven-dried film is significantly greater than that of an air-dried film as will be demonstrated by following experiments. Therefore, ambient air-dried films are tensile strength tested in all further experiments herein to obtain accurate results.

Figure 3.3. Scanning electron micrograph of air-autoxidized alkyd IV emulsion, non-catalyzed, 50x magnification.

iranchembook.ir/edu

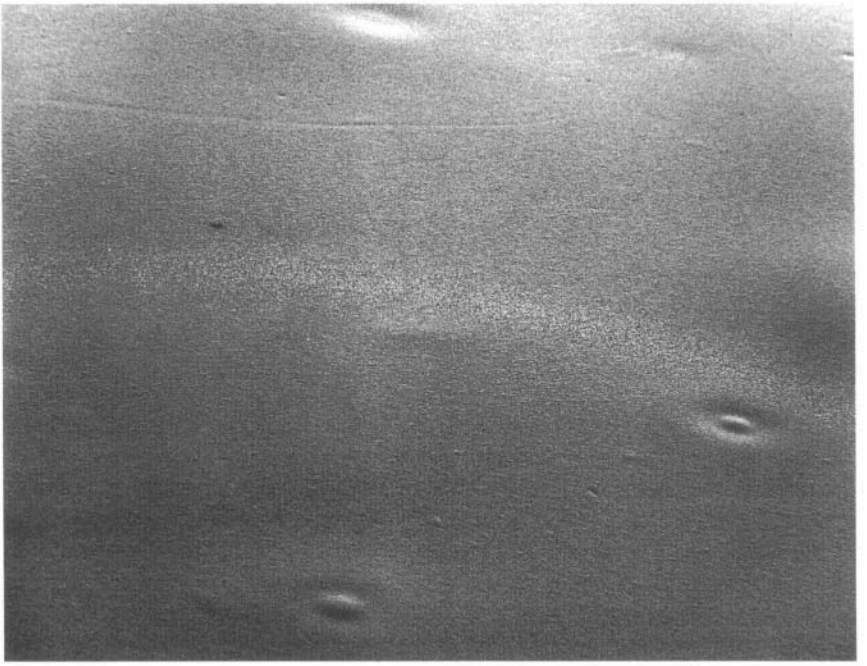

Figure 3.4. Scanning electron micrograph of air-autoxidized alkyd IV emulsion with 0.04% cobalt metal added to emulsion after autoxidation, 50x magnification.

iranchembook.ir/edu

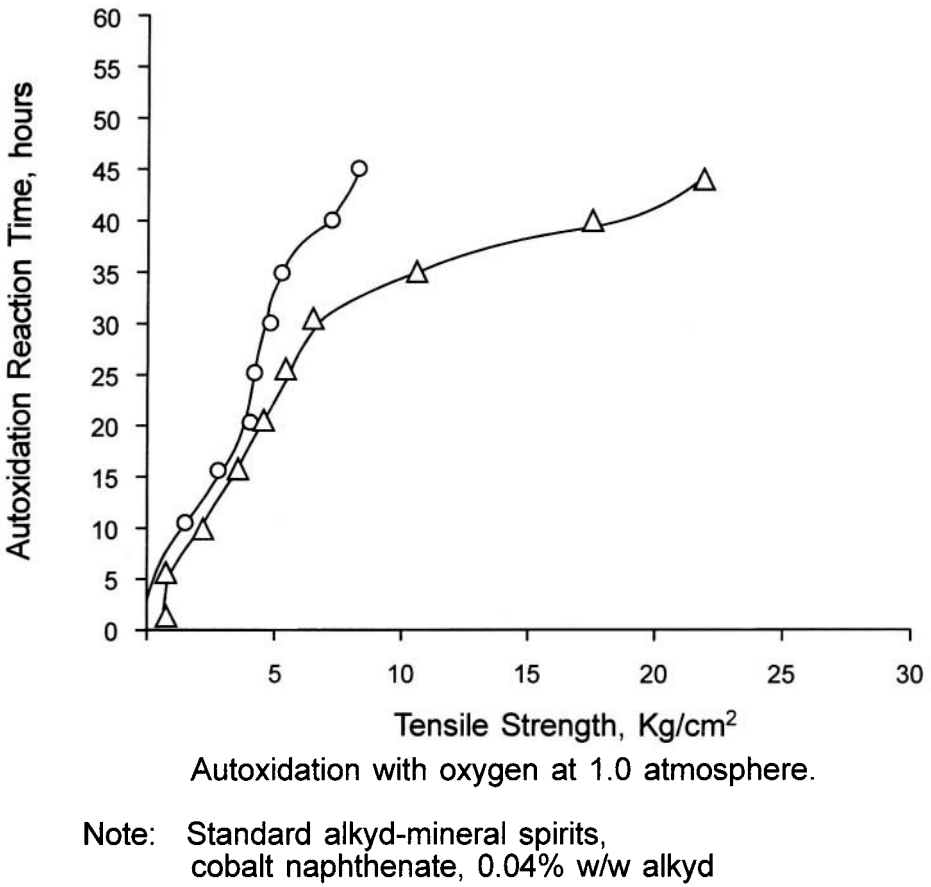

Figure 3.5. Tensile strength vs. reaction time for cobalt catalyzed and noncatalyzed films from alkyd IV emulsion, O – catalyzed and Δ – noncatalyzed.

The utilization of pure oxygen instead of air to process alkyd III eliminated the large voidage volumes within the dried films and, therefore, oxygen was employed to autoxidize the emulsion. An additional advantage of using oxygen that was expected was to enhance the rate of the reaction due to a greater solubility in the aqueous phase of the emulsion compared to air solubility.

The alkyd IV emulsion was autoxidized in two experiments. The first experiment consisted of 0.04% by weight of cobalt naphthenate in the aqueous phase of the emulsion and the second experiment consisted of autoxidation of the alkyd III with no catalysis. Table 3.21 represents the reaction time and subsequent dry times found for the catalyzed and non-

iranchembook.ir/edu

catalyzed systems. The solvent-alkyd system without emulsification is also represented in Table 3.21. The dry time of the catalyzed solvent-alkyd system was two hours, as expected, but the same alkyd, emulsified and catalyzed, did not dry for more than five hours. The emulsifier was suspected of plasticizing the film and preventing proper drying. The same emulsion was prepared again without emulsifier and the dry time was comparable to the solvent-alkyd system. The emulsifier and film property study will be further described herein, but it was found that Igepal CO-430, nonylphenoxypoly $(ethyleneoxy)_4$ alcohol, produced poor tensile strength even when catalyzed with 0.04% cobalt naphthenate (Refer to Table 3.1). This emulsifier was responsible for the slow rate of drying even when catalyzed. Table 3.22 represents the tensile strength and percent elongation for the samples from Table 3.21. The solvent-alkyd system produced the expected $21.79\ kg/cm^2$. The tensile strength increased with autoxidation time, both catalyzed and non-catalyzed. The percent elongation increased with tensile strength. Tensile strength and percent elongation increased with cobalt naphthenate added to the emulsion after the autoxidation reaction.

Table 3.23 represents reaction time with dried film hardness as determined by the Sward Hardness Test. On inspection of Table 3.23, it can be seen that hardness increases with reaction time. The hardness from this table corresponds to the same reaction time for the previously discussed film properties. It can be seen by reviewing the emulsifier studies contained in Table 3.1 that Igepal CO-430 contains a phenolic ring, which is often capable of scavenging free radicals. This could retard the autoxidation of the drying film and appear to be doing so here.

In addition to the measurements discussed, the percent solids value of the emulsion, with reaction time, was determined for each sample. Table 3.24 represents the percentage of dry alkyd by weight in each emulsion sample with respect to reaction time. The percent of alkyd increases due to loss of water and/or co-solvent, mineral spirits, during the autoxidation process.

iranchembook.ir/edu

Table 3.21 Effect of Catalysis on Film Dry Time

Reaction Time, hours	Dry Time, hours	
	Cobalt [a]	No Cobalt
Solvent-Alkyd [b] Standard	2.0	------
0	-----	------
5	5.0	------
10	4.5	------
15	4.0	8.0
20	3.0	3.0
25	2.5	3.0
30	2.0	2.0
35	1.0	2.0
40	0.8	1.0
45	0.8	1.0

[a] Cobalt naphthenate, 0.04% w/w alkyd, dry basis.

[b] Alkyd IV in mineral spirits (50/50% weight/weight)

iranchembook.ir/edu

Table 3.22 Effect of Oxygen and Cobalt Naphthenate on Alkyd IV Emulsion

Oxygen Reaction Time, hours	Tensile Strength, Kg/cm^2		% Elongation	
	Cobalt [a]	No-Cobalt	Cobalt	No-Cobalt
Solvent-Alkyd System [b]	21.79	0.00	130.0	0.0
0	.40	0.00	12.5	0.0
5	.71	0.00	40.0	0.0
10	1.62	1.48	60.0	62.5
15	3.23	3.01	71.2	81.2
20	4.58	4.61	67.5	81.2
25	5.29	4.75	65.0	51.2
30	6.22	4.88	65.0	62.5
35	10.51	5.48	101.2	98.7
40	17.11	7.20	105.0	102.5
45	21.58	7.98	161.2	109.3

a Cobalt naphthenate, 0.04% w/w Alkyd, alkyd IV in mineral spirits, 50% alkyd w/w

b Dry time: All films were dried for 7.0 days prior to testing at 20°C. Catalyst was added after reaction to emulsion.

iranchembook.ir/edu

Table 3.23 Reaction Time and Film Hardness

Reaction Time, hours	Sward hardness Test	
	Cobalt[a]	No-Cobalt
Solvent-alkyd[b]	10	---------
0	0	0
5	0	0
10	2	2
15	2	2
20	4	4
25	4	4
30	4	4
35	4	4
40	6	6
45	6	6

[a] Cobalt naphthenate, 0.04% w/w alkyd IV

[b] Alkyd IV in mineral spirits (50/50%, w/w)

iranchembook.ir/edu

Table 3.24 Reaction Time and Percent Solids

Hours	Reaction Time % Solids
0	26.311
5	27.011
10	27.424
15	27.013
20	27.538
25	27.852
30	28.424
35	28.619
40	29.311
45	30.766

Note: Emulsion comprised of alkyd IV

3.4.5. Autoxidized Emulsion Characterization

Alkyd III was oxygen autoxidized at atmospheric pressure and samples were taken hourly in order to characterize the change of percent solids, pH, particle size, relative and absolute viscosity with respect to reaction time. Table 3.25 represents the result of this characterization.

Percent solids of alkyd increased again with increasing reaction time as expected and discerned above. The emulsion pH decreased with increasing reaction time and this observation will be investigated further in a later study. The particle size was estimated by the microscopic examination of a diluted emulsion sample. The particle size did not change significantly until 30 hours of reaction time and then thereafter. The relative viscosity decreases slightly initially, and then begins to increase again after fifteen hours of reaction. The absolute viscosity steadily decreases. It is important to note at this point the difference between the two viscosity methods. The relative viscosity is obtained by effluxing the emulsion through a capillary viscometer and obtaining a ratio of its efflux time to that of distilled water or the aqueous phase of the emulsion. The capillary is very sensitive to percent

iranchembook.ir/edu

non-volatile and since the percent non-volatile changes by more than eight percent, relatively speaking, during the process, one would expect the relative viscosity to increase. At the same time, the particles crosslink and become more dense thereby reducing the emulsion viscosity. The non-volatile change is the over-riding parameter here.

Table 3.25 Emulsion Reaction Characterization

Reaction Time, Hours	% Solids	pH	Particle Size, microns [a]	Emulsion Relative	Viscosity Centipoise
0	22.8727	4.27	0.5-10.0	1.6597	23.0
5	23.0493	4.22	0.5-10.0	1.6840	18.2
10	23.1596	41.5	0.5-10.0	1.6632	18.3
15	23.3109	4.08	1.5-10.0	1.6563	18.5
20	23.4343	3.95	0.5-10.0	1.7622	18.4
25	23.6592	3.72	1.0-15.0	1.7512	18.2
30 (insoluble)	23.8605	3.43	1.0-15.0	1.7743	17.5
35 (insoluble)	24.8213	3.20	10.0-20.0	1.8930	16.3
40 (insoluble)	16.1696	3.05	10.0-20.0	2.0879	5.6
45 (insoluble)	unstable	unstable	unstable	unstable	unstable

Note: Alkyd IV: 50.0% non-volatile (N.V.) in mineral spirits.
Emulsifier: 2.0% w/w alkyd, Igepal CO-850 and dodecyl sodium sulfate, 30/50% weight basis initial intrinsic viscosity alkyd: 0.040

[a] Microscopic examination utilized for the above oxygen autoxidation reaction of emulsion.

The absolute viscosity is determined by measuring the resistance to rotation of a cylindrical spindle within the emulsion. As the crosslinking increases within the particle with time and the particles eventually become hard "spheres" in the water. A decrease in centipoise (absolute) viscosity was with reaction time is observed thereby demonstrates that the particle crosslinking overrides the percent solids increase with reaction time. After 40.0 hours reaction time, the viscosities change dramatically. At this point in

iranchembook.ir/edu

the reaction, the percent transmittance in acetone decreased significantly, indicating that the polymer is highly crosslinked. After 45 hours of run time, the emulsion is visibly unstable and sedimentation is observed. Thus, the viscosities, relative and centipoise, demonstrate the onset of instability.

Table 3.26 represents the dry times of films formed from emulsions processed in Table 3.25. Dry time decreases rapidly after 30.0 hours of reaction. Time required for the film to become tack-free (surface dry) is usually smaller than total film dryness or set time. It is obvious after inspection of Table 3.26 that the film qualities develop during the final stages of crosslinking of the emulsified particles. The solubility of the particles with reaction time is described by percent transmittance in acetone. As the solubility decreases, as shown by turbidity in the sample and decreasing light transmittance, the crosslink density increases with decreasing swelling ratio. The clean-up or washability with soap (10% dodecyl sodium sulfate in water) was rated from one to ten as shown in Table 3.26. The trend is that the ease of cleanup is greatest during the advanced stages of reaction.

The alkyd phase within the emulsion particle was increased in order to study this influence on the emulsion characteristics during reaction. Table 3.27 represents reaction of the emulsion containing 74.4% alkyd in the alkyd solution phase or 37.20% alkyd in the total emulsion. These data demonstrate that the percent solids of alkyd increases with reaction time. The pH of the emulsion decreases with reaction, as previously observed (See Table 3.25). The particle size was estimated to be an average of 1.0 micron. The relative viscosity unexpectedly (based upon observations in Table 3.25) decreased slightly with reaction time until 35.0 hours, then increased. The region of 40.0 to 45.0 hours of reaction time appears to be the time frame in which emulsion instability begins and therefore drastic changes of all parameters occur.

However, observing relative viscosity from 0.0 to 35.0 hours of reaction demonstrates a decrease in both relative and absolute viscosity together with a decrease in centipoise viscosity. The change of percent solids is smaller than the percent solids observed in Table 3.25. Therefore, increasing crosslink density or decreasing swelling ratio with reaction time decreases the viscosity of the emulsion when the percent solids are at about 74.4 percent of alkyd solution phase. The diffusion of co-solvent from the alkyd particle changes the percent solid per unit volume of emulsion, but with higher percent solids in the alkyd polymer phase there is a proportionally greater influence of crosslinking influence on viscosity compared to percent solid change with reaction time.

iranchembook.ir/edu

Table 3.26 Film Dry Time and Emulsion Reaction Time

Emulsion [a] Reaction Time, hours	Dry Time, [b] Tack Free, Hours	Set-Time, [c] To-Touch, Hours	Emulsion % Transmittance in Acetone [d]	Water Clean Up [e]
0	--	--	--	1
5	--	--	--	--
10	--	--	--	--
15	25.0	35.0	--	--
20	15.0	25.0	--	--
25	8.0	20.0	--	--
30	5.0	10.0	30.0	--
35	3.5	7.0	25.0	--
40	2.0	5.0	15.0	10

[a] Alkyd III-xylene co-solvent emulsion autoxidized with oxygen.

[b] Dry to touch is tack-free or surface dry time.

[c] Set-time is total film dry time.

[d] Dilution of 1.0 gram alkyd (dry basis) to 200 milliliters acetone.

e Ability to clean in detergent water, 1 = poor and 10 = excellent

iranchembook.ir/edu

Table 3.27 Emulsion Reaction Characterization, Alkyd III in Xylene (74.4% w/w, N.V.[a])

Reaction Time, Hours	% Solids In Emulsion	PH	Average Particle Size Microns	Emulsion Viscosity	
				Relative	Centipoise
0	36.98	6.41	0.5 - 10.0	1.9231	48.3
5	37.01	5.35	0.5 - 10.0	1.9024	44.3
10	37.09	4.56	0.5 - 10.0	1.8926	43.9
15	37.17	3.66	0.5 - 10.0	1.8625	42.8
20	37.21	3.52	0.5 - 10.0	1.7213	19.3
25	37.30	3.31	0.5 - 10.0	1.8734	19.1
30 (insoluble)	37.41	3.20	0.5 - 10.0	1.7016	18.9
35 (insoluble)	37.52	2.89	0.5 - 20.0	1.6990	18.3
40 (insoluble)	37.79	2.45	1.0 - 20.0	1.9228	17.1
45 (insoluble)	40.89	2.31	10.0 - 20.0	unstable	23.8

[a] N.V. is non-volatile or alkyd matter in alkyd phase.

Note: Oxygen flow rate of 708.0 cm^3/minute.

Table 3.28 represents the film properties previously discussed in Table 3.27. The 15.0-hour sample possesses a greater tensile strength than the more advanced stage films. The flowability of the 15.0-hour film was greater than during the advanced stages of reaction, but the amount of crosslinking was lower compared to 40.0 hours of reaction. Elongation was greater at 15.0 hours and elongation increased again at 45.0 hours, but with lower tensile strength. The flowability with tensile strength merits further study later in this chapter. The emulsion stability of the emulsion after processing is reported in Table 3.28 together with freeze-thaw stability. The mechanical stability represents exposure to agitation of the reacted emulsion in minutes before instability occurs.

iranchembook.ir/edu

Table 3.28 Autoxidized Emulsion Characterization, Alkyd III in Xylene Solvent (74.4% N.V.)

Reaction Time, Hours	Tensile Strength, Kg/cm^2	% Elongation	Shelf Stability, Days	Freeze-Thaw, Cycles	Mechanical Stability, minutes
15	11.1	85.0	13	1	2.0
20	13.9	72.0	13	1	2.0
40	6.08	28.0	13	1	2.0
45	9.20	106.0	13	1	2.0
45 (pH=7.0)[a]	22.5	104.0	6	0	0.0

[a] pH was post-reaction adjusted to 7.0 with 6.0 molar NH_4OH and a pale yellow color developed.

Note: Oxygen flow rate of 708.0 cm^3/minute.

3.4.6. Post pH-Adjustment of Autoxidized Emulsion

The post-adjustment of pH of the 45.0-hour sample increased the tensile strength of the drawn film but drastically reduced the emulsion stability. From this observation, it is apparent that pH effects require further study. Table 3.29 represents a study to determine pH adjustment effect on emulsion stability of the 45.0-hour sample. It can be seen that emulsion pH of less than 7.0 improves stability. However, the tensile strength improves near 7.0.

Table 3.29 Emulsion Stability with Post-Adjusted pH[a]

pH	Stability, days 62.8°C
2.61	8
7.00	6
8.00	4

[a] pH adjusted with ammonium hydroxide.

iranchembook.ir/edu

3.4.7. pH Adjustment Prior to the Autoxidation

A study was initiated to observe the effect of pH adjustment prior to autoxidation. Table 3.30 represents the emulsion system from Table 3.27, but with the pH adjusted to 7.29 before reaction as shown in Table 3.30. It can be seen from inspection of Table 3.30 that the pH continues to decrease with reaction time and the percent solids continues to increase with reaction. The relative viscosity does not change significantly until the region of emulsion instability is reached, at about 40.0 hours of reaction. The centipoise viscosity decreased with reaction time.

Table 3.30 Emulsion Reaction Characterization, Alkyd III in Xylene (74.4% N.V.) with pH Adjustment Prior to Processing

Reaction Time, Hours	% Solids	pH[a]	Average Particle Size, Microns	Emulsion Viscosity	
				Relative	Centipose
0	39.57	7.29	1.0	1.524	55.8
5	39.98	7.59	1.0	1.532	39.6
10	40.57	6.80	1.0	1.538	27.9
15	40.63	6.15	1.0	1.555	25.0
20	40.79	5.75	1.0	1.563	23.7
25	40.78	5.35	1.0	1.557	20.7
30	40.05	4.98	1.0	1.555	19.3
35 (yellowing)	41.77	4.00	1.0	1.551	18.5
40 (unstable)	41.25	3.10	1.0	1.602	17.4
45 (emulsion broken)	-------	---------	-------	------	-----

[a] pH adjustment made with 6.0 Molar NH_4OH

Note: Oxygen flow rate of 708.0 cm^3/minute.

Table 3.31 represents the film properties of the emulsion processed in Table 3.30. The tensile strength did not develop at the same rate as in Table 3.27, which represents the identical reaction without post-pH

iranchembook.ir/edu

adjustment of the emulsion. Therefore, increasing the pH closer to 7.0 retarded the autoxidation reaction. The elongation of the films was comparable to those from Table 3.27. Mechanical stability was similar to those of Table 3.27.

Table 3.31 Autoxidized Emulsion Characterization, Alkyd III in Xylene (74.4% N.V.) with pH Adjustment Prior to Processing

Emulsion	Tensile Strength, kg/cm^2	% Elongation	Shelf Stability, Days	Freeze-Thaw Cycles	Mechanical Stability Minutes
20 hours	7.30	62.2	13	1	5.0
35 hours	7.92	56.7	0	1	5.0

Note: Oxygen flow rate of 708.0 cm^3/minute.

3.4.8. Cobalt Naphthenate Catalysis in Alkyd Phase

An attempt to catalyze the reaction from Table 3.32 was initiated for the purpose of improving the film integrity and reducing the reaction time. Cobalt naphthenate, 0.04% by weight alkyd, was dissolved in the alkyd solution phase and then emulsified as discussed. The reaction is characterized in Table 3.32. The percent solids increased significantly with reaction time, the pH decreased with reaction time and centipoise viscosity decreased with reaction time. The relative viscosity increased with reaction time. The particle size was estimated by the microscopic method.

The tensile strength of the 25.0-hour sample was greater than the same sample with cobalt naphthenate catalysis. The film tack-free dry time was 0.5 hour, which was unexpectedly fast. The stability of the emulsion was comparable to stability of uncatalyzed reactions, Table 3.33.

3.4.9. Post-Addition of Emulsifier

A study of "post-addition of an emulsifier to greatly enhanced the stability of the alkyd prior to autoxidation," that was destroyed by the autoxidation process, was utilized in an attempt to increase the stability of autoxidized emulsions. The emulsifier, Gafac RE-960, was post-added to

iranchembook.ir/edu

each autoxidized emulsion in the amount of 20.0 grams per liter of emulsion. Table 3.34 represents the resulting stabilities. It can be seen by comparing these data with those in Table 3.33 that post addition of Gafac RE-960 enhanced the heat accelerated shelf stability by about two days, but the freeze-thaw stability was not changed.

Table 3.32 Emulsion Reaction Characterization, Cobalt Naphthenate (0.04% w/w) Catalysis in Alkyd III

Reaction Time, Hours	% Solids	pH	Average Particle Size, Microns	Emulsion Viscosity Relative	Centipoise
0	25.75	6.16	1.0	1.6234	56.5
5	26.21	6.07	1.0	1.6205	50.2
10	26.35	5.82	1.0	1.6123	48.6
15	26.90	4.93	1.0	1.6021	29.2
20	27.31	3.24	2.0	1,8286	27.1
25	26.95	3.08	3.0	1.8098	20.7
30 (unstable)	----	----	-----	------	19.3
35	----	----	-----	------	------
40	----	----	-----	-----	------
45	----	----	-----	-----	-----

[a] Microscopic examination.

Note: Oxygen flow rate of 708.0 cm^3/minute.

iranchembook.ir/edu

Table 3.33 Autoxidation Emulsion Characterization, Alkyd III with Cobalt Naphthenate Catalysis [a]

Emulsion	Tensile Strength Kg/cm^2	% Elongation	Stability Day, 62.8°C	Freeze-Thaw Cycles	Mechanical Stability [c]
25 hours	9.69	50.0	2	1	Stable during Processing

Note: Film dry time was faster than expected, 0.5 hours, tack free.

[a] Cobalt naphthenate in medium soya alkyd, 0.4% weight/weight dry alkyd basis.

[b] Freeze-thaw cycles, -5 to +20°C over 25 hour period, ASTM method.

[c] Mechanical stability comprises constant 60 revolutions per minute agitation in reaction vessel.

Table 3.34 Post Addition of Emulsifier [a]

Hours Blown	Shelf Stability 62.8°C	Freeze-Thaw Stability (-5°C - 20°C)
15	14	<1
20	14	<1
30	14	<1
35	14	<1

[a] Addition of Gafac RE-960 to each sample, 20 grams per liter of emulsion.

Note: Initial Emulsion: 900 grams medium soya alkyd
900 grams water
18 grams sodium lauryl sulfate
Shelf Stability – 10 days
Freeze-Thaw Cycles - <1 cycle

iranchembook.ir/edu

3.4.10. pH Effect on Reaction Rate

The effect of pH on the autoxidation reaction is described in Table 3.35. The progress of crosslinking with time at a constant pH is monitored by the percent transmittance method of measuring crosslinking. Changes in percent solids were corrected in order to measure 1.00 gram of dry weight alkyd from an emulsion sample and dilute to 200.00 milliliters of acetone. It is obvious from inspection of Table 3.35 that only acidic conditions enable the autoxidation reaction to proceed.

Table 3.35 Emulsion Particle Crosslinking Development with pH Adjustment Prior to Reaction

Reaction Time, Hours	Average Particle Diameter [c]	% Transmittance [a]		
		pH = 9.0 [b]	pH = 7.0	pH = 6.0
0	1.0	99.5	98.5	99.6
5	1.0	99.5	99.3	99.5
10	1.0	99.6	99.4	99.4
15	1.0	99.7	98.7	99.0
20	1.0	99.3	99.5	98.6
25	1.0	99.2	99.5	92.5
30	1.0	99.5	99.5	61.2
35	1.0	99.6	99.4	9.2
40	1.0	99.4	99.1	4.9

[a] % transmittance is adjusted for change in % solids of medium soya alkyd.

[b] pH is the initial pH measurement of the emulsion before reaction.

[c] Microscopic examination

Note: Emulsion was prepared from alkyd II and autoxidized at 1.0 atmosphere oxygen pressure.

The decreasing pH with increasing reaction time from previous reactions merited further study. The acid values of the unreacted alkyd, autoxidized emulsion and the separated dried alkyd from the autoxidized

iranchembook.ir/edu

emulsion were determined by titration. From inspection of Table 3.36, the medium soya emulsion increased in acid value with autoxidation.

Table 3.36 Acid Value from Titration [a] of Reacted Emulsion

Alkyd III	Autoxidized Emulsion 15 hours	Alkyd from Autoxidized Emulsion
10.4 [c]	11.8	18.9

[a] Standard KOH = 0.1 N Titrant

[b] Emulsion: Alkyd III, emulsifier (T-DET A026, sodium lauryl sulfate), reacted with oxygen for 15 hours.

[c] Acid value = milligrams KOH to neutralize 1.0 gram of alkyd, milliequivalents acid = acid value/5.619.

3.4.11. Increased Oxygen Concentration and Catalysis

In another study of medium soya alkyd emulsion autoxidation, the oxygen pressure was increased to 20.0 pounds per square inch, which increased the oxygen concentration from 0.029 to 0.069 grams per liter, Table A.6 in the Appendix. The alkyd III was catalyzed with 0.02% by weight cobalt naphthenate and 0.02 percent by weight 0.02% by weight cobalt naphthenate and 0.02 percent by weight zirconium naphthenate. Theoretically, the combination of increased oxygen and catalysis should decrease the drying time and data in Table 3.37 demonstrates that the drying time decreases with time on an accelerated basis as expected. Crosslinking is again followed with percent transmittance of an acetone solution. Tensile strength and percent elongation are optimal at 10.2% transmittance. From this study and Table 3.37, it can be seen that film properties go through an optimum and then decrease. Monitoring the percent transmittance, which is referred to in Chapter 2 as the turbidimetric method of measuring crosslinking, identified this optimum point or reaction time. Therefore, by measuring the crosslinking by percent transmittance produced by the emulsion in acetone, the point during the reaction that produces optimal film properties has been detected. The only remaining action is to stop the

iranchembook.ir/edu

reaction at this point by releasing the oxygen pressure and lowering the temperature to ambient conditions.

Table 3.37 Reaction Time and Physical Properties

% Transmittance	Dry Time, hours	Tensile Strength	% Elongation
51.7	2.0	--	--
23.2	1.0	4.6	67
10.2	0.5	10.7	95
5.5	0.4	8.4	55
3.5	0.3	8.5	50
2.7	0.3	8.4	57

Note: Emulsion contained alkyd III, 50% T-Det RA26 + 50% Sodium lauryl sulfate, 0.02% zirconium naphthenate + 0.2% Cobalt naphthenate, 20.0 psi oxygen pressure.

3.4.12. Scanning Electron Microscopy

The film from Table 3.37, taken at 10.2% transmittance, produced the greatest tensile strength and a fast drying time. A free film was prepared and examined by scanning electron microscopy. Figure 3.6 represents the film surface magnified 5000 times. The particles appear to be coalescing and forming a continuous film. Coalescence is necessary for film formation and the degree of coalescence with further autoxidation determines the integrity of the final dried film. Figure 3.7 represents the same film surface, but magnified 13,000 times. The outlines of the original particles are vaguely visible. The individual particles can be seen to be coalescing with each other and forming a continuous film. If the particles had been too highly crosslinked prior to film formation, the particles would not coalesce as well as in Figure 3.6. However, if the particles had been too lightly crosslinked, then complete coalescence would occur, but the resultant film would require an excessive drying time. The phenomenon is evidence by Table 3.37.

iranchembook.ir/edu

Controlling the crosslinking reaction is imperative if one is to maintain optimal film integrity.

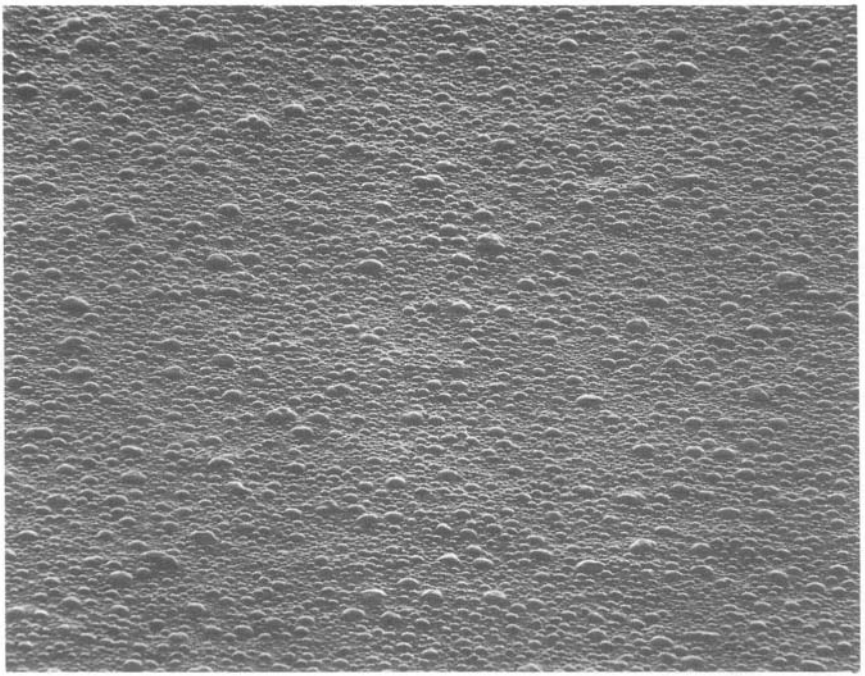

Figure 3.6. Scanning electron micrograph 80.0 psig oxygen alkyd II emulsion, 7.0 hour sample, 5000x magnification.

iranchembook.ir/edu

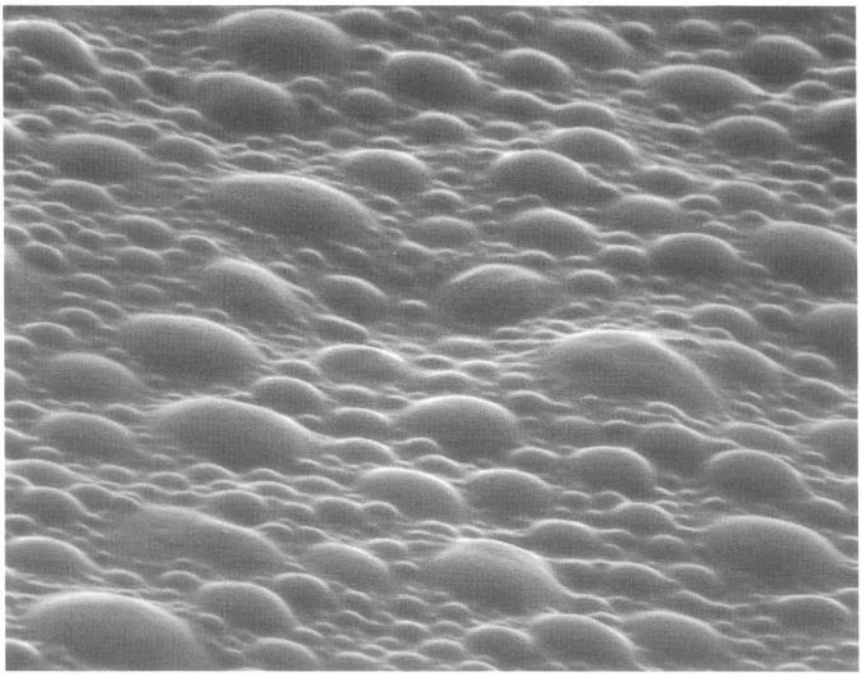

Figure 3.7. Scanning electron micrograph 80.0 psig oxygen autoxidized alkyd II emulsion, 7.0 hour sample, 13,000x magnification.

3.4.13. Water Clean-Up of Emulsion

The emulsion from Table 3.37 was brushed on a wood surface with a two-inch width paintbrush and then cleaned by rinsing with mild detergent. The results of the brush cleaning operation are described in Table 3.38. The emulsion is less sticky and far more cleanable after having been reacted 7.0 hours by autoxidation.

iranchembook.ir/edu

Table 3.38 Water Clean-Up of Emulsion

Reaction Time, Hours	Clean-up Rating, 5 minutes of drying on brush
0	1
1	1
2	1
3	1
4	1
5	1
6	8
7	8
8	8
9	8

Rating: 1- Failure to clean- up
10 - Complete clean-up

Emulsion: Alkyd III, Plurafac RA20, Sodium lauryl sulfate, autoxidized at 80.0 psi with 0.02% Zirconium naphthenate and 0.02% Cobalt naphthenate

3.4.14. Comparison to Alkyd-Solvent System

Alkyd III in a 50.0% mineral spirits solution was compared to an autoxidized emulsion sample. The solvent-alkyd solution was catalyzed by 0.04% cobalt naphthenate by weight of alkyd III. The film was dried at ambient conditions for 7.0 days. The autoxidation reacted emulsion film was processed at 80.0 psig pressure for 7.0 hours and the film was dried for 7.0 days.

iranchembook.ir/edu

Table 3.39 represents a direct comparison between the two films for drying of the films and their tensile strengths. The solvent-alkyd system possesses a higher tensile strength than the autoxidized emulsion, but the autoxidized emulsion possesses a shorter drying time.

Table 3.39 Comparison of Autoxidized Emulsion to Alkyd-Solvent System

System	Tensile Strength Kg/cm^2	Film Dry Time, hours
Solvent Borne-Alkyd III	14.3	7.0
Autoxidized Emulsion Alkyd [a]	9.8	1.0

[a] Alkyd II emulsion, reacted for 7.0 hours at 5.62 Kg/cm^2, 80.0-psi oxygen pressure.

3.4.15. Effect of Emulsifier Structure on Reaction Rate

Many emulsifier variations have been used during the course of this research effort. The effect of emulsifiers has been observed on numerous properties of the emulsions generated. This study was conducted (see pages 63-73) which ascertained that film properties varied as a function of the emulsifiers employed to stabilize alkyd III. A subsequent study was also initiated to determine the effect of emulsifier structure on the autoxidation rate of reaction. Figure 3.8 represents the oxygen pressure variation during successive reactions as a function of the time required to reach a densely crosslinked state. The Gafac RE-960 system is dramatically slower relative to the autoxidation rate when T-Det and dodecyl sodium sulfate or Igepal CO-850 and dodecyl sodium sulfate surfactants are employed. The chemical structures of these compounds are found in Chapter 2, Table 3.1.

Referring to Chapter 2, Table 3.1, one finds that Gafac RE-960 contains a phosphoric acid group together with an aryl group. Both of these groups are capable of stabilizing a radical through resonance. The Igepal CO-850 structure contains an aryl group. The T-Det AO26 does not contain any substituent or groups capable of stabilizing a radical. Since the diffusion of oxygen through the emulsifier region surrounding the polymer particle is

iranchembook.ir/edu

necessary if autoxidation within the polymer particles is to occur, the emulsifying agent should not characteristically possess an ability to retard oxygen diffusion. If it does, the crosslinking reaction will proceed at a slower rate than expected as evidenced in Figure 3.8. Figure 3.6 illustrates the geometrical configuration of the particle in relation to the emulsifier layer, which presents a barrier to oxygen diffusion. It can be seen that the lipophile segment of the emulsifier is soluble in the alkyd particle phase and the hydrophile segment is soluble in the aqueous phase.

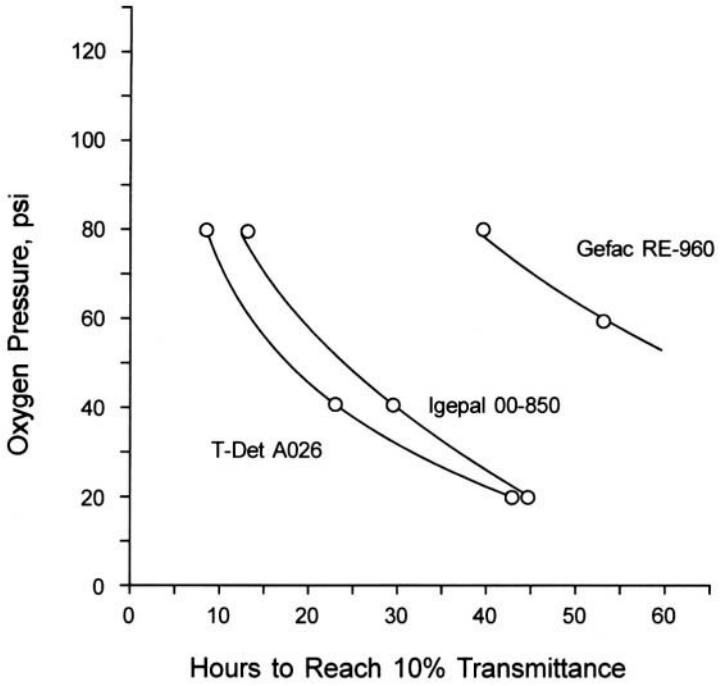

Figure 3.8. Effects of emulsifier structure on reaction rate.

As indicated in Figure 3.6, the oxygen must diffuse from the aqueous phase through the emulsifier region and into the alkyd particle phase in order

iranchembook.ir/edu

to initiate autoxidation. If the emulsifier is capable of retarding the diffusion of oxygen by radical stabilization or a formidable intermolecular reaction, then the crosslinking reaction by autoxidation is slowed. A total explanation of how emulsifiers retard the reaction is not within the scope of this dissertation, but demonstration that the factor exists is clearly made here. A discussion of possible mechanisms may be found in references Lenz (1967) and Odian (1970).

3.5. Kinetic Study

3.5.1. Oxygen Concentration Relationship

By controlling the oxygen partial pressure, the influence on the autoxidation reaction of oxygen concentration can be studied. If all other variables are constant within the reaction, the oxygen concentration can be varied and the swelling ratio method of determining the degree of crosslinking can be measured per unit time. Figure 2.1 represents the apparatus for accomplishing this purpose. From inspection of Figure 2.1, it can be seen that the rate of agitation within the reaction vessel is controlled by a tachometer. An electrical heating mantle that is controlled by a proportional temperature-controller generates the heat within the reaction vessel. The oxygen pressure within the reaction vessel is controlled by an oxygen pressure-regulator that is attached to a cylinder of dry oxygen.

The Bench Scale^{R} pressure reactor is illustrated in cross-section in Figure A. 1 in the Appendix section of this dissertation. Figure A.2 illustrates the top view of the pressure vessel. Figure A.3 represents the assembly that seals the drive shaft from the vessel (stainless steel, 1000 cm^3). Table A.8 in the Appendix describes in detail each numbered component of the pressure reactor. By utilization of this vessel, the autoxidation reaction can be controlled for the variables of oxygen concentration, agitation rate, and temperature. The Bench Scale pressure reactor is here as a "batch" type reactor (Levenspiel, 1972).

It is important to understand the influence of oxygen concentration on the autoxidation reaction. Methods to monitor the progress of the autoxidation reaction with time have been discussed by measuring percent transmittance as a function of swelling ratio. The relationship of oxygen concentration to oxygen partial pressure has been discussed as being a linear relationship. It is now possible to determine the oxygen concentration influence on the rate of reaction by varying oxygen concentration for each reaction and monitoring the percent transmittance.

iranchembook.ir/edu

3.5.2. Correlation of Swell Ratio and Percent Transmittance

Correlation of percent transmittance with swelling ratio is illustrated in Figure 3.9. One gram of polymer sample was diluted to 200.0 cm^3 with acetone and the degree of turbidity was determined with a Spectronic^R 710 Spectrophotometer, Bausch & Lomb Mfg. One hundred percent acetone was calibrated at 100.0% transmittance at 509 nm. Because 509 nm is the wavelength of maximum transmittance for acetone, it was chosen for the turbidity analysis. A percent solids of the sample must be known prior to measuring 1.0 gram of polymer in emulsion in order to compensate for the mass of the other constituents of the emulsion, surfactant and water. This method of measuring swelling ratio requires ten minutes, nominally.

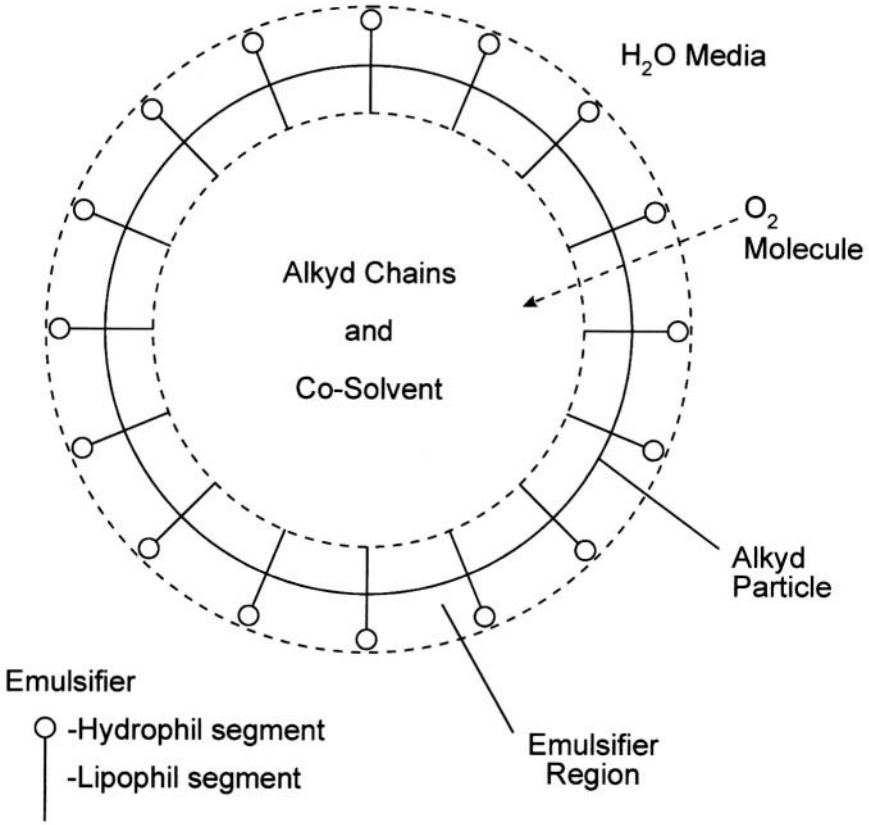

Figure 3.9. Emulsified alkyd particle and oxygen diffusion.

iranchembook.ir/edu

Figure 3.10 was constructed from data collected in Table A.9 in the Appendix for percent transmittance of autoxidized emulsion samples and swelling ratio of the dry alkyd polymer phase as discussed. Figure 3.11 was constructed from identical data in Figure 3.10, and was analyzed with linear regression. The resulting linear curve in Figure 3.11 consists of data from the same three-autoxidation experiments in Figure 3.10 and the data is listed in Table A.10 in the Appendix.

It has been discussed that the turbidimetric method of measuring swelling ratio is more sensitive and faster than the direct hydrodynamic volume method of measuring swelling ratio. Therefore, the turbidimetric method of measuring swelling ratio was utilized to monitor the crosslinking development of the emulsified alkyd polymer particles.

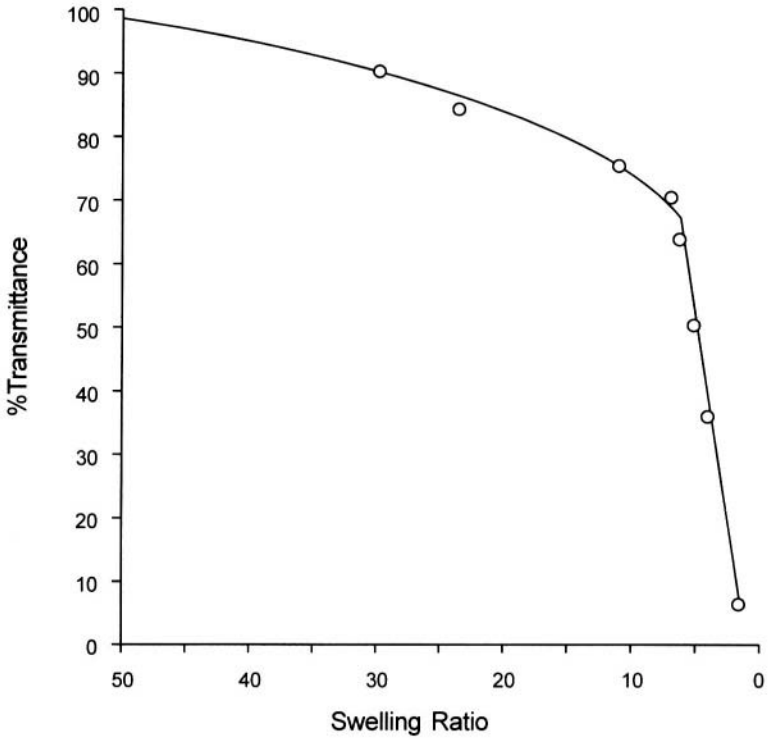

Note: Alkyd III emulsion autoxidized with oxygen
Catalysis: 0.04% (w/w) zirconium naphthenate
Temperature: 55.0°C
Agitation rate, RPM: 300
Pressure, oxygen, psi: 20

Figure 3.10. Swelling ratio vs. % transmittance.

iranchembook.ir/edu

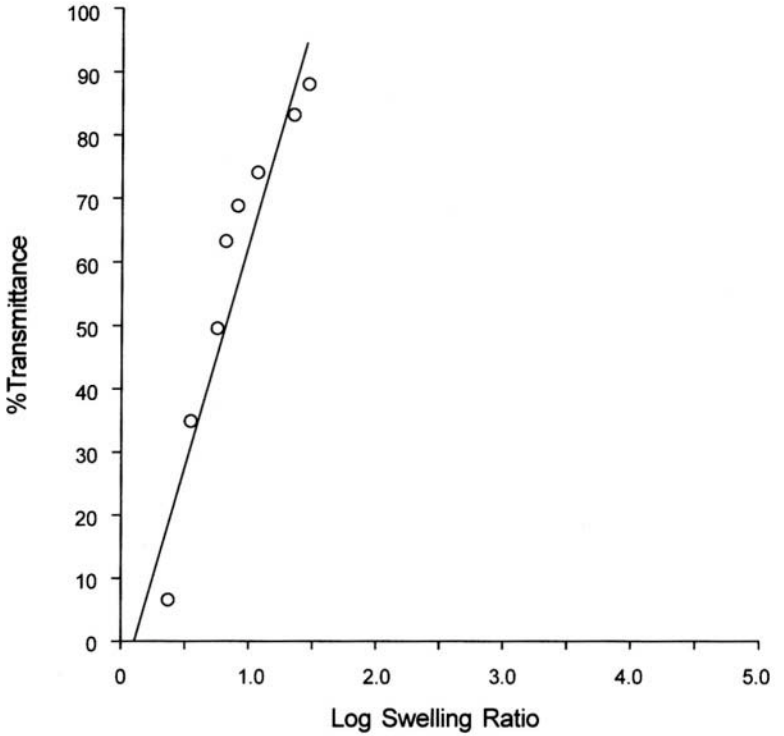

Figure 3.11. Log swelling ratio vs. % transmittance.

The autoxidation reaction was studied in the Bench Scale[R] laboratory pressure vessel, 1.0-liter capacity. Figure A.1 represents the apparatus and configuration of materials and direction of material flow for studying the influence of oxygen concentration within the emulsion by controlling oxygen partial pressure. The oxygen pressure regulator requires manual adjustment for a specific oxygen pressure that was controlled at the system. The temperature was constant at 55°C and was controlled by the proportional temperature controller in Figure 2.1. The rate of agitation was controlled at 300 rpm for each reaction. Therefore, the only variable present within this system, illustrated by Figure 2.1, was oxygen pressure. For the following series of autoxidation reactions, the oxygen pressure was varied at

iranchembook.ir/edu

10.0-psig (0.71 kg/cm^2) increments over a range of 10 psig to 80 psig. The maximum safe pressure for the Bench Scale^R pressure vessel is 100 psig (7.09 kg/cm^2). Samples were taken hourly and Figures were plotted for each autoxidation reaction. The emulsion composition was exactly the same for each sample. Table 3.40 represents the formulation for the emulsion. It is important to understand that the quality of the dodecyl sodium sulfate is important. It will be shown later that a technical grade (95% purity) of dodecyl sodium sulfate will increase the total reaction time.

Table 3.40 Formulation for Oxygen Concentration Dependence on Autoxidation Reaction Study

Component	Weight of Component, grams
Alkyd III	345.0
Xylene co-solvent	155.0
Water, distilled	480.0
Dodecyl sodium sulfate [a]	10.0
T-Det A020	10.0
Total	1000.0 grams

[a] Dodecyl sodium sulfate, Aldrich Chemical Company, reagent grade.

The influence of oxygen concentration on autoxidation of alkyd III emulsions was studied by observing the percent transmittance change of the emulsion dissolved in acetone that has been discussed as the turbidimetric method of measuring swelling ratio. This study was conducted by autoxidizing the emulsion at a fixed oxygen pressure for each reaction while taking hourly samples for crosslinking measurements. Figures A.5 – A.12 (in the Appendix) represent the autoxidation reaction of 10, 20, 30, 40, 50, 60, 70, and 80 psig of oxygen pressure with respect to percent transmittance. Figure 3.12 represents a composite curve for Figures A.5 -A.12. Points for

iranchembook.ir/edu

Figure A.10 were plotted as hours required as to reach 10% transmittance. Significant autoxidation beyond 10% transmittance produces instability within the emulsion. It can be seen from Figure A.10 that autoxidation time required to reach 10% transmittance decreases exponentially with oxygen pressure.

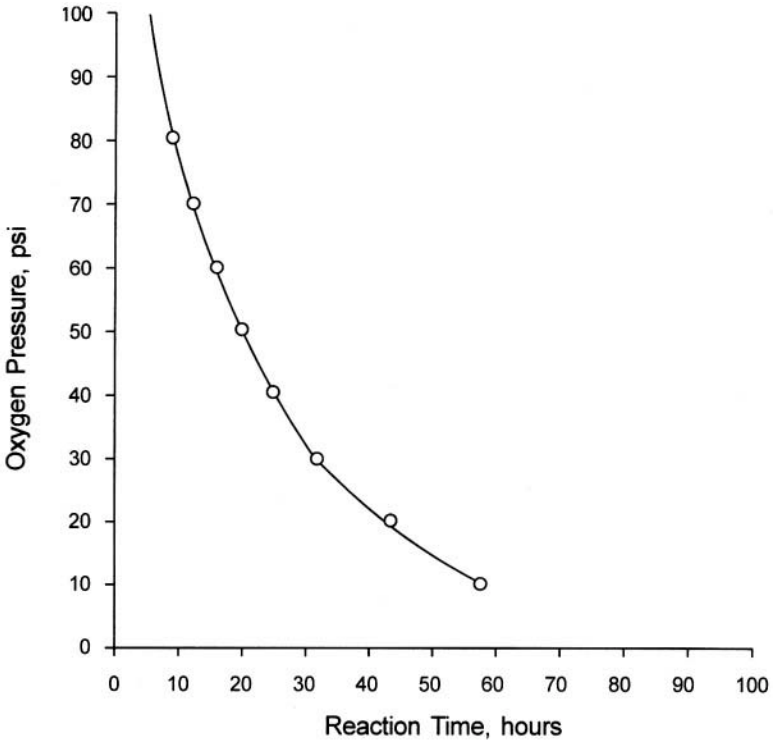

Figure 3.12. Total reaction time vs. oxygen pressure.

Referring again to Figures A.5-A12, it can be seen that the same shape of curve exists in each figure. There is an initial slope that continues for some period of time, and a greater slope that continues for another period of reaction time. The intervals of reaction for the initial slope were determined by observing the time before the second and greater slope began.

iranchembook.ir/edu

The interval of time required for the greater or second slope was measured by measuring the time from the first point of the second slope to the point represented by 10% transmittance. Since the initial slope is gradual and represents a very low rate of crosslinking, this period is generally before a rapid rate of crosslinking occurs. The functions of this induction period are shown in Table 3.41. The crosslinking period obviously occurs during the second time interval as evidenced by the rapidly decreasing percent transmittance in Figures A.24 – A.31. The sum of the induction period and crosslinking period is equivalent to the total reaction time. Table 3.42 lists these values for Figures A.5-A.12. A plot of induction time and oxygen pressure, form Table 3.42 and is illustrated by Figure 3.13. It is apparent that increasing oxygen pressure reduces induction time. A plot of crosslinking time from the same figures is shown in Figure 3.14. The crosslinking time decreases with increasing oxygen pressure to 40.0 psig. After 40.0 psig, the time does not change with increasing oxygen pressure. However, after this same point of oxygen pressure as related to oxygen concentration, induction time does decrease with increasing oxygen pressure. Therefore the net result of increasing oxygen pressure above 40.0 psig is to reduce the induction time of the reaction.

Table 3.41 Functions of Induction Period

1. Oxygen diffusion through aqueous phase
2. Oxygen diffusion through emulsifier barrier
3. Oxygen diffusion through viscous alkyd polymer particle
4. Oxygen initiation of radicals for autoxidation reaction

iranchembook.ir/edu

Table 3.42 Oxygen Concentration, Induction Time, Crosslinking Period, Total Reaction Time and Log Reaction Time

Oxygen Concentra -tion, psig	Induction Period, Hours	Crosslin king Period, hours	Total Reaction Time, hours	Oxygen Concentra- tion mole/liter	Log Reaction Time, Hours
80	4	5	9	1.53×10^{-3}	1.792
70	7	5	12	2.16×10^{-3}	1.623
60	2	4	16	2.85×10^{-3}	1.491
50	16	5	21	3.53×10^{-3}	1.380
40	19	5	24	4.21×10^{-3}	1.279
30	24	7	31	4.88×10^{-3}	1.204
20	29	16	42	5.51×10^{-3}	1.079
10	36	22	58	6.13×10^{-3}	0.9542

iranchembook.ir/edu

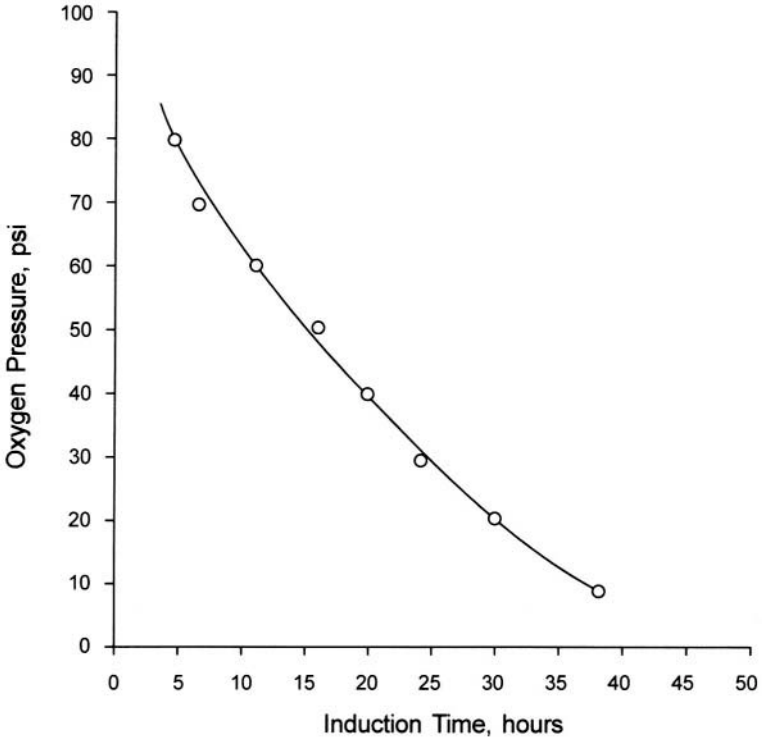

Note: Alkyd III and water emulsion auto-oxidized with oxygen
Temperature: 55.0°C
Catalysis: None
Agitation rate, RPM: 300

Figure 3.13. Induction time vs. oxygen pressure.

iranchembook.ir/edu

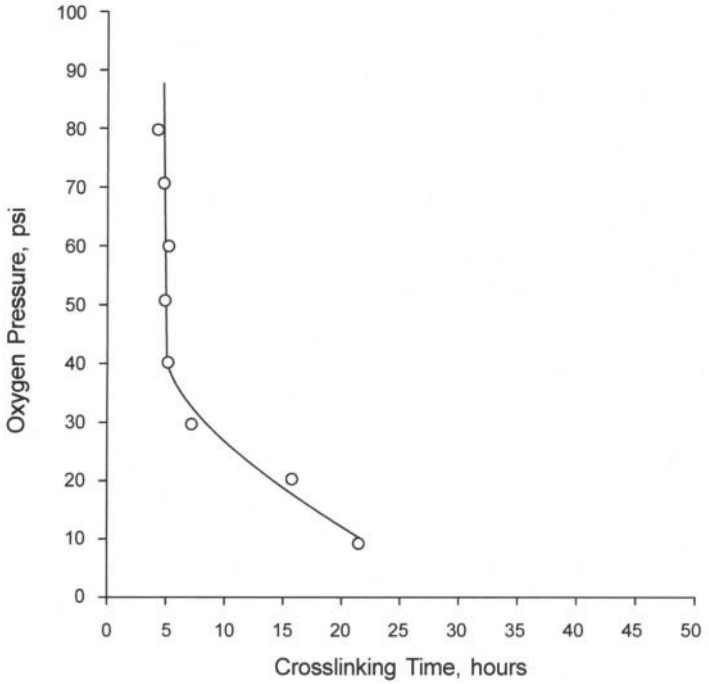

Figure 3.14. Crosslinking time vs. oxygen pressure.

The induction period consists of more than a period of radical formation for initiation in a typical free radical polymerization. The induction period in this reaction includes the time required for oxygen to diffuse through the aqueous phase, the emulsifier barrier on the surface of the alkyd particle and the viscous alkyd particle.

After these significant mass transfers occur, then the formation of radicals occurs for initiation of the autoxidation reaction as summarized in Table 3.41. Fick's Law (Barrow, 1973) use mass transfers as a function of mass per unit area per unit time. Summarizing, the induction period includes the total time before significant crosslinking occurs.

Intrinsic viscosity of the dry polymer particles indicates that crosslinking begins before the polymer becomes insoluble and before a significant decrease in light transmittance occurs. Light transmittance

iranchembook.ir/edu

decreases only after crosslinking has significantly developed. Figure 3.15 illustrates more accurately the change of intrinsic viscosity with reaction time. The initial increase in intrinsic viscosity marks the beginning of the reaction time or initial crosslinking period. During this period, molecular weight is increasing by virtue of crosslinking and as evidenced by the increase in intrinsic viscosity, which is related directly to viscosity molecular weight by the Mark-Houwink Equation (Collins, 1973). However, a significant degree of crosslinking does occur before insolubility of the polymer particle and intrinsic viscosity measurements describe this trend in Figure 3.15. Therefore, a more accurate determination for induction period is performed. The emulsion autoxidized for the construction of Figure 3.13 was the material from the previous 80.0 psig oxygen experiment (Figure A.12) for determination of total reaction time dependence on oxygen concentration.

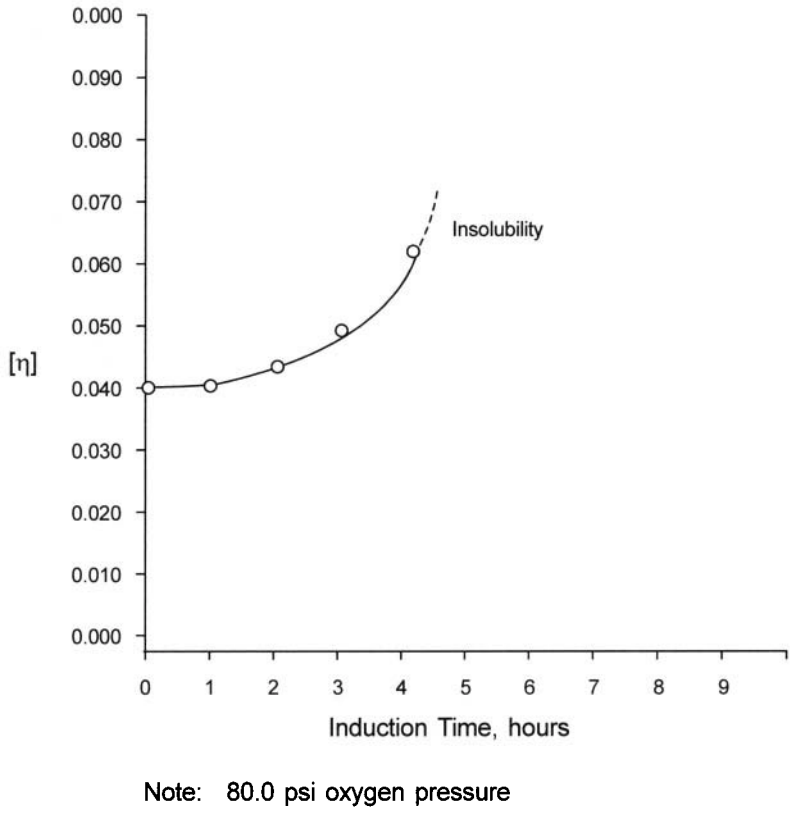

Figure 3.15. Intrinsic viscosity vs. induction time.

iranchembook.ir/edu

Emphasis is placed most heavily on the swelling ratio with respect to reaction time because the polymer film properties develop after the swelling ratio reaches less than ten. Control of the swelling ratio by the rapid turbidimetric method enables accurate control of film properties.

The relationship of oxygen concentration and total reaction time can be expressed in a kinetic equation where the concentration of oxygen and alkyd polymer are expressed with their respective reaction orders. The concentration of alkyd polymer is constant for all reactions and will react to constant percent conversion for all reactions. The alkyd polymer concentration cannot be utilized to control the autoxidation reaction. Therefore, it is of utmost importance to control the oxygen concentration and have knowledge of the oxygen concentration and reaction order with respect to the constant initial alkyd polymer-concentration and the constant final alkyd polymer-concentration. A kinetic relationship can be developed employing the reaction data from Figure 3.12. Equations were developed from the basis of a constant conversion of polymer material. The following kinetic treatment of the data from Figure 3.12 is based on the assumption that the alkyd polymer is initially of the same concentration and that the final degree of crosslinking is the same for each reaction as measured by the swelling ratio method. By allowing the reaction conversion to remain constant for each reaction, the concentration differential of alkyd polymer becomes a constant, m. Temperature and agitation rate are controlled at the same values for each reaction. Therefore, the existing variable in the series of autoxidations represented in Figure A. 5-A.12, and combined in Figure 3.12, is oxygen concentration. Referring to Figure 3.12, the points on this curve represent time required to autoxidize the alkyd polymer particles to 10% transmittance and the following equations develop as shown.

$$\frac{d[A]}{dt} = k\ [A]^{a}\ [O_2]^{b}$$

$$\frac{d[A]}{[A]^{a}} = k\ [O_2]^{b} \int dt$$

because $[A]_f - [A]_i$ = constant, m

where $[A]$ = concentration of alkyd, moles/liter emulsion

$[A]_i$ = concentration of alkyd, initially

iranchembook.ir/edu

$[A]_f$ = concentration of alkyd at end of reaction
$[O_2]$ = concentration of oxygen, mole/liter emulsion
b = order of reaction with respect to $[O_2]$
a = order of reaction with respect to [A]
m = constant representing a constant change in concentration with respect to $[A]$
t = reaction time, hours
k = reaction constant

$$m = [O_2]^b t$$

$$m/t = [O_2]^b$$

$$\log m - \log t = b \log [O^2]$$

$$\log t = b \log [O_2] - \log m$$

and solve for b by plotting the equation

$$\log t = -b \log [O_2] + \log m \text{ and } -b = \frac{\log m - \log t}{\log [O_2]}$$

From Table 3.43, the order of reaction with respect to $[O_2]$ is

b = order, $[O_2]$
= 1.324
m = constant, $[O_2]$
= 1.271×10^{-2} mole/liter

and $$\frac{d[A]}{dt} = k [A]^a [O_2]^{1.324}$$

Conversely, $[O_2]$ can be constant and [A] may vary in order to compute a, order with respect to [A].

$$\frac{d[O_2]}{dt} = k [A]^a [O_2]^b$$

iranchembook.ir/edu

$$\int_{[O_2]_i}^{[O_2]_f} \frac{d[O_2]}{[O_2]^b} = k\,[A]^a \int dt$$

$$n =]^a \; t$$

To solve for a, plot the equation

$$\log t = -a \log [A] + \log n \text{ or } \log t \text{ vs. } \log [A]$$

$$a = \text{slope}$$

$$n = \text{intercept}$$

To find k, plot the equation (Levenspiel, 1972)

$$\ln \frac{[A]_t \quad [O_2]_i}{[A]_i \quad [O_2]_t} = \ln \frac{[A]}{M\,[O_2]}$$

where $M = \dfrac{[A]_i}{[O_2]_i}$ and $[A]_i \neq [O_2]i$

$$\text{Slope} = ([A]_i - [O_2])\; k$$

$$\text{Intercept} = \ln \frac{[A]_i}{[O_2]_i} = \ln M$$

iranchembook.ir/edu

Table 3.43 Oxygen Concentration Correlation with Reaction Time

Log Oxygen Concentration Moles/liter	Log Reaction Time, hour
-2.815	1.792
-2.666	1.623
-2.545	1.491
-2.452	1.380
-2.376	1.279
-2.311	1.204
-2.259	1.079
-2.213	0.954

Correlation coefficient = 0.989
Degrees of freedom = 6
Slope = -1.324
Intercept = 1.896

It is not within the scope of this dissertation to study the kinetic relationships beyond those pertinent to the immediate processing of the emulsion. However, the possibilities for additional and more thorough investigation of kinetic relationships will be discussed in Chapter 4.

3.5.3. Catalysis Effect

The effect of catalysis was studied at an oxygen pressure of 80.0 psig (6.13×10^{-3} moles/liter H_2O). The catalysts selected for this study were catalysts that were successful for catalyzing the alkyd in a solvent system. Cobalt naphthenate catalysis in concentrations of about 0.04%

iranchembook.ir/edu

(weight/weight alkyd) produced instability within the emulsion and therefore this catalyst was not used singularly, but in combination with zirconium naphthenate, which does not degrade the stability of the emulsion. Figure 3.14 represents an autoxidation reaction catalyzed by 0.02% cobalt naphthenate and 0.02% zirconium naphthenate (weight/weight alkyd). The time required to crosslink the emulsion particles to 10.0% transmittance is about two hours less than non-catalyzed autoxidation.

It would be obvious to increase the catalyst concentration in order to further reduce autoxidation time required to densely crosslink the alkyd polymer particles. Figure 3.15 represents the formidable effects of increasing the concentration of zirconium naphthenate to 0.05% and cobalt naphthenate to 0.05%. When the emulsion was subjected to 80.0 psig, the autoxidation reaction was uncontrollable as illustrated in Figure 3.15. Therefore, the concentration of catalysts is critical.

Zirconium naphthenate does not impart instability to the emulsion as cobalt naphthenate does. Considering reduction of autoxidation time and emulsion stability, zirconium naphthenate was selected to study catalyst concentration with autoxidation reaction time. Figure 3.16 represents the effect on reaction time with increasing zirconium naphthenate concentration. After 0.05 grams/1000 grams alkyd polymer, instability within the emulsion occurs. Therefore, concentrations below 0.05 grams zirconium naphthenate/ 1000 grams alkyd should be employed to catalyze the reaction. Table 3.44 represents a plot of zirconium naphthenate concentration and log reaction time to reaction 10.0% transmittance (10% T). The correlation coefficient of this curve is acceptable and therefore the relationship of zirconium naphthenate concentration to reaction time to reach 10.0% transmittance is a logarithmic relationship described by the slope and intercept of the curve from Table 3.44.

iranchembook.ir/edu

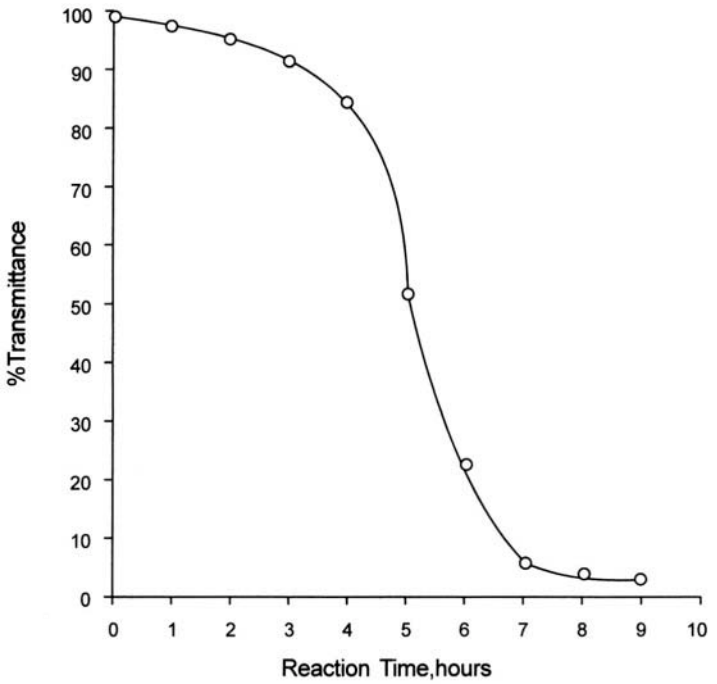

Note: Medium soya alkyd and water emulsion auto-oxidized with oxygen
Temperature: 55.0°C
Catalysis: 0.02% cobalt naphthenate + 0.02% zirconium naphthenate
Agitation rate, RPM: 300
Pressure, oxygen, psi: 80

Figure 3.16. Reaction time vs. % transmittance.

iranchembook.ir/edu

Table 3.44 Zirconium Naphthenate Concentration vs. Reaction Rate

Zirconium Naphthenate grams/1000 grams alkyd	log Hours (10% T)
0.00	0.9542
0.01	0.9395
0.02	0.9294
0.03	0.8976
0.04	0.7993
0.05	0.6628
0.06	0.5682

Correlation coefficient = 0.934089
Degrees of freedom = 5
Slope = -6.576
Intercept = 1.0188

3.5.4. Temperature Effect

The effect of temperature on the autoxidation reaction was studied at 80.0 psig of oxygen pressure and uncatalyzed. The study was designed to include an emulsion autoxidized at 20, 30, 40, 50, and 60°C at 80.0-psig oxygen pressure. Each reaction would be considered complete at 10.0% transmittance. Figure 3.17 represents the decreasing reaction times to reach 10.0% transmittance with increasing temperature. Table 3.45 represents a plot of temperature with log hours to reach 10.0% transmittance. The correlation coefficient is acceptable, which is indicative of the quality of the curve. Therefore, the best fit of the data form Figure 16 is represented by the data described in Table 3.44 and by the slope and intercept form linear regression of Reaction Temperature vs. Log Reaction Time.

iranchembook.ir/edu

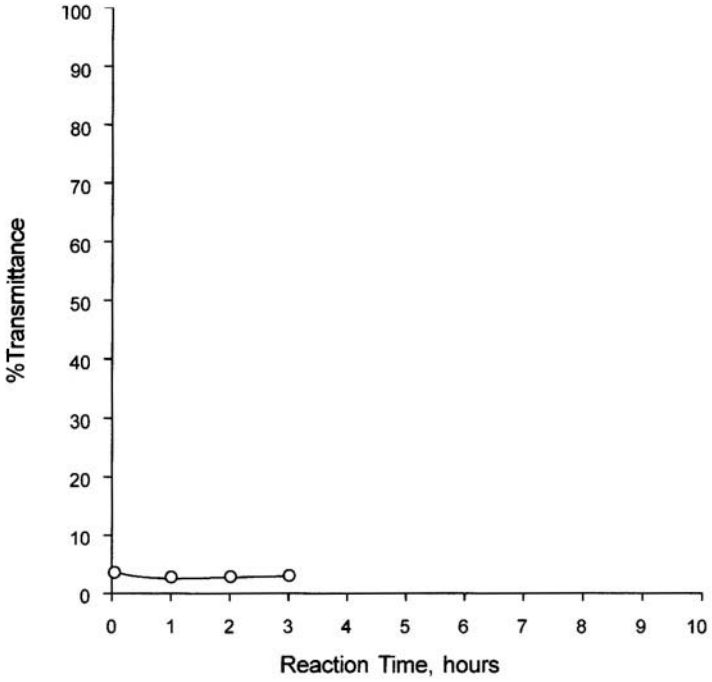

Note: Medium soya alkyd and water emulsion auto-oxidized with oxygen
Temperature: 55.0°C
Catalysis: 0.05% cobalt naphthenate + 0.05% zirconium naphthenate
Agitation rate, RPM: 300
Pressure, oxygen, psi: 80

Figure 3.17. Reaction time vs. % transmittance.

iranchembook.ir/edu

Table 3.45 Reaction Temperature vs. Log Reaction Time

Temperature, °C	log Hours (10% T)
20	---
30	1.5798
40	1.3222
50	1.0792
60	0.9031

Correlation Coefficient = 0.99654
Degrees of freedom = 2
Slope = -0.02273
Intercept = 2.24397

3.5.5. Agitation Rate Effect

The agitation within the autoxidizing emulsion is responsible for circulating the alkyd polymer particles within the aqueous phase and constantly exposing peripheral surfaces of the polymer phase to oxygen dissolved in the aqueous phase. The effect of agitation rate on oxygen diffusion into the particle was studied with respect to autoxidation time required to convert the alkyd polymer to a percent transmittance of 10.0, which is near 100% reaction conversion of the alkyd polymer.

The effect of agitation rate was studied by observing the time required to autoxidize the alkyd polymer to 10.0% transmittance with respect to revolutions per minute of the turbine agitator within the pressure vessel. The oxygen pressure was controlled at 80.0 psig. Figure 3.18 represents the reaction described utilizing a reagent grade of dodecyl sodium sulfate and Figure 3.19 represents the same reaction utilizing a technical grade (95% purity) of dodecyl sodium sulfate in combination with T-Det AO26. The total emulsifier concentration was 4.0% by weight of the alkyd solution before emulsification. Attempts to linearize these curves were not successful due to the lack of a sufficient number of data points. The curves illustrated in Figure 3.18 and Figure 3.19 are representative of general strands of reaction time and agitation rate.

iranchembook.ir/edu

In summary, the reaction increases with increasing agitation rate above zero agitation rate. The technical grade of dodecyl sodium sulfate contained impurities that slowed the autoxidation reaction compared to emulsification by reagent grade dodecyl sodium sulfate. Therefore, the emulsifier purity is significant together with the proper agitation rate of the processing emulsion. It is important to understand that the emulsion host stability above approximately 300 revolutions per minute and therefore this rate of agitation has been a standard throughout these studies.

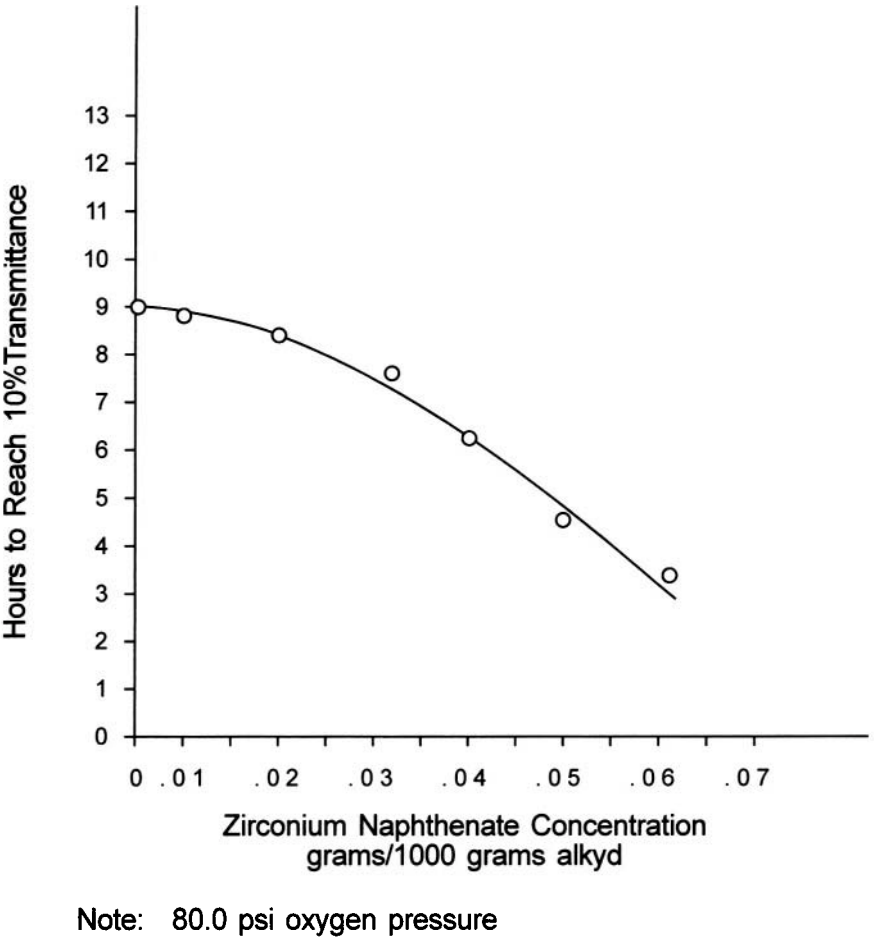

Figure 3.18. Zirconium naphthenate concentration vs. reaction rate.

iranchembook.ir/edu

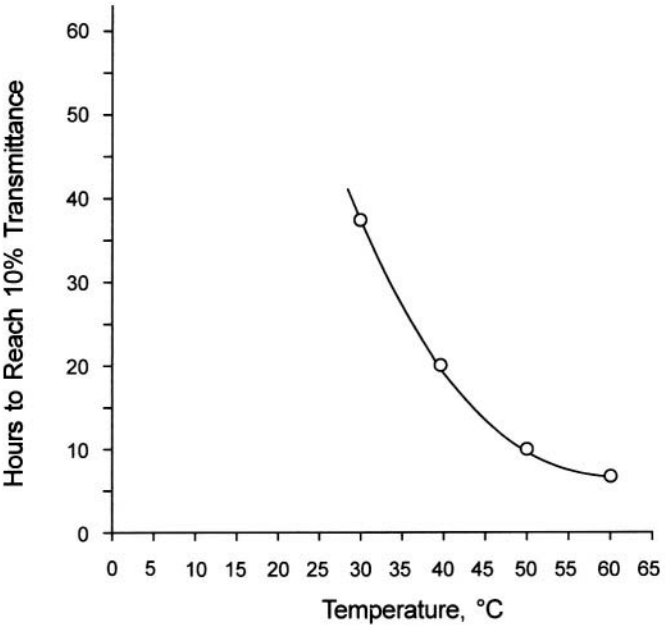

Figure 3.19. Reaction temperature vs. reaction time, reagent grade.

3.5.6. Molecular Weight Effect

Gel permeation chromatography (GPC) was used to evaluate molecular weight and observe the effects of autoxidative polymerization. The weight-average molecular weight (M_w) of unreacted alkyd resins ranged from 789-934 grams/mole and between 2550-3500 grams/mole after autoxidation, but not completely crosslinked or gelled that would have made the alkyd only swellable and not soluble in the hydrofuran carrier phase. The K and a constants (Mark-Houwink Equation) used to generate the GPC chromatograms were developed for medium oil linseed alkyd resins. In all cases these molecular weights, before and after autoxidation, were similar, regardless of the reaction conditions and catalysis. After about 3500

iranchembook.ir/edu

grams/mole the polymerized resin was insoluble, as evidence by the swelling data discussed above, and actually was lightly crosslinked. The GPC chromatograms showed less retention time and a more narrow single peak for the polymerized alkyd emulsions compared to a bimodal peak for the unpolymerized emulsions. The polymerized alkyd particles flowed into each other and coalesce to form a smooth continuous film on glass plates, but further crosslinking produced more viscous particles that dried to form rough films. As proven previously in swelling experiments, the polymerization mechanism proceeds via crosslinking of alkyd molecular chains which quickly increases the viscosity of an alkyd particle compared to chain- or step-polymerization mechanism.

3.6. Studies on Emulsion Particle Size

The emulsion by itself is not defined without specifying the average particle size and particle size distribution of the polymer within the emulsion. The particle analysis of these emulsions will be determined individually in studies consisting of series of samples. The first study will consist of particle size change with respect to reaction time (Figure 3.20). The second study (Figure 3.21) will determine particle size change with respect to homogenization, which will ascertain the minimum amount of energy needed to disperse the oil or alkyd phase. The third study will examine particle size after one year of shelf storage to yield actual shelf stability data.

3.6.1. Particle Size with Reaction Time

A Coulter-Counter^{R} model TAII was used with an M3 Data Converter, and a 15-micron aperature to investigate the particle size changes during autoxidations. The limiting particle size changes during autoxidation. The limiting particle diameter for this method is 0.20 microns. Figure 3.22, Particle size vs. Reaction Time, illustrates that the average particle size decreases slightly with increasing reaction time. Table A. 11 in the Appendix lists the data points for Figure 3.22. The data for Table A. 11 was collected for the individual reaction time samples and the particle size distributions are shown in Figures A.4-A.17 in the Appendix as cumulative and differential curves. The data for construction of these curves was taken from data pints listed respectively in Tables A.13-A.16 in the Appendix.

iranchembook.ir/edu

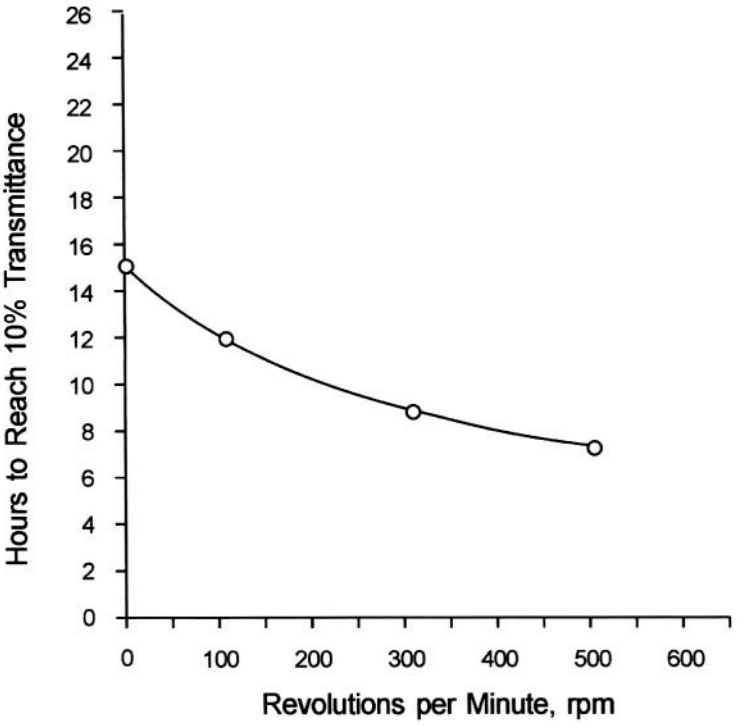

Figure 3.20. Agitation rate vs. reaction time, technical grade.

iranchembook.ir/edu

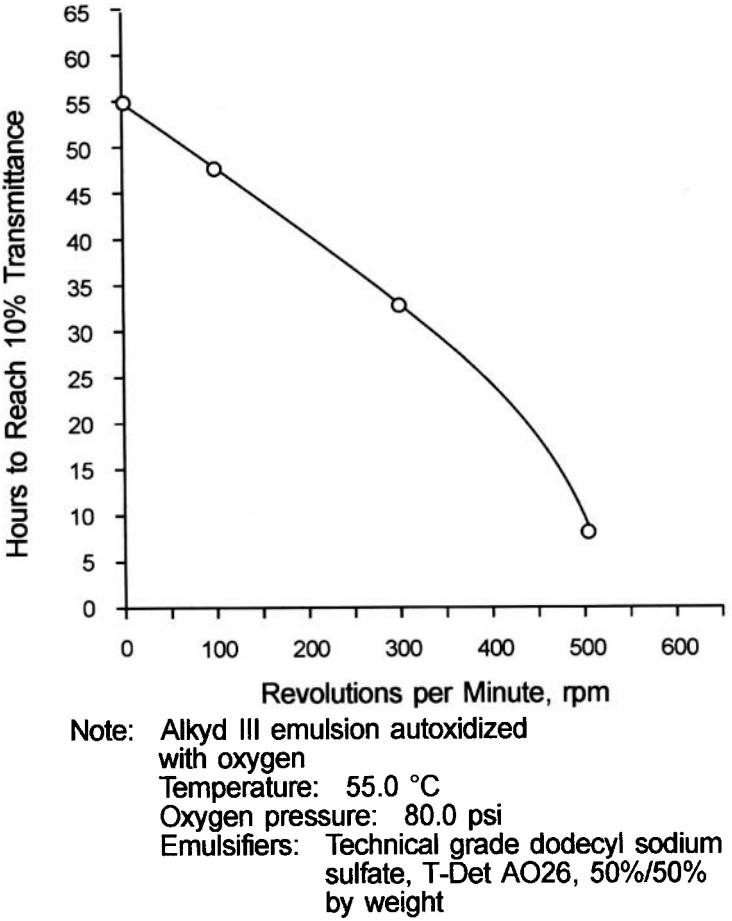

Figure 3.21. Agitation rate vs. reaction time, reagent grade.

iranchembook.ir/edu

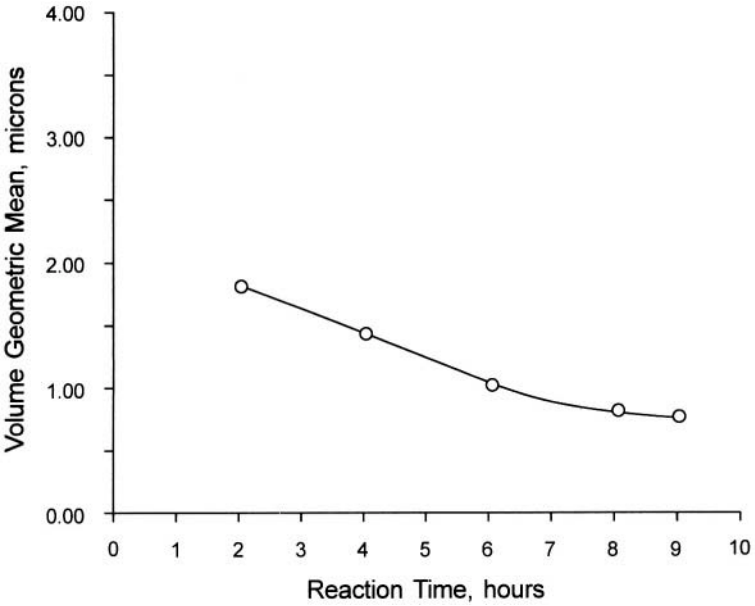

Figure 3.22. Particle size vs. reaction time, technical grade.

The particle diameters are based on data contained in Figures A.23-3.27 and Tables A.12-A.16. The volumetric particle diameter is indicated by the relative volume occupied by particles in a given volume of emulsion. The population of particles of a given diameter is indicative of the number of particles of that diameter within a volume. As a particle decreases in diameter, it also decreases in volume and increases with surface to mass ratio. Therefore, the term that best expresses the average particle diameter is volume geometric mean, microns. The population geometric mean is different from volume geometric mean as noted in Figures A.28-3.32 in the Appendix and Tables A.17-A.21, also in the Appendix. The explanation for this difference is related to the different statistical methods for calculation of these mean values. Volume geometric mean is calculated from percent particle size by volume and population geometric mean is calculated from the number of particles of each diameter.

iranchembook.ir/edu

By observing Figure 3.22, it is obvious that the average particle size (volume geometric mean) is decreasing slightly. The explanation for this trend can be understood by observing the particle distribution of the samples. It can be seen from Figures A.13-A.22 and Tables A.12-A.21 that the larger particle diameters are decreasing, which increases the percentage of particles are subdivided into smaller particles due to the constant turbulent agitation during autoxidation within the reaction vessel. There is no opportunity for sedimentation under these conditions. However, change of average particle diameter was insignificant. In conclusion, Figure 3.22, and the accompanying study have proven that average particle diameter does not change significantly with reaction time.

3.6.2. Average Particle Size with Homogenization

The energy required to homogenize or disperse the alkyd polymer phase within the aqueous phase, corresponds to the final average particle diameter, assuming sufficient emulsifier is present. It is useful and important to know the reduction of particle size with homogenization. The Gaulin Laboratory **Homogenizer**^{R} (Technical Bulletin, 1977) was employed to the particle size of the pre-emulsified medium soya alkyd particles. A sample was taken after each homogenization cycle and analyzed for particle size distribution and average particle diameter. The homogenizer was operated at a shearing force of 3500 pounds per square inch (**248 kg/cm**^{2}).

Figure 3.23, Particle Size vs. Homogenization Cycles, illustrates the change of average particle diameter with increasing homogenization. The change is insignificant after the first cycle and this demonstrates that one cycle is sufficient to reduce the particle size to an acceptable figure and that additional homogenization does not significantly change the average particle size. Table A.22 in the Appendix lists the data points for Figure 3.23. These data points were collected from an individual analysis of each sample by utilization of the **Coulter-Counter**^{R}. The particle distribution of each emulsion sample is illustrated in Figures A.23-30 in the Appendix and data points for construction of these Figures are listed in Tables A.23-A.30 in the Appendix. The average particle diameter (volume geometric mean, microns) is found at the bottom of each table, together with median, mode, and standard deviation.

3.6.3. Particle Size after One Year of Shelf Life

It is important to know the emulsion stability with relation to shelf life. Therefore, a sample of alkyd III was set aside in the laboratory for

iranchembook.ir/edu

twelve months and the particle size was measured by the Coulter-Counter^{R}. Table 3.46, Emulsion Particle Size after One Year, represents the average particle diameters one-day after preparation of the emulsion and one year after preparation of the emulsion and after having been autoxidized with oxygen.

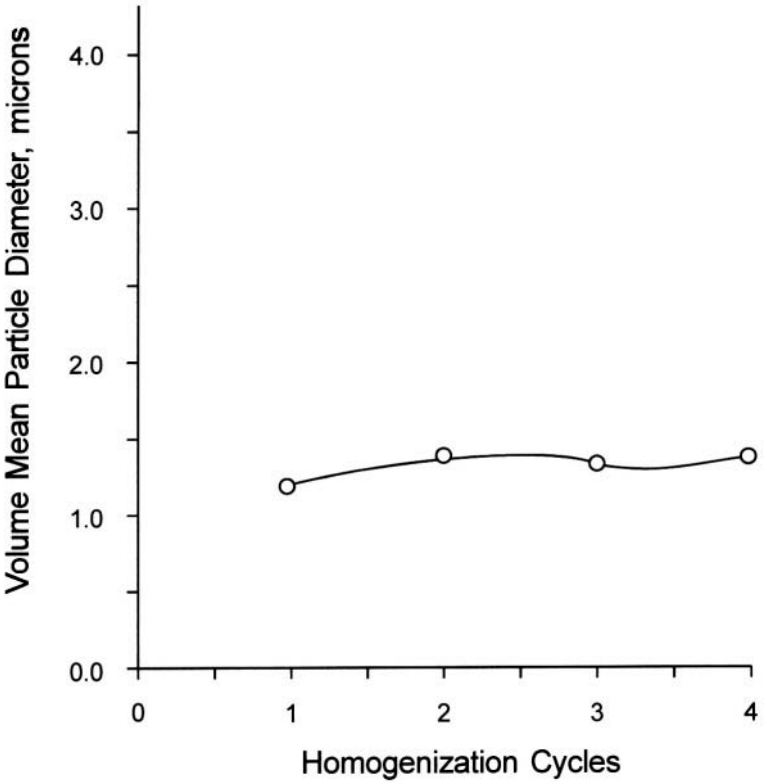

Figure 3.23. Particle size vs. homogenization cycles.

iranchembook.ir/edu

Table 3.46 Emulsion Particle Size after One Year

Volume Geometric Mean Diameter, Microns	
One Day	One Year
0.41	0.81

Note: soya urethane alkyd emulsion

The average particle diameter increased significantly, but remained under one micron in diameter. The one year aged sample was stirred to insure a uniform sample for particle size analysis. The aged sample was intact and showed no indications of instability. Referring to the one-day sample, Figure A.31 in the Appendix is the particle distribution by volume. Figure A.32 in the Appendix is the particle distribution for the one-year sample by volume. Tables A.31and A.32, also in the Appendix, are the lists of the data points and mean values for each figure and follow each figure consecutively.

In summary, the autoxidation reaction does not change the average particle size of the emulsion significantly while the emulsion is stable and intact. Homogenization after one cycle at 3500 psig (246 kg/cm^2) does not reduce the average particle size significantly. Soya urethane emulsion remains stable after one year of shelf life and the average particle size does not increase significantly enough to destabilize the emulsion.

3.7. Alkyd Oil Length and Conjugation Study

Variation of the amount of vegetable oil present in an alkyd polymer was studied to determine the effect of vegetable oil, or oil length, on the reaction time. The significance of this study is related directly to the required composition of the alkyd polymer for crosslinking of the emulsified polymer particles. The oil length of the alkyd polymer influences the crosslinking reaction and the degree of change with respect to reaction time must be determined. The autoxidation experiments were conducted at atmospheric pressure and with pure oxygen. The results are based upon a constant 48.0-hour reaction time.

The amount of conjugation within the alkyd polymer can influence the reaction time of the crosslinking reaction. It is therefore important to ascertain the degree of influence on the reaction from the viewpoint of

iranchembook.ir/edu

polymer conjugation within the total polymer composition. The experiments that will establish these trends will consist of an identical series of reactions with the percent conjugation of oil in the alkyd composition as the single variable.

3.7.1. Alkyd Oil Length Study

Alkyd oil length variation was studied with respect to dry time, tensile strength and intrinsic viscosity. Alkyds of varying percent soya oil were selected for this together with a soya urethane alkyd and short tall oil alkyd. The structure of alkyd materials and nomenclature are described by Martens (1974) and the only variation in this study will be oil length or percentage of oil in the alkyd structure.

Table 3.47 represents a series of alkyd materials having been autoxidized with oxygen for 48.0 hours each. The tables lists the initial characterization of the alkyds with dry time after reaction and Table 3.48 represents the properties after 48.0 hours of reaction with oxygen at atmospheric pressure. Upon inspection of Table 3.45, it can be seen that intrinsic viscosity increases in each case, but alkyds containing 30, 52, and 60 percent soya oil crosslink beyond solubility and therefore the intrinsic viscosity cannot be measured. The greater crosslinking in each of these alkyds is accompanied by an increasing drying time after 52% soya oil. Therefore, dry time increases with an increasing percent of soya oil in the same basic alkyd structure. Referring to tensile strength, it can be seen that tensile strength decreases with increasing soya oil in the alkyd. Elongation increases with increasing soya oil in the alkyd.

The soya urethane alkyd consists of a urethane linkage in the chain structure of the alkyd polymer. It can be seen that the soya urethane alkyd develops a comparable dry time with the mentioned soya alkyds, but the intrinsic viscosity is obtained which means that the emulsified alkyd particles are not gelled, but still flowing. The tensile strength is greatest of the alkyds described in Table 3.47 and the elongation of the soya urethane free film is comparable to the other materials. The short tall oil alkyd produced a dry time comparable to the soya oil alkyds and its dried free films produced a tensile strength slightly greater than the soya oil alkyds. However, the soya urethane alkyd possessed the highest tensile strength.

iranchembook.ir/edu

Table 3.47 Characterization of Oxygen Reacted Alkyd Emulsions[a] of Varying Oil Length at Atmospheric Pressure – Part A

Alkyd Type[b]	Intrinsic Viscosity		Tensile Strength Kg/cm^2	% Elongation
	Initial	Final		
VII	0.048	0.090	21.47	51.2
II	0.030	Insoluble	5.2	43.4
III	0.040	Insoluble	4.3	56.8
V	0.056	Insoluble	3.60	117.5
VI	0.020	0.022	---	---
VIII	0.036	Insoluble	5.18	304.0

[a] Emulsions were prepared by identical methods in each reaction, 50.0% alkyd, 2.0%Igepal CO-850 and 2.0% Dupanol, weight/weight alkyd, and 46.0% water.

[b] Each Alkyd material was utilized from standard industrial source together with solvent.

Note: Constant agitation rate of 60.0 rpm for all reactions in 1.0-liter reaction vessels and atmospheric pressure conditions for 48.0 hours.

Emulsion studies were conducted on the alkyd emulsions autoxidized in Table 3.48. The mentioned emulsion samples were studied for accelerated heat stability as described in Table 3.49. The emulsifier combination is also described in this table and it can be seen that the emulsifier combination is constant for each emulsion. The stability of these emulsions is decreasing with increasing oil content in the alkyd structure. The soya urethane alkyd possesses a good stability since 14.0 days is considered excellent stability for an emulsion. The soya extra-long oil alkyd does not appear in the table since it did not produce an acceptable film and

iranchembook.ir/edu

was eliminated from this study. Short tall oil alkyd was omitted from Table 3.49 since it is not a soya oil alkyd ad this study is attempting to eliminate variables. The oil length or content is the only variable in Table 3.49. The freeze-thaw stability is described in Table 3.50, utilizing emulsion samples from Table 3.48. It can be seen upon inspection of this table that the freeze-thaw stability is constant except for the soya long oil alkyd, which possesses a improved freeze-thaw stability. Three-to-five cycles are preferred for freeze-thaw stability. However, the freeze-thaw stability of these systems may be improved by addition of ethylene glycol to the aqueous phase.

Table 3.48 Characterization of Oxygen Reacted Alkyd Emulsions of Varying Oil Length at Atmospheric Pressure – Part B

Alkyd Type	Acid Value (max.)	% Oil (Oil Length)	Dry Time, Hours Tack-free	Oxygen Flow cm^3/min.	Temperature ^oC
VII	4	62	1.0	708	55
II	12	30	1.0	708	55
III	10	52	1.0	708	55
V	12	60	1.1	708	55
VI	8	80	---	708	55
VIII	12	36	1.0	708	55

iranchembook.ir/edu

Table 3.49 Accelerated Shelf Emulsion Stability

Alkyd	Emulsifier	Maximum Stability, Days @ 62.8 °C
VII	Nonylphenoxy (ethylene oxide)$_{20}$ alcohol + Dodecyl sodium sulfate	12
VII	Nonylphenoxy (ethylene oxide)$_{20}$ alcohol + dodecyl sodium sulfate	11
VII	Nonylphenoxy (ethylene oxide)$_{20}$ alcohol + dodecyl sodium sulfate	9
VII	Nonylphenoxy (ethylene oxide)$_{20}$ alcohol + dodecyl sodium sulfate	14

Note: Emulsions were autoxidized for 48.0 hours at 1.0 atmosphere of oxygen.

iranchembook.ir/edu

Table 3.50 Emulsion Freeze-Thaw Stability

Alkyd	Emulsifier	Freeze-Thaw, Stability Cycles
VII	nonylphenoxypoly- (etheneoxy)$_{20}$ alchol + dodecylsoldiumsulfate	1
VII	nonylphenoxypoly- (etheneoxy)$_{20}$ alchol + dodecylsoldiumsulfate	1
VII	nonylphenoxypoly- (etheneoxy)$_{20}$ alchol + dodecylsoldiumsulfate	1
VII	nonylphenoxypoly- (etheneoxy)$_{20}$ alchol + dodecylsoldiumsulfate	2

Note: Emulsions were autoxidized for 48.0 hours at 1.0 atmosphere of oxygen.

3.7.2. Alkyd Conjugation Study

The amount of conjugation of the olefinic unsaturation present in an alkyd should have a significant effect on the autoxidation rate. Experiments were designed to study the effects of conjugation upon reaction time. Table 3.49 represents the formulations for synthesis of alkyds for the study of conjugation effects on the autoxidation reaction. The only variable in the formulation of this series of alkyds is the percentage of conjugation in the fatty acids employed in synthesizing the alkyd. The fatty acids selected are described in Table 2.3. It can be seen upon inspection of this table that the percent of conjugation varies. It can also be seen from inspection of the same table that there are two different sources of fatty acids. **Pamolyn**^{R} fatty acids are products manufactured by the Hercules Corporation and **Sylfat**^{R} fatty acids are products of the Sylvachem Corporation. All of these materials are vegetable derivatives. Differences between the sources are a result of method of manufacture. The specific amount of conjugated lenoleic acid is listed for each fatty acid together with reaction time required to achieve

iranchembook.ir/edu

10.0% transmittance, equivalent to a swelling ratio of 3.2. Figure 3.24 represents a plot of percent conjugation and reaction time for both sources of vegetable derived fatty acids. The curves in Figure 3.24 show the trends of reaction with increasing conjugation for each fatty acid source.

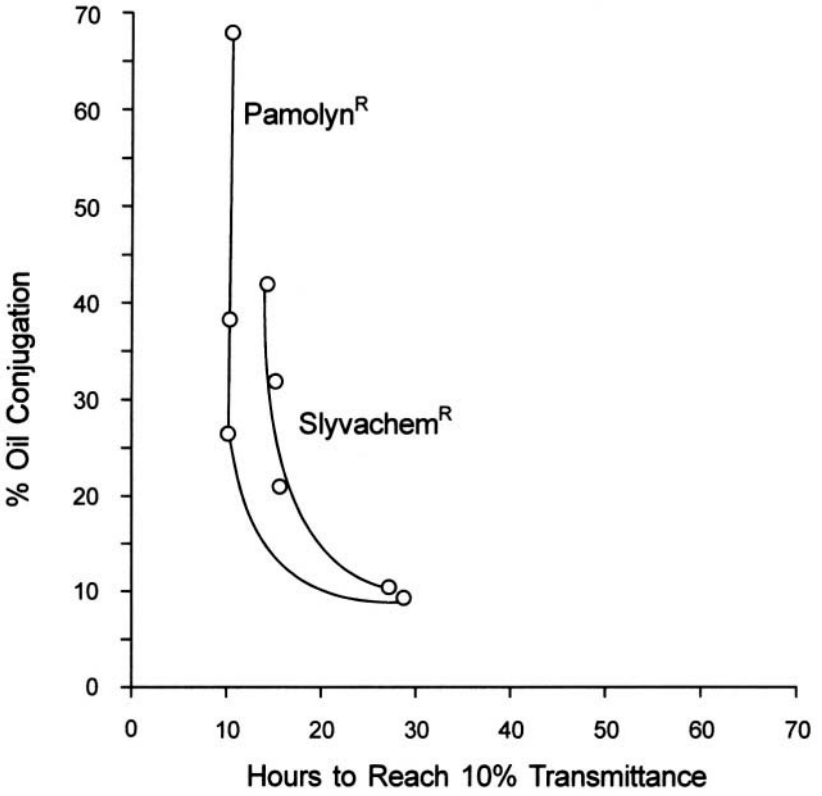

Figure 3.24. Oil conjugation vs. reaction time.

In summary, the effect of increasing oil length for pure soya alkyds decreases tensile strength with a slight increase in elongation. The tack-free dry time increases about 0.1 hour from 30% oil length to 60% oil length, there is a very long dry time.

The soya urethane alkyd possesses an oil length of 62%, but the tensile strength of the dried free film was about four times greater than the leading pure soya film. It is obvious that the urethane unit within the soya urethane alkyd enhances the physical properties of this material. The

iranchembook.ir/edu

elongation of the urethane alkyd was comparable to that of the pure soya alkyds was tensile strength of the dried films.

The short tall oil alkyd possessed an oil length of 36% with a tensile strength comparable to the short soya oil alkyd, which was expected due to similarity of structure. Dry time of the short tall oil alkyd was comparable to the short soya oil alkyd counterpart as shown in Table 3.47. Therefore, there is little difference between the tall oil and soya oil equivalent structures based on the evidence from Table 3.47. The emulsion stability of the soya urethane alkyd was good, but pure soya oil alkyd stability was greatest for the long oil alkyd and the short and medium oil alkyds were stable. All of these emulsions possessed acceptable stability for processing and examination.

The effect of conjugation definitely influences the reaction rate as graphically illustrated by the curves in Figure 3.24. Since conjugation typically is capable of stabilizing radicals, it was expected that reaction rate would increase, but the small change in rate between 20% and 70% conjugation was not expected. These data must be interpreted to indicate either that the amount of unsaturation present is of greater importance than the "percentage of it that is conjugated," provided that the non-conjugated unsaturation is only separated by a single methylene unit as was the case here. Otherwise, the interpretation must be that once an optimized rate is achieved through conjugated unsaturation, other "parameters in the system" become rate determining.

iranchembook.ir/edu

Chapter 4

EXPERIMENTAL RESULTS, RESEARCH AND COMMERCIALIZATION OF TECHNOLOGY

The primary conclusion to be drawn from the previous chapters relates directly to the autoxidative crosslinking processability of emulsions prepared from vegetable oils and vegetable oil derived alkyds. The emulsification parameters and conditions for autoxidative crosslinking have been studied in detail for optimization of emulsion stability after processing together with film properties from the emulsions.

4.1. Autoxidative Crosslinking of Vegetable Oil

It has been shown that stable emulsions may be prepared from soya oil as described in Chapter 2. Accelerated heat stabilities were obtained in excess of 14.0 days and equivalent to over six months of shelf stability at ambient conditions. However, the autoxidative crosslinking of the emulsified soya oil was very slow and produced films of poor tensile strength which were slow to dry, i.e., the films were tacky even after more than two days. These results were encouraging from the viewpoint that vegetable oil derived materials of higher molecular weight such as alkyds would autoxidize at a faster rate and films there-from should dry more completely.

Observing the intrinsic viscosity of the autoxidation reaction, it became obvious that an intrinsic viscosity of 0.046 of the oil would necessarily be surpassed in order to achieve improved film integrity. Catalysis did not achieve this purpose nor did increasing heat of reaction for processing of the emulsion. The preliminary result of this study served to investigate the autoxidative crosslinking of vegetable oil alkyds.

iranchembook.ir/edu

4.2. Autoxidative Crosslinking of Vegetable Oil Alkyds

After emulsifying an alkyd resin, processing conditions were studied for autoxidation at atmospheric pressure utilizing air and pure oxygen. Air autoxidation produced significant gas voids within the film that reduced film tensile strength, but did not impair drying of the films. Measurement of intrinsic viscosity demonstrated that the autoxidation reaction crosslinked the alkyd beyond the maximum intrinsic viscosity obtained with soya oil. The crosslinked alkyd produced an alkyd particle that possessed a small swelling ratio, less than 10.0, which indicates that the material is densely crosslinked. Oxygen autoxidation of the alkyd emulsion developed crosslinks faster than air and the alkyd emulsion formed a film of medium tensile strength and elongation. Increased oxygen pressure further increased the reaction rate. By observing the swelling ratio, the degree of crosslinking could be monitored and observing the swelling ratio could compromise a combination of drying time and crosslink density compromised for maximum tensile strength, i.e., flow and drying time of the films. Table 4.1 compares two leading acrylic emulsions with the vegetable oil alkyd films prepared in these laboratories. It can be seen that the commercial emulsions possess higher tensile strength than the medium soya alkyd, but the alkyd emulsion had a comparable dry time. The soya urethane emulsion possessed a tensile strength within the range of the commercial products, but its elongation is lower, though adequate in our opinion. The heat accelerated shelf stability test results are comparable. The freeze-thaw stability test results of all of the emulsions synthesized herein are less than is desired, but are improved by the post-addition of ethylene glycol.

Table 4.1 Comparison of Commercial Emulsions to Autoxidized Emulsions

Emulsion	Dry Time, Hours	Tensile Strength kg/cm^2	% Elongation	Stability (62.8 ^{o}C) days
Rhoplex AC-64	0.5	35.53	475	15
Amsco 3077	0.7	24.61	707	12
Autoxidized:				
Alkyd III	0.5	10.70	95.0	14
Alkyd VIII	1.0	21.47	51.2	15

iranchembook.ir/edu

4.3. Emulsification

Vegetable oil alkyds have been emulsified successfully and have remained stable after processing. The screening of emulsifying agents has eliminated slow emulsion reaction rates, low tensile strength and slow drying of films. Evidence from these chapters shows clearly that emulsifying agents preferably are aliphatic alcohols with ethylene oxide adducts in combination with an equivalent amount of dodecyl sodium sulfate.

The studies conducted in Chapter 3 give evidence that the average particle size changes insignificantly during the crosslinking reaction, the homogenization of emulsions is accomplished in a single cycle and additional homogenization is redundant. One year of aging of a soya urethane emulsion does not affect the average particle size significantly. The particle size studies demonstrate that the emulsions described in these chapters are processable and stable. These statements have been made in view of the imperatively correct emulsifier selection of emulsification.

The reaction rate increases with percent conjugation to about 20% conjugation and then other parameters appear to be autoxidation rate determining. Increasing oil length of alkyds decreases the tensile strength of dried alkyd films, but the urethane alkyd film tensile strength with 62% soya oil length. The urethane alkyd structure is apparently responsible for the tensile strength property of the dried film.

4.4. Continuing Research and Developments

Research continues inpart within the kinetic studies performed in Chapter 3. The relationship of oxygen concentration to the reaction rate of the emulsified to the reaction rate of the emulsified alkyd particles was determined, but the relationship of the alkyd concentration with reaction rate was discussed, but not performed. Experiments could be designed to determine the alkyd reaction order and the reaction constant in order to define the kinetics of the reaction more concisely.

The importance of the emulsifying agent together with its chemical structure was emphasized in Chapter 3, but the study did not concisely correlate emulsifier chemical structure with reaction rate. Also, the distinction between oxygen diffusion rate and autoxidation retardation was not clearly made for lack of experimental data. Since the emulsifier is a factor for autoxidation reactions of emulsified alkyd particles, then it follows that this investigation should continue. The vegetable oil materials have been purposefully limited in chemical structure and type in order to eliminate variables for these studies. However, the same studies could be expanded in

iranchembook.ir/edu

order to determine the processability of many different types of vegetable oil resins having been emulsified, and some examples follow.

Gooch and Hofland (1991) experimented with inverse-phase emulsification of alkyds in an aqueous solution of acrylic monomers. The acrylic monomers polymerized during the slow continuous feed of the aqueous solution of monomers into the warm alkyd resin, and the result was a stable emulsion of alkyd resin stabilized by acrylic polymer around each particle of resin. The free films formed from these emulsions were clear and uniform, but requiring drying metal catalysts. Autoxidative polymerization of the emsulsified alkyd particles reduced the dry-to-touch drying time of free films.

Naburs (1997) initiated a study on the polymerization and the morphology development of "alkyd-acrylic" composite emulsions as a continuation in-part of the above alkyd emulsion research. Alkyd-acrylic composite emulsions may offer opportunities toward the development of solvent-free binders in coatings thereby, providing the optimal properties of both alkyd and acrylic resins or polymers in one binder. In order to allow for the preparation of alkyd-acrylic composite emulsions containing no surfactant, alkyds were developed with built-in sulfonate groups. These alkyds were prepared according to a three-stage polymerization process. It was that incorporating sulfonate groups that the color of the alkyd was strongly affected. This effect was suppressed by adding a base during the second step of the polymerization process. The viscosity of alkyds synthesized with sulfonate groups increased at sulfonate concentrations of 100×10^{-6} mole/gram of alkyd. The interfacial tension between alkyd and waster was found to decrease sharply up to a sulfonate group concentration of 25×10^{-6} mole/gram, after which there is no change. Emulsifcation of alkyd with sulfonate groups, resulting in alkyd emulsions without free surfactant, was found to be more efficient at higher sulfonate group concentrations. The diameter of the emulsified alkyd-acrylic particle increases with very high sulfonate group concentration. The autoxidative initiation of polymerization for the alkyd component in the emulsified alkyd resin-acrylic monomers was performed using atmospheric oxygen (air) in the liquid emulsion at 60°C. It was shown that the molecular weight of the alkyd molecule increased due to chemical grafting of acrylic oligomers onto the alkyd chains by using Gradient Polymer Elution Chromatography. No phase separation was observed between alkyd resin and acrylic polymers. An applied film-formation and testing stage is planned for the materials prepared from these emulsions at the Laboratory of Polymer Chemistry, Eindhoven University, Eindhoven, The Netherlands.

Dong et al (2001) and Gooch et al (2000) developed novel products by grafting oil modified polyurethane resins onto acrylic polymeric moieties, via hydrogen abstraction mechanisms, in rniniemulsions. Draw-down films

iranchembook.ir/edu

on glass demonstrated acceptable hardnesses and adhesion. Wang et al (1996) prepared miniemulsions by grafting alkyds resins onto acrylic polymeric moieties. Miniemulsion polymerization offers some advantages over conventional emulsion (macroemulsion) polymerization systems. Among the advantages are a process that is more tolerant of contaminants, and a product with more uniform copolymer composition, narrow particle size distribution, and high shear-stability. The miniemulsion polymerization is a "batch" reaction compared to emulsion polymerization which is a continuous feed operation and subsequently, continuous. More specifically, each emulsified particle in a miniemulsion is an individual reaction separate from all other particles and with no continuous feed of monomers (Novel Water-Borne Coatings via Hybrid Miniemulsion Polymerization).

In some ways, the preparation of autoxidative polymerization of alkyd resins and vegetable oils was one of the first miniemulsions, possibly with the exception that the average particle size of the typical miniemulsion particle is significantly smaller. Miniemulsion polymerization involves the use of a more effective emulsifying system to produce very small monomer droplets (<500 nm). Particle nucleation occurs primary via radical entry into the small monomer droplets. These must be stabilized against coalescence and diffusional degradation. Coalescence may be precluded by the addition of an appropriate surfactant. Diffusional degradation, or Ostwald ripening can be eliminated by the addition of a small amount of a water-insoluble (hydrophobe), monomer-soluble stabilizer. Polymers, comonomers, and chain transfer agents have been reviewed as hydrophobes. Miniemulsions have some unique and desirable properties: They are far more robust to variations in the recipe or to contaminant levels than conventional emulsions. Particle number is less sensitive by at least an order of magnitude to changes in initiator, water-phase retarder, and oil-phase inhibitor concentrations than macroemulsion polymerizations from which typical latex paint dispersions are derived. Perhaps because of this robustness, it was possible to produce latex with a narrow polydispersity. Hydrophobic comonomers have been used successfully as hydrophobes. It has been found that such systems will give a more uniform copolymer composition since the supply of hydrophobic comonomer is not mass-transfer limited than in macroemulsion polymerization. Miniemulsion polymerization also can be used to produce copolymers in which one of the comonomers (i.e. macromers) is almost completely insoluble in water. Such copolymers are often not possible with macroemulsion polymerization. Finally, graft copolymers with alkyds, polyesters, urethanes, etc., can be made by hybrid miniemulsion polymerization, and may be the basis for a new generation of low volatile organic compound (VOC) alkyd coatings. A major effort in the development of miniemulsion technology is the Reaction Engineering Group (Director-

iranchembook.ir/edu

Dr. F. Joseph Schork), School of Chemical Engineering at the Georgia Institute of Technology, Atlanta, Georgia.

4.5. Commercialization of Alkyd Emulsions

The studies referred to in previous chapters were successful, and those innovations were patented by Gooch, Bufkin and Wildman (U.S. Patent 4,419,139), and the technology was applied to commercial "emulsified alkyd" products, originally by the Cargilll Corporation, but followed by other resin manufacturers. The exact nature of the manufacturing technology remains proprietary, but individual segments of the above work were applied to products including the emulsification of alkyd resins, without autoxidative polymerization, and allowed to form a cured hard film on a surface using a metal drier. This has been referred to as a "green" technology because is an environmentally friendly material and the materials utilized are renewable.

Sam Sung LTD Corporation of Seoul, Korea (Gooch, 1986) emulsified fish oil based alkyd resins and autoxidatively polymerized them to form consistent, flexible and hard films for can coatings including vegetable cans, toothpaste and others. The pigmented coatings exhibited a shorter dry-to-touch period that reduced the time from application of the coating to sheet metal stock to forming the container and filling the containers with product.

As petroleum prices rise and coating manufacturing regulations require lower VOC values, "green" technologies become more attractive in United States, Europe and other international markets.

iranchembook.ir/edu

APPENDIX - FIGURES

iranchembook.ir/edu

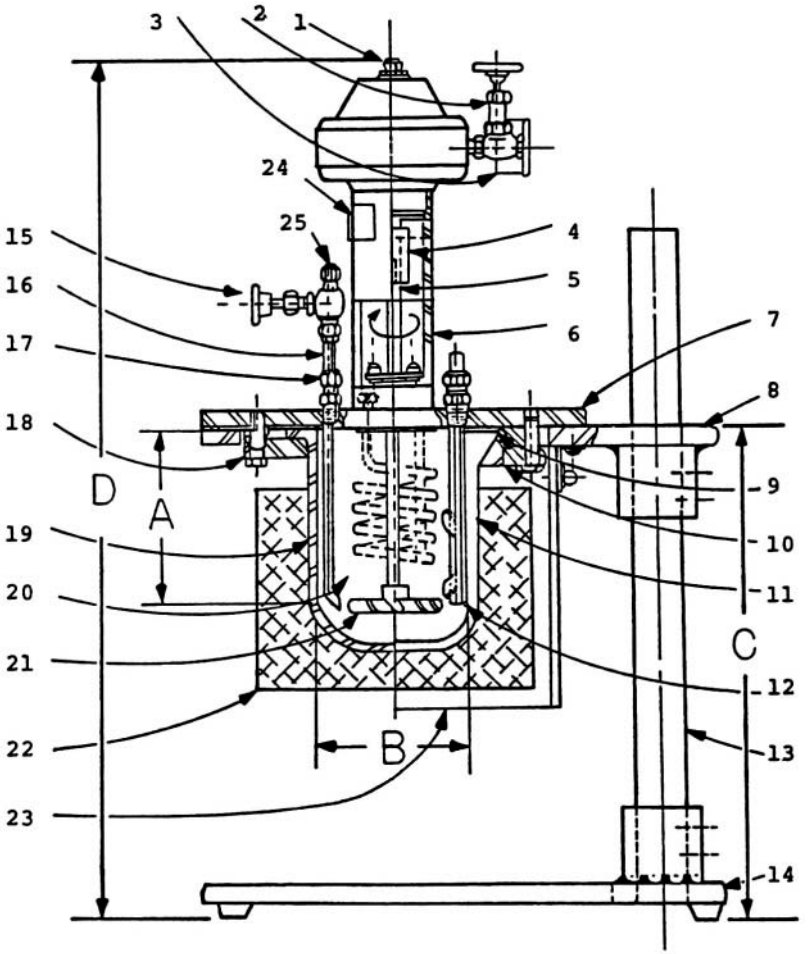

Figure A.1. Bench scale[R] mini-reactor pressure vessel, cross-sectional view.

iranchembook.ir/edu

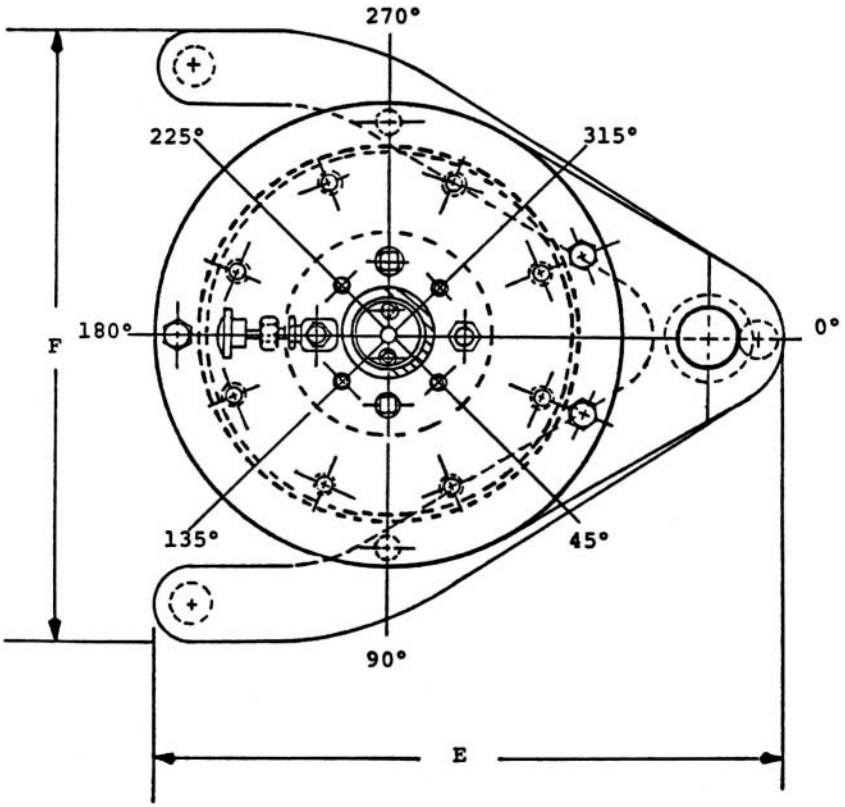

Figure A.2. Bench scale[R] mini-reactor pressure vessel, top view.

iranchembook.ir/edu

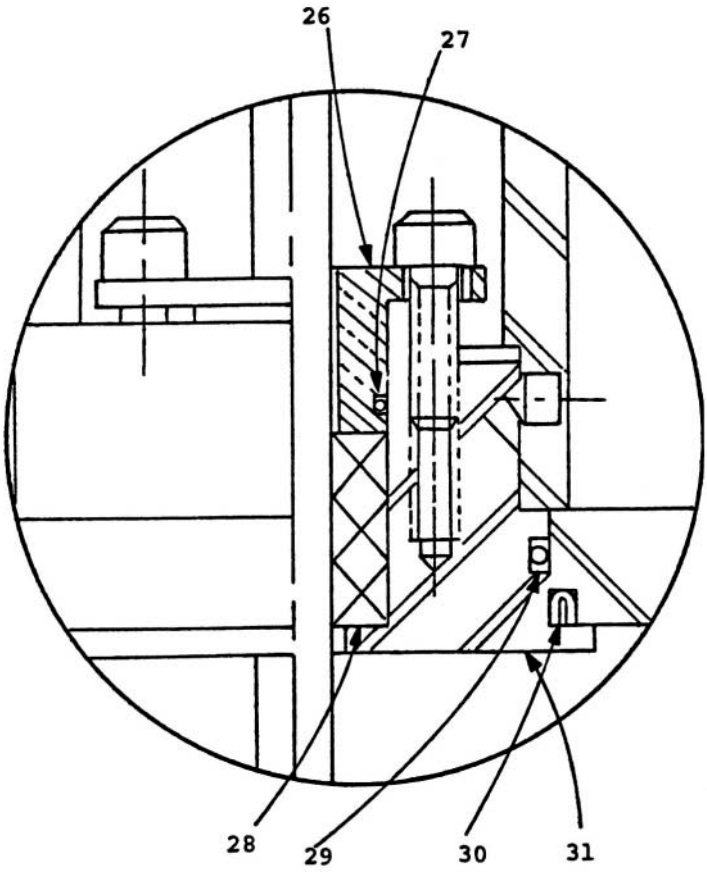

Figure A.3. Bench scale[R] mini-reactor pressure vessel, seals and packing cross-sectional view.

iranchembook.ir/edu

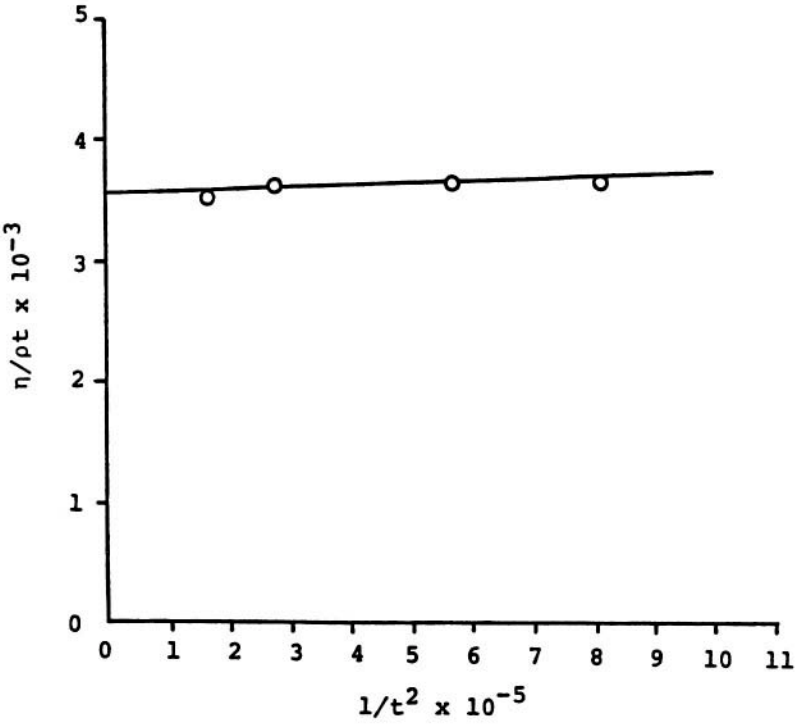

Figure A.4. Viscometer calibration curve.

iranchembook.ir/edu

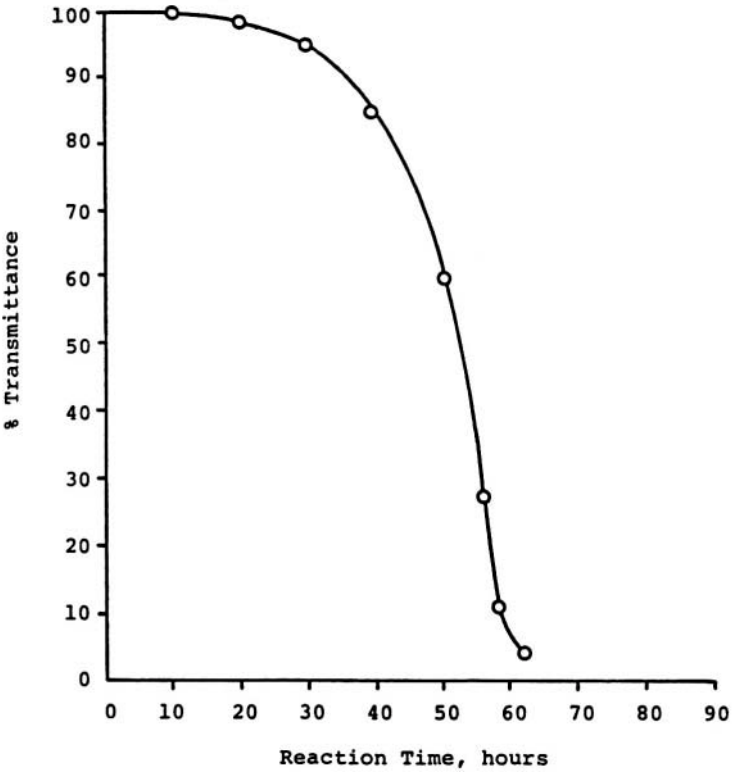

Note: Medium soya alkyd and water emulsion
autoxidized with oxygen
Temperature: 55°C
Catalysis: None
Agitation Rate, RPM: 300
Pressure, oxygen, psi: 10

Figure A.5. Reaction time vs. % transmittance, 10 psi.

iranchembook.ir/edu

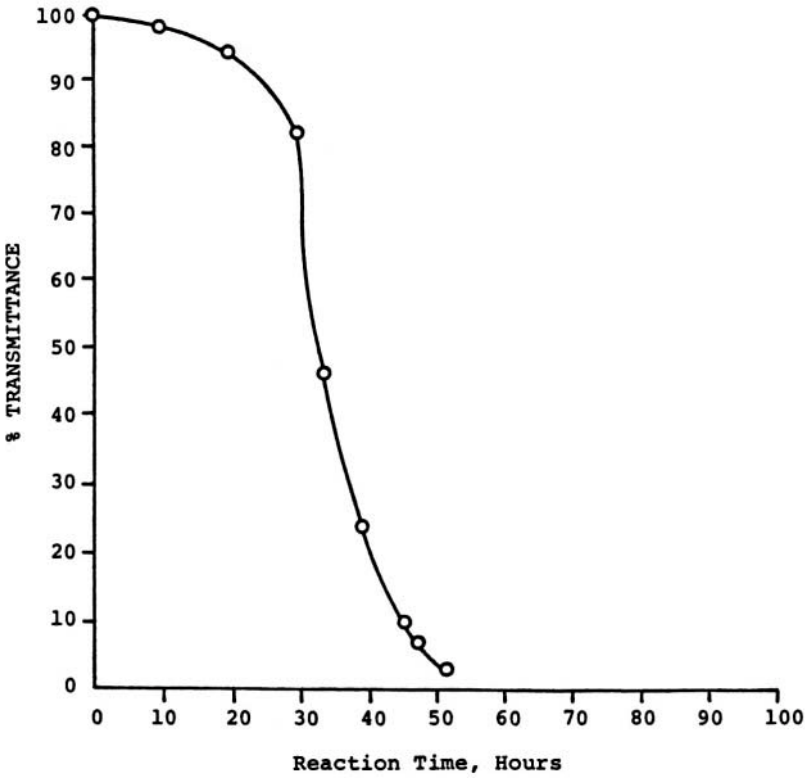

Note: Medium soya alkyd and water emulsion auto-oxidized with oxygen
Catalysis: None
Temperature: 55°C
Agitation Rate, RPM: 300
Pressure, Oxygen, psi: 20

Figure A.6. Reaction time vs. % transmittance, 20 psi.

iranchembook.ir/edu

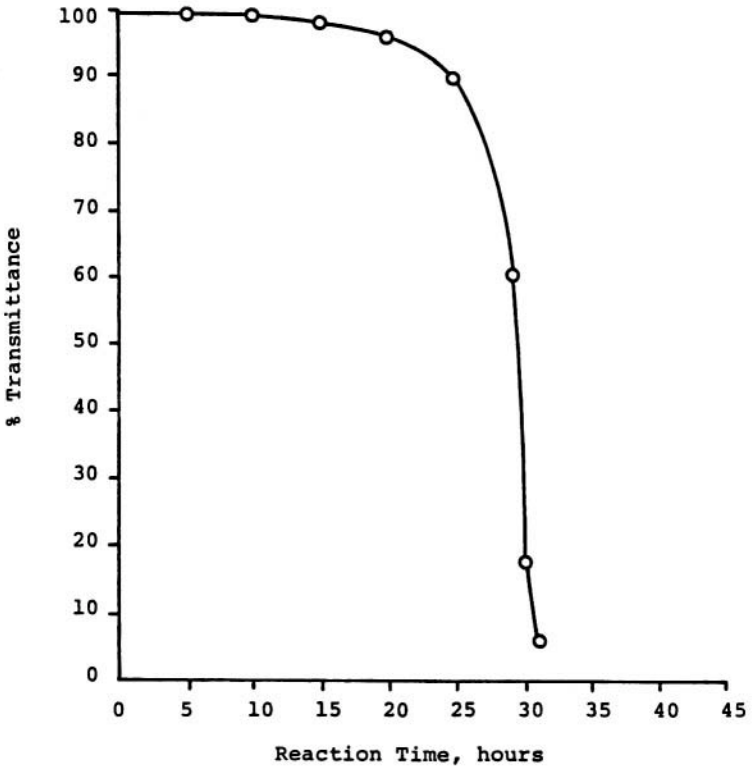

Note: Medium soya alkyd and water emulsion
autoxidized with oxygen
Temperature: 55°C
Catalysis: None
Agitation Rate, RPM: 300
Pressure, oxygen, psi: 30

Figure A.7. Reaction time vs. % transmittance, 30 psi.

iranchembook.ir/edu

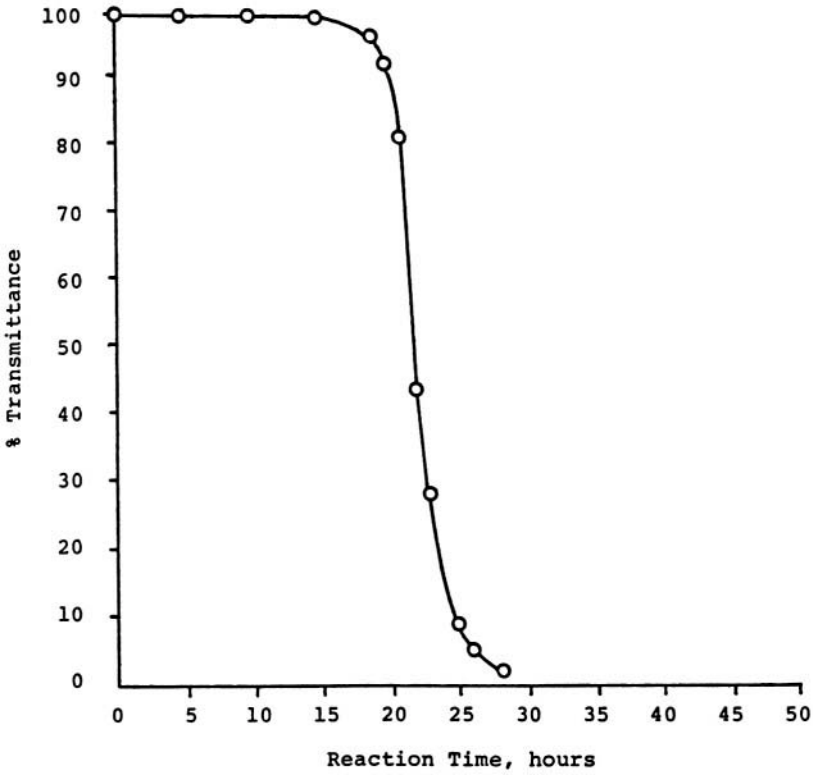

Note: Medium soya alkyd and water emulsion auto-oxidized with oxygen
Temperature: 55°C
Catalysis: None
Agitation Rate, RPM: 300
Pressure, Oxygen, psi: 40

Figure A.8. Reaction time vs. % transmittance, 40 psi.

iranchembook.ir/edu

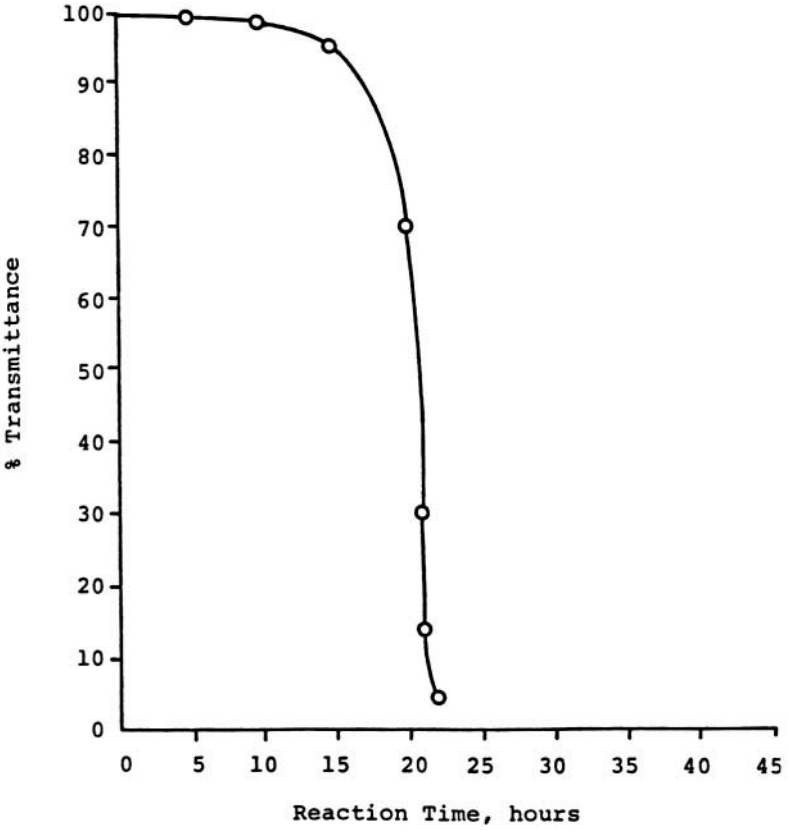

Note: Medium soya alkyd and water emulsion
autoxidized with oxygen
Temperature: 55°C
Catalysis: None
Agitation Rate, RPM: 300
Pressure, oxygen, psi: 50

Figure A.9. Reaction time vs. % transmittance, 50 psi.

iranchembook.ir/edu

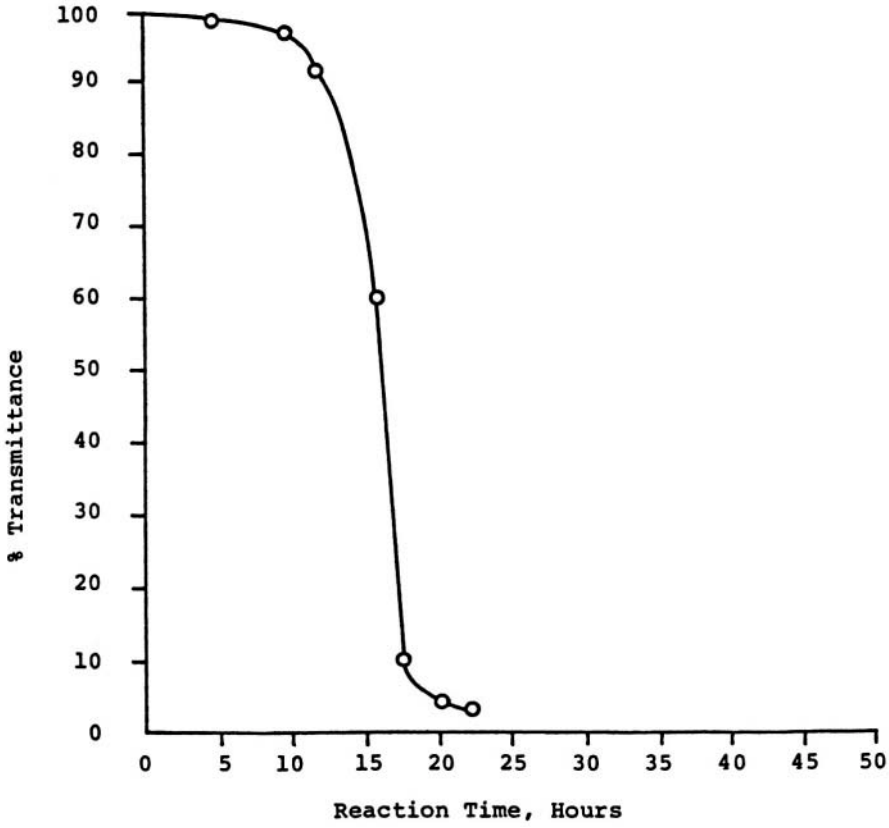

Note: Medium soya alkyd and water emulsion auto-oxidized with oxygen
Catalysis: None
Temperature: 55°C
Agitation Rate, RPM: 300
Pressure, Oxygen, psi: 60

Figure A.10. Reaction time vs. % transmittance, 60 psi.

iranchembook.ir/edu

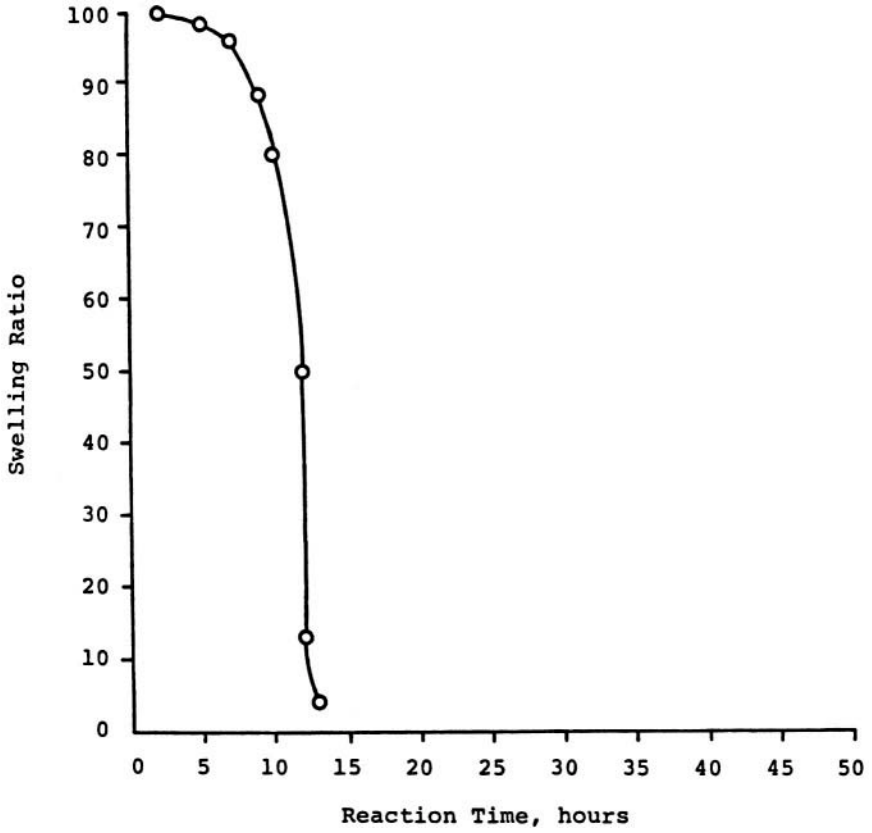

Note: Medium soya alkyd and water emulsion
autoxidized with oxygen
Temperature: 55°C
Catalysis: None
Agitation Rate, RPM: 300
Pressure, oxygen, psi: 70

Figure A.11. Reaction time vs. % transmittance, 70 psi.

iranchembook.ir/edu

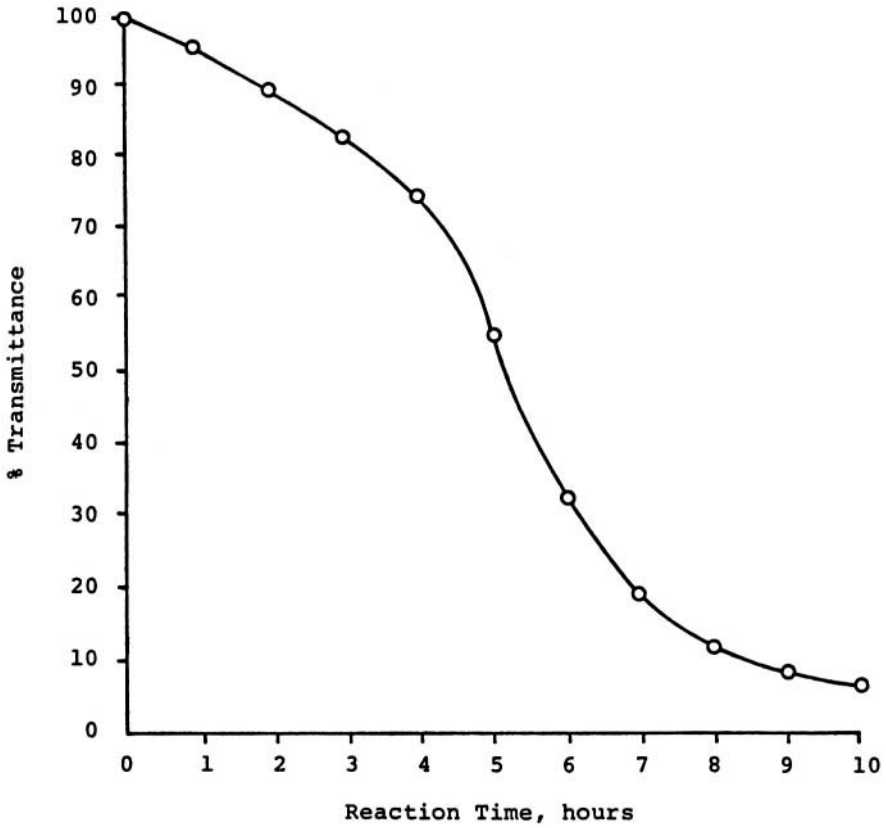

Note: Medium soya alkyd and water emulsion auto-oxidized with oxygen
Temperature: 55°C
Catalysis: None
Agitation Rate, RPM: 300
Pressure, Oxygen, psi: 80

Figure A.12. Reaction time vs. % transmittance, 80 psi.

iranchembook.ir/edu

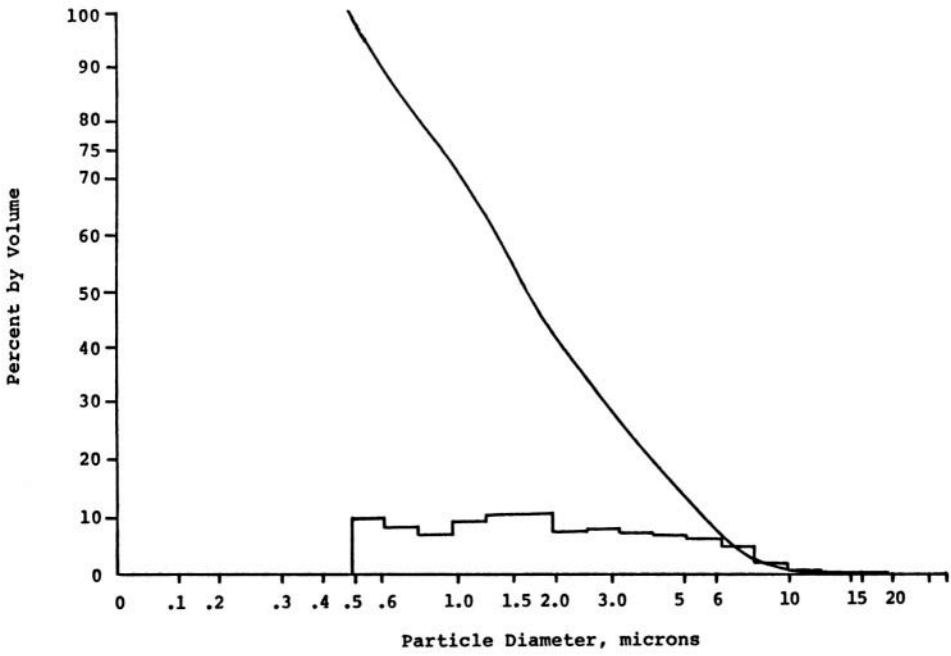

Figure A.13. Particle size distribution, 2.0 hours, by volume.

iranchembook.ir/edu

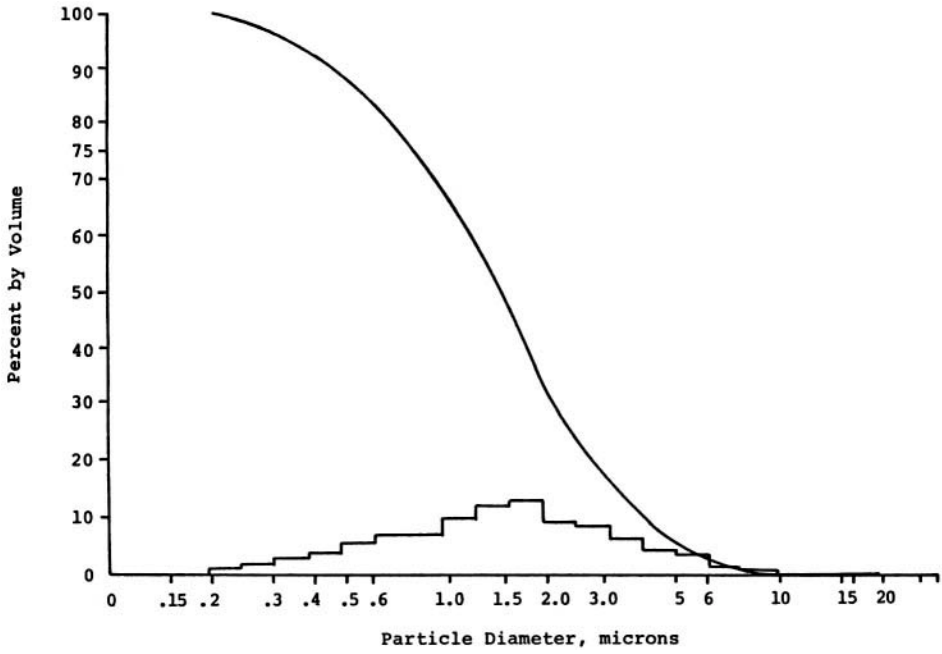

Figure A.14. Particle size distribution, 4.0 hours, by volume.

iranchembook.ir/edu

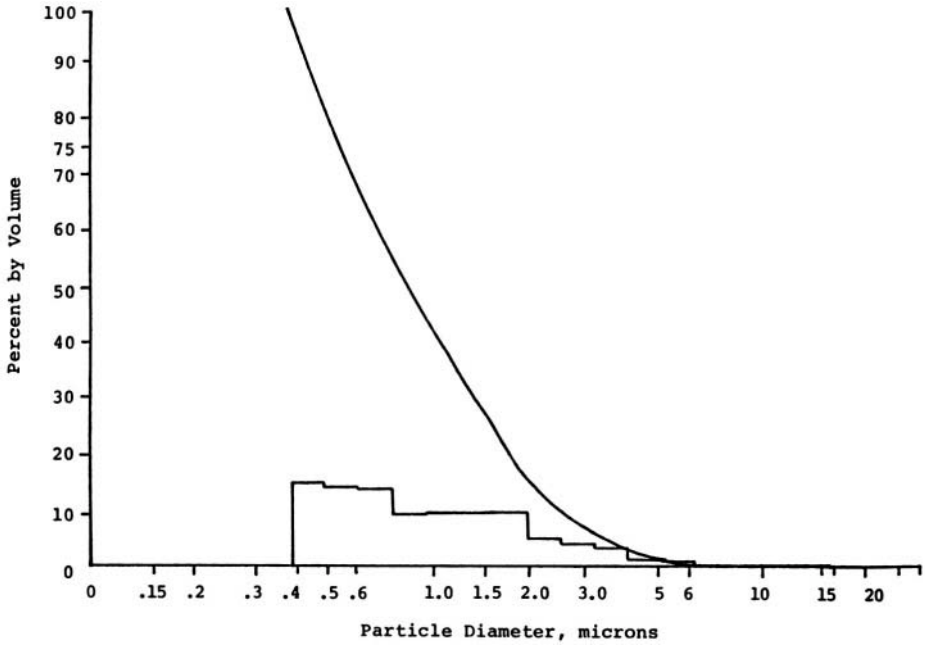

Figure A.15. Particle size distribution, 6.0 hours, by volume.

iranchembook.ir/edu

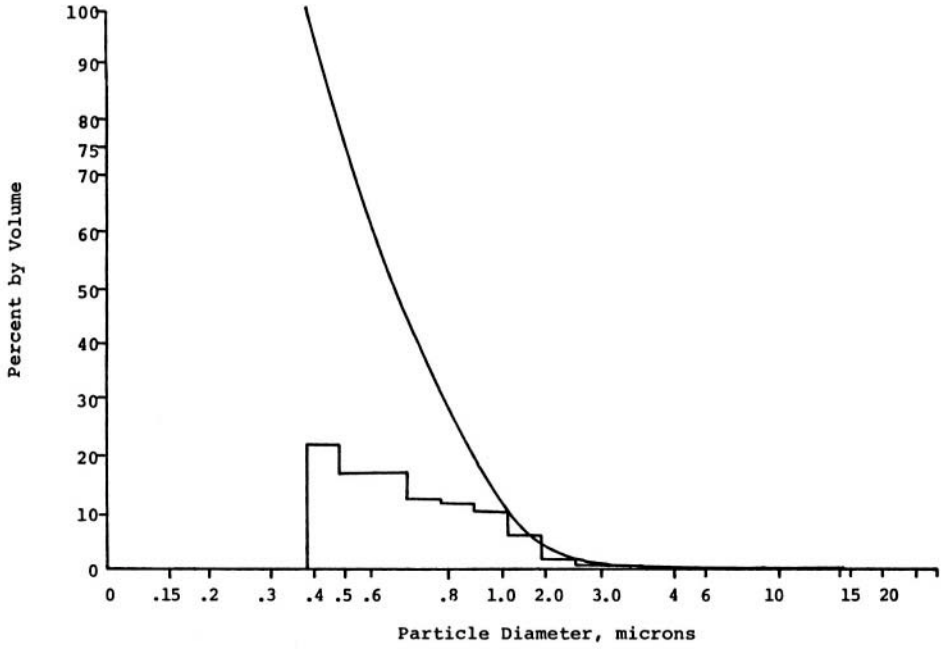

Figure A.16. Particle size distribution, 8.0 hours, by volume.

iranchembook.ir/edu

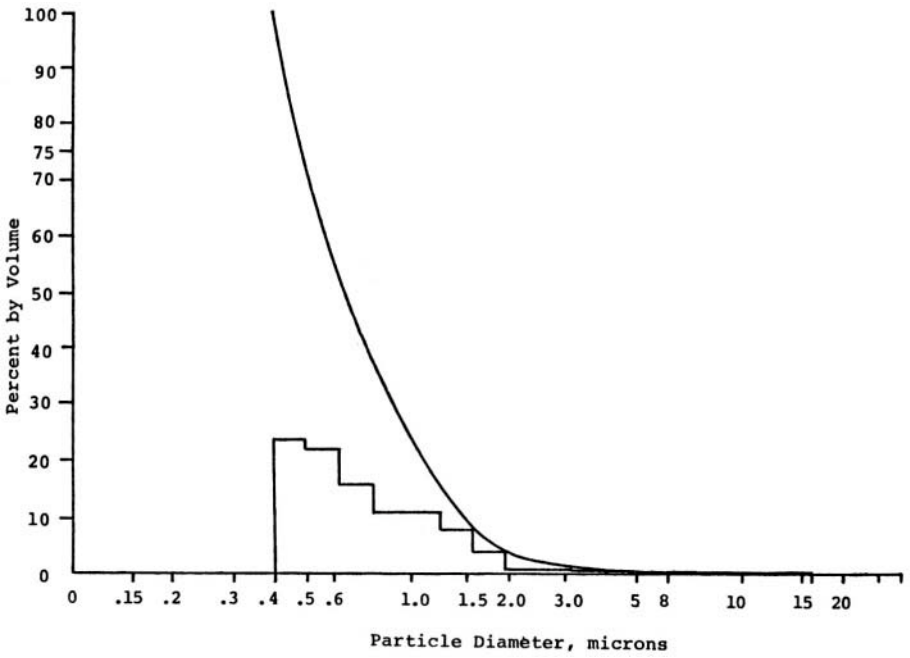

Figure A.17. Particle size distribution, 9.0 hours, by volume.

iranchembook.ir/edu

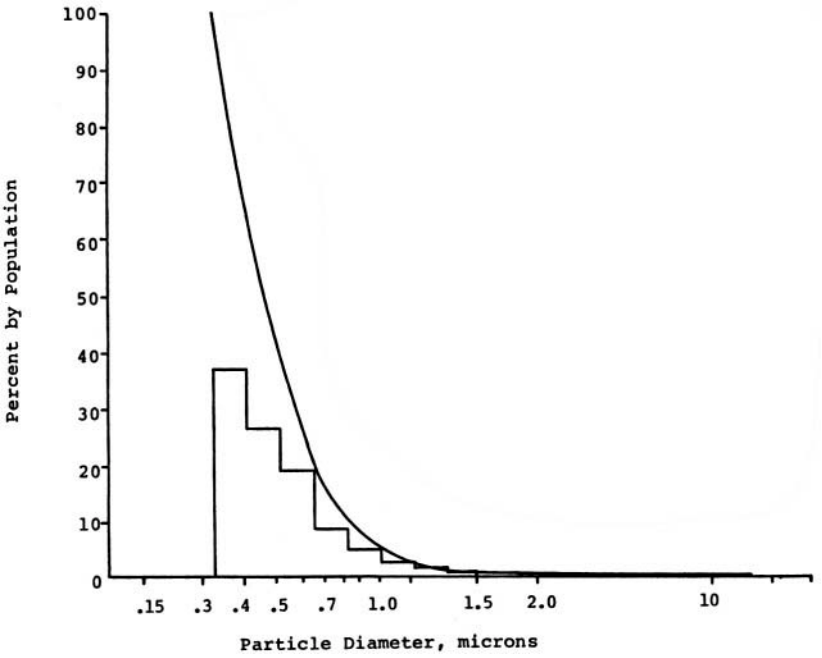

Figure A.18. Particle size distribution, 2.0 hours, by population.

iranchembook.ir/edu

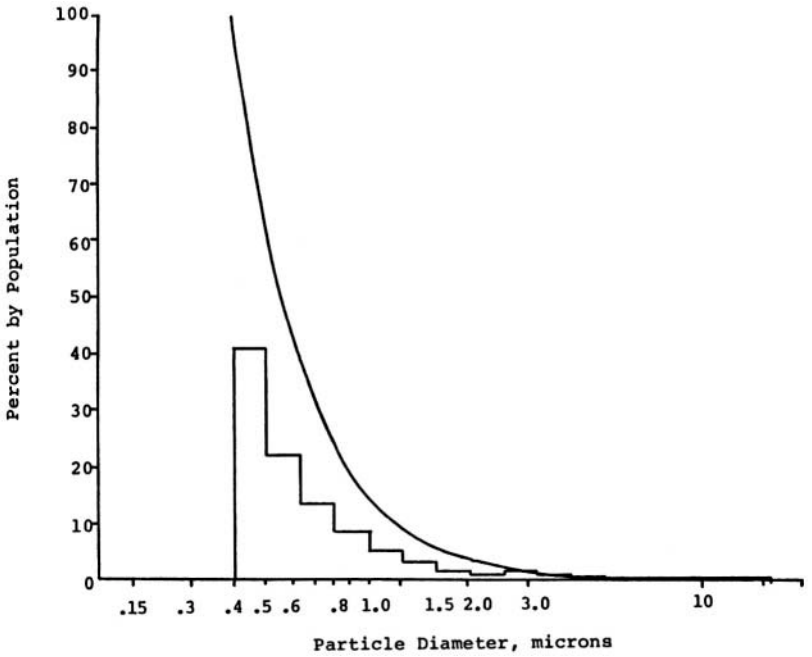

Figure A.19. Particle size distribution, 4.0 hours, by population.

iranchembook.ir/edu

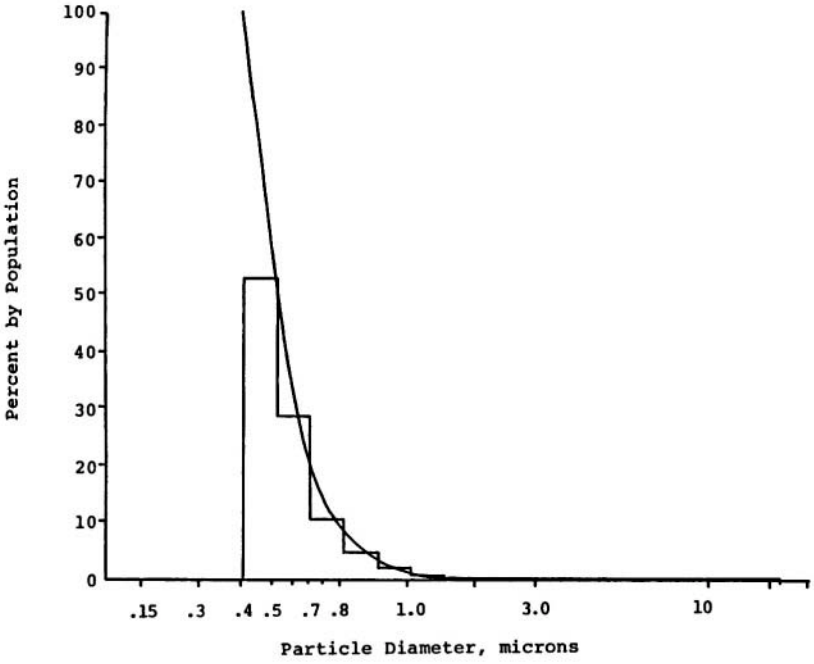

Figure A.20. Particle size distribution, 6.0 hours, by population.

iranchembook.ir/edu

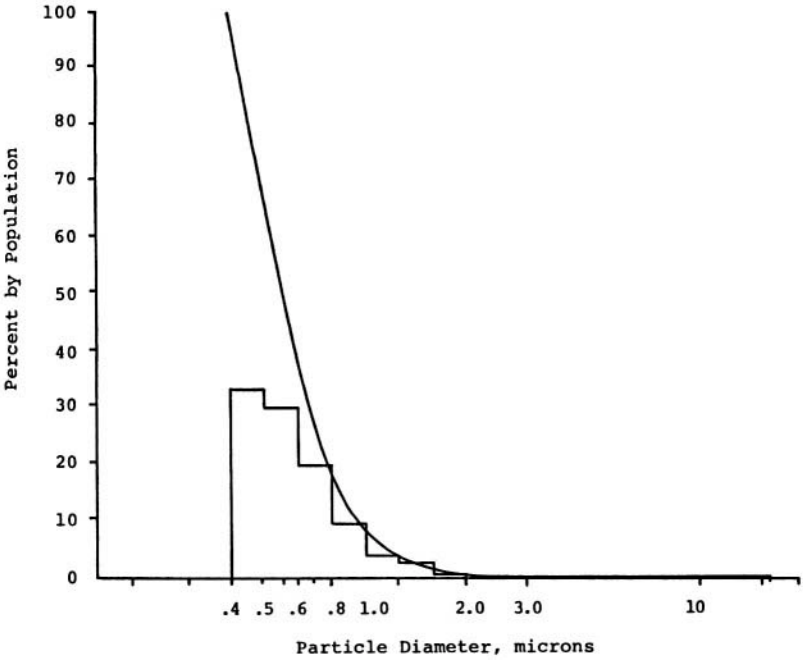

Figure A.21. Particle size distribution, 8.0 hours, by population.

iranchembook.ir/edu

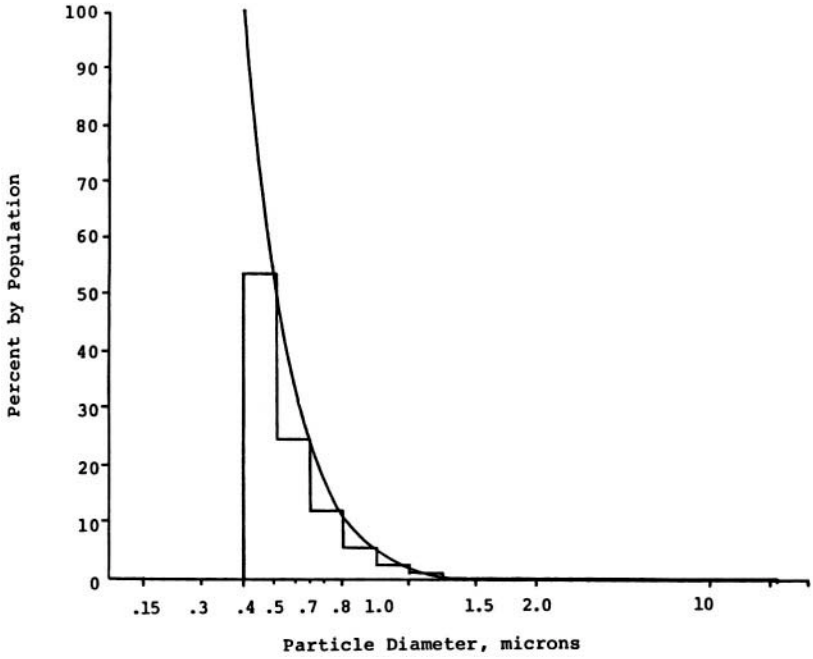

Figure A.22. Particle size distribution, 9.0 hours, by population.

iranchembook.ir/edu

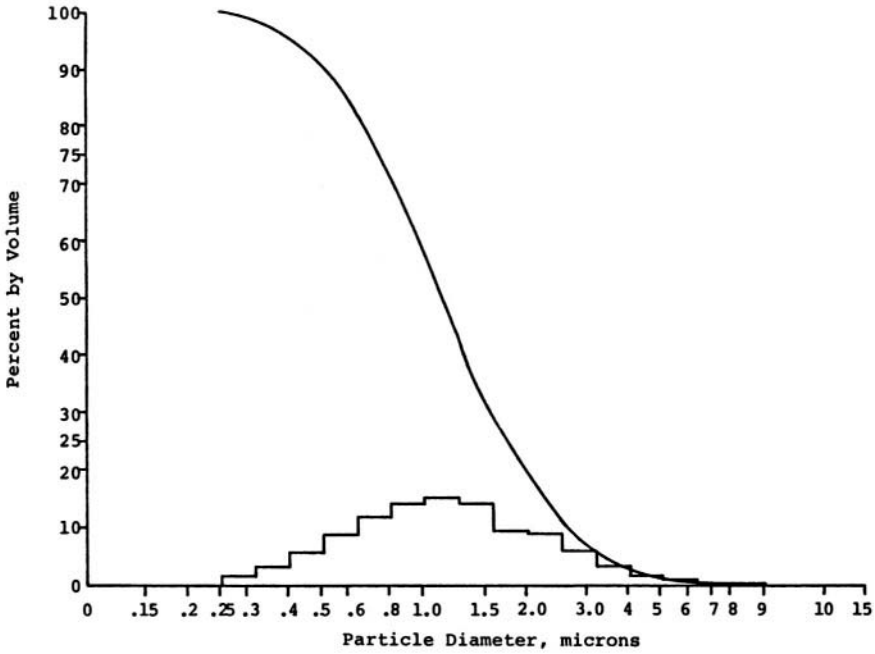

Figure A.23. Particle size distribution, 1 cycle, by volume.

iranchembook.ir/edu

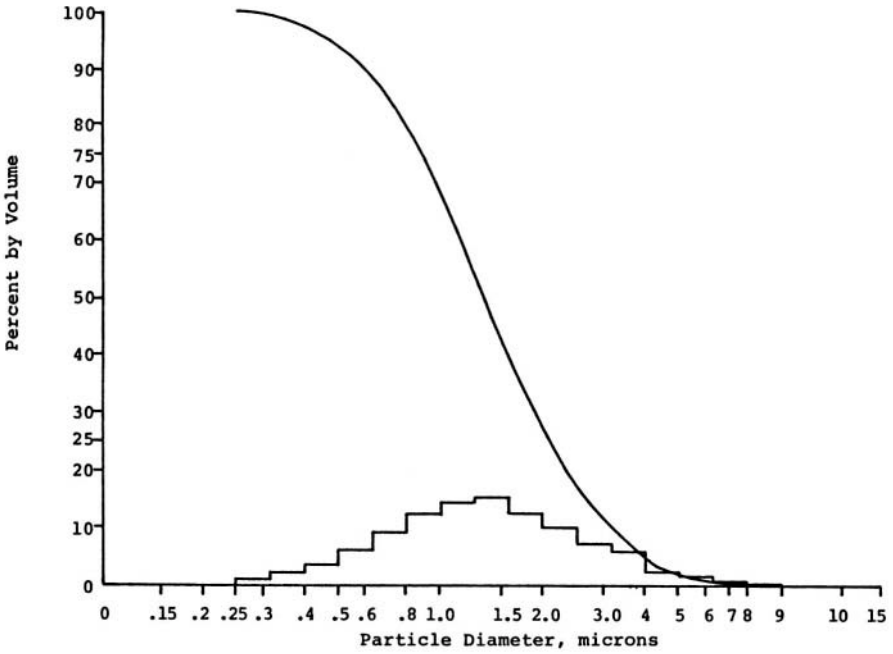

Figure A.24. Particle size distribution, 2 cycles, by volume.

iranchembook.ir/edu

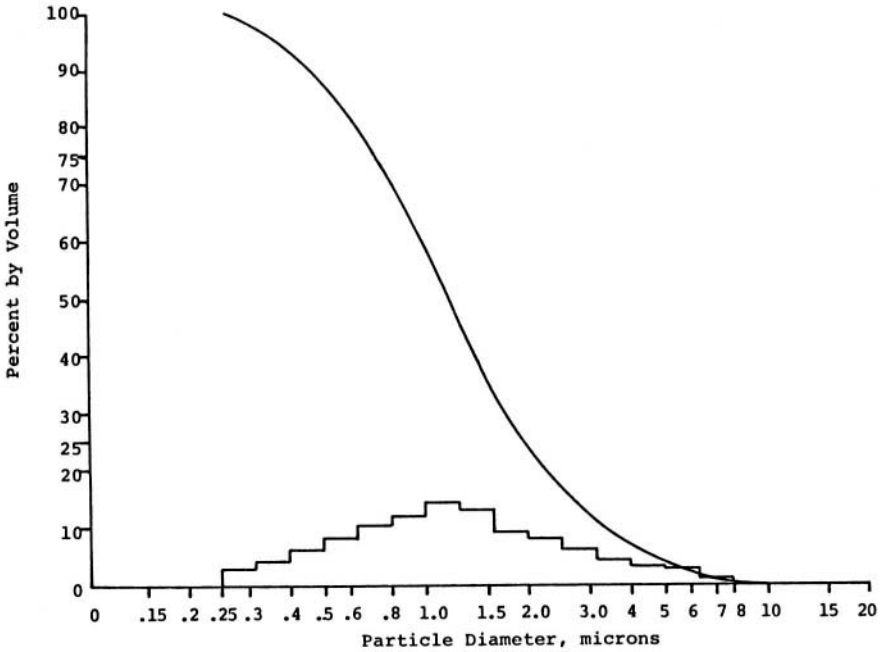

Figure A.25. Particle size distribution, 3 cycles, by volume.

iranchembook.ir/edu

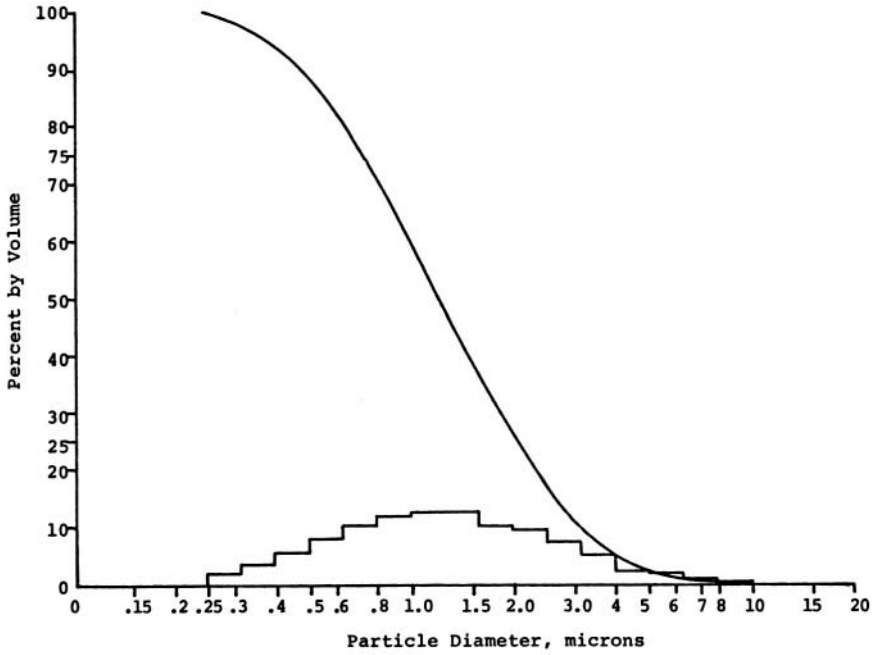

Figure A.26. Particle size distribution, 4 cycles, by volume.

iranchembook.ir/edu

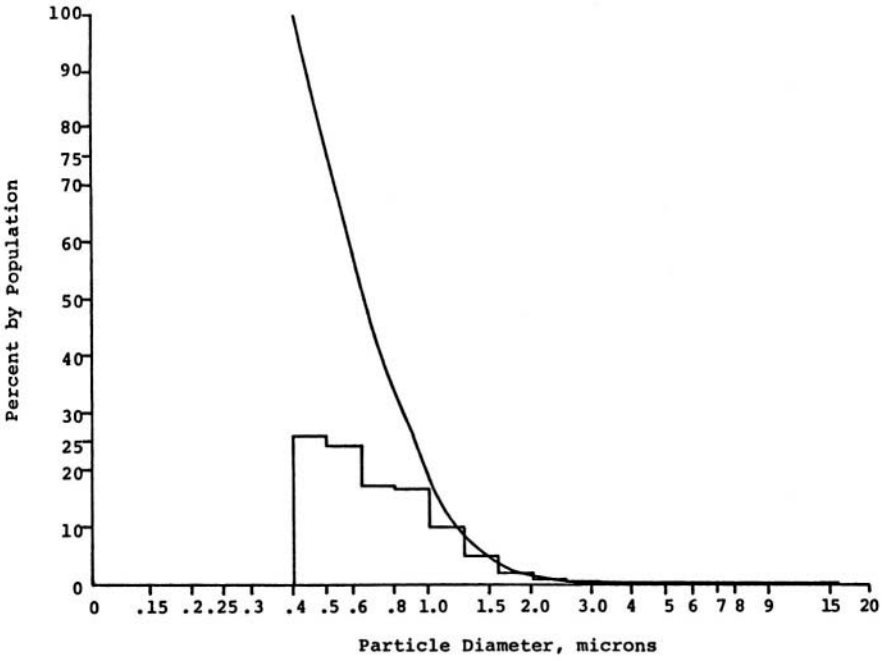

Figure A.27. Particle size distribution, 1 cycle, by population.

iranchembook.ir/edu

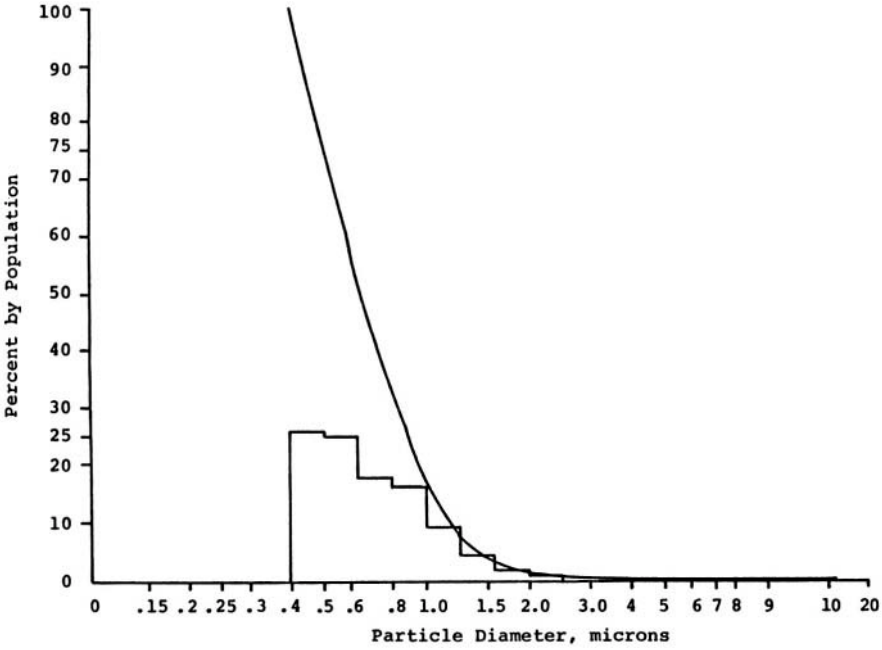

Figure A.28. Particle size distribution, 2 cycles, by population.

iranchembook.ir/edu

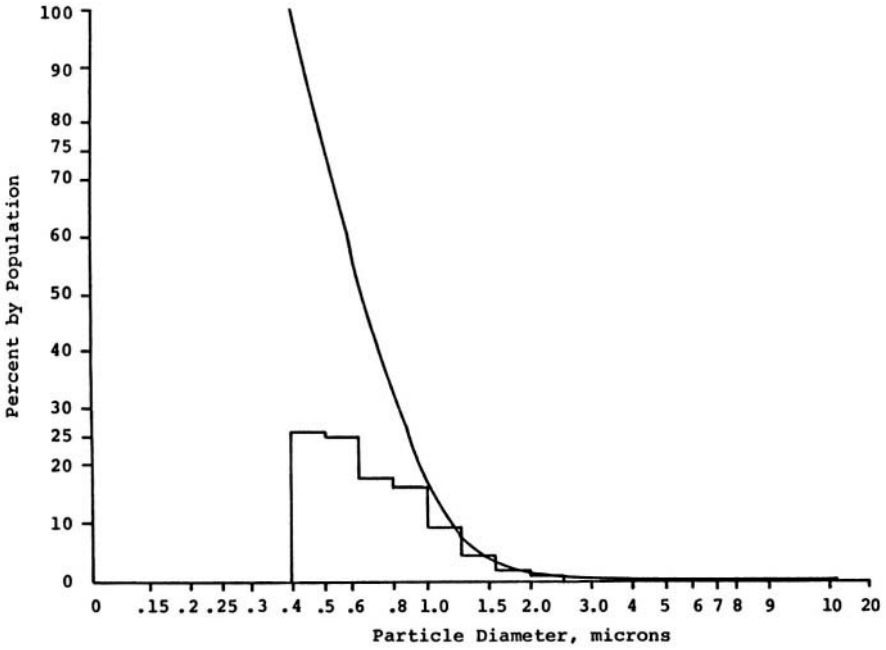

Figure A.29. Particle size distribution, 3 cycles, by population.

iranchembook.ir/edu

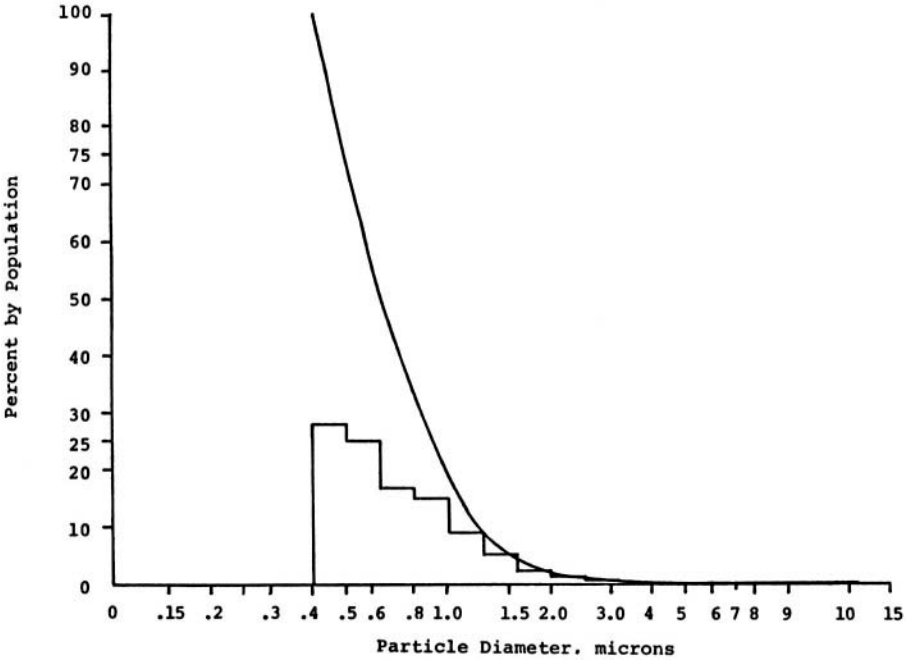

Figure A.30. Particle size distribution, 4 cycles, by population.

iranchembook.ir/edu

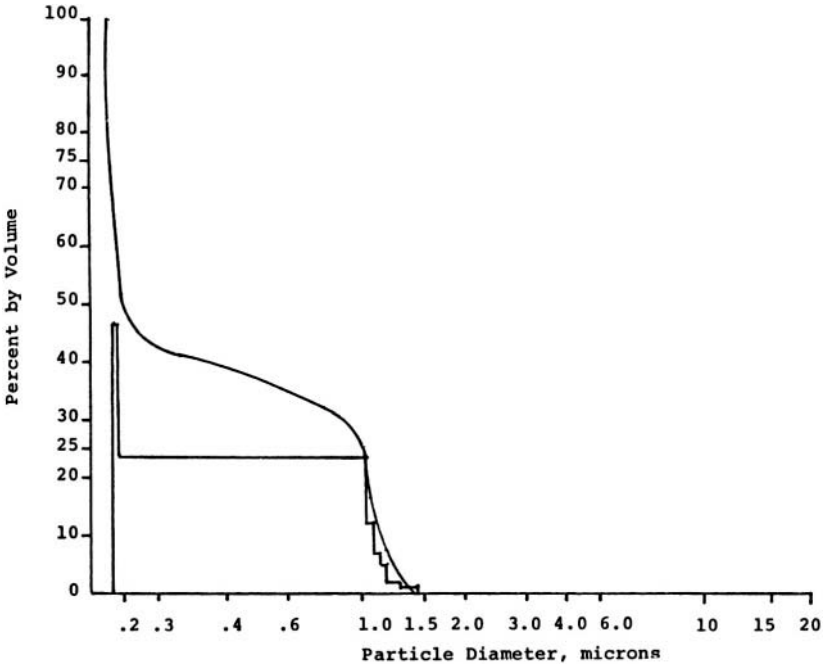

Figure A.31. Particle size distribution, 1 day, by volume.

iranchembook.ir/edu

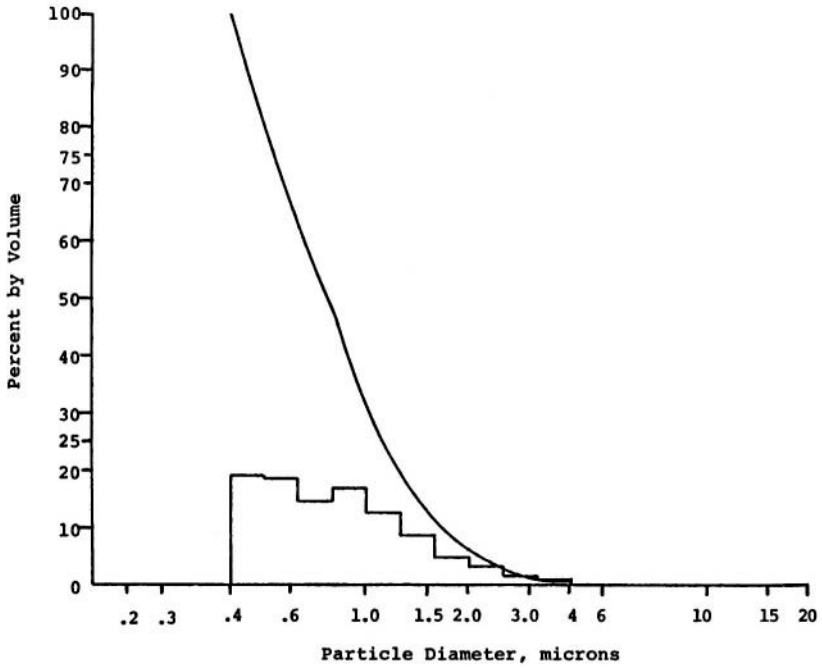

Figure A.32. Particle size distribution, 1 year, by volume.

iranchembook.ir/edu

APPENDIX - TABLES

iranchembook.ir/edu

Table A.1 Henry's Law Constants for Oxygen

t, °C	0	5	10	15	20	25	30	35
10^4 x H	2.55	2.91	3.27	3.64	4.01	4.38	4.75	5.07

t, °C	40	45	50	60	70	80	90	100
10^4 x H	5.35	5.63	5.88	6.29	6.63	6.87	6.99	7.01

Source: "International Critical Tables," vol.3, 257.

iranchembook.ir/edu

Table A.2 Henry's Law Constants for Air

t, °C	0	5	10	15	20	25	30	35
10^4 x H	2.55	2.91	3.27	3.64	4.01	4.38	4.75	5.07

t, °C	40	45	50	60	70	80	90	100
10^4 x H	5.35	5.63	5.88	6.29	6.63	6.87	6.99	7.01

Source: "International Critical Tables," vol.3, 257.

iranchembook.ir/edu

Table A.3 Air Dissolved in Water

Air Pressures Psi	Air Atmospheres	Air in Water Concentrations Moles/liter	Oxygen [a] in Dissolved Air Concentration Grams/liter
0	1.00	5.67×10^{-4}	3.43×10^{-3}
10	1.68	9.53×10^{-4}	5.76×10^{-3}
20	2.36	1.34×10^{-3}	8.10×10^{-3}
30	3.04	1.73×10^{-3}	1.05×10^{-2}
40	3.72	2.11×10^{-3}	1.28×10^{-2}
50	4.40	2.50×10^{-3}	1.50×10^{-2}
60	5.08	2.88×10^{-3}	1.74×10^{-2}
70	5.76	3.27×10^{-3}	1.98×10^{-2}
80	6.39	4.43×10^{-3}	2.68×10^{-2}

[a] Mole fraction of oxygen in air is 0.189 or 18.9%, oxygen is 20.946% in air by weight.

Note: Henry's Constant for air at 55°C = 9.78×10^4 atmospheres/mole oxygen in 1.0-liter water.

iranchembook.ir/edu

Table A.4 Oxygen Concentration Expressions

Oxygen Pressures Psi	Oxygen Concentration Grams/liter H_2O	Oxygen [a] Concentration Moles/liter
0	0.029	9.07×10^{-4}
10	0.049	1.53×10^{-3}
20	0.069	2.16×10^{-3}
30	0.101	2.85×10^{-3}
40	0.133	3.53×10^{-3}
50	0.145	4.21×10^{-3}
60	0.156	4.88×10^{-3}
70	0.176	5.51×10^{-3}
80	0.196	6.13×10^{-3}

[a] Henry's Constant at 55°C = 6.085×10^4 atmospheres/mole oxygen in 1.0 liter water.

iranchembook.ir/edu

Table A.5 Calibration of Viscometer A627 Viscometer Size 50

Sample	ρ25°C	$\frac{\eta}{C_P}$	t	η/pt	$1/t^2$
Acetone	0.7908	0.316	110.2	0.00363	0.0000823
Benzene	0.8790	0.608	189.9	0.00364	0.0000279
Ethyl Acetate	0.901	0.441	131.9	0.00371	0.0000575
Water	0.99707	0.894	256.5	0.00349	0.0000152

A = 0.003533
B = -1.84793
t = Flow time

iranchembook.ir/edu

Table A.6 Oxygen Concentration and Oxygen Partial Pressure in H_2O at 55°C

Kg/cm^2	0	1.41	2.81	4.22	5.62	7.03
$Lbs./in.^2$ (Relative)	0	20	40	60	80	100
Atmospheres	1.00	2.36	3.72	5.08	6.39	7.80
Millimeters Hg	760	1793.6	2827.2	4058.4	4856.4	5928.0
$\frac{\text{Grams } 0_2}{\text{Liter } H_20}$	0.029	0.069	0.113	0.156	0.190	0.228

iranchembook.ir/edu

Table A.7 Emulsifiers and Manufacturers

Trade Name	Manufacturer
Plurafac A-24	BASF Wyandotte Corporation, Chemical Group
Plurafac B-26	"
Plurafac D-25	"
Plurafac RA-20	"
Plurafac RA-30	"
Plurafac RA-40	"
Pluronic L61	"
Dupanol C	Du Pont Company
Gafac RA-960	GAF Corporation, Chemical Products
Igepal CO-430	"
Igepal CO-520	"
Igepal CO-530	"
Igepal CO-850	"
Triton X-207	Rohm and Haas Company
Triton X-363M	"
T-Det A026	Thompson-Hayward Chemical Company
T-Det C-40	"
T-Det TDA-65	"
T-Mulz 565	"
T-Mulz 596	"
T-Mulz 776	"

iranchembook.ir/edu

Table A.8 Legend for Figures 8-10

Item Number	Description
1.	Air motor for turbine drive, ½ horsepower maximum
2.	Air needle valve, ¼ inch, National Pipe Thread
3.	Air motor muffler
4.	Sleeve coupling with bronze bushing
5.	Shaft, 5/16 inch diameter, 316 stainless steel
6.	Drive alignment tube
7.	Vessel head, 316 stainless steel
8.	Support plate, carbon steel
9.	Vessel gasket, Teflon®
10.	Flange with soft rubber insert
11.	Pipe cap, glass
12.	Thermowell-baffle, ¼ inch inside diameter
13.	Support post, 1 3/8 inches diameter x 24 inches length
14.	Support plate, carbon steel
15.	Oxygen regulating valve, 316 stainless steel
16.	Sparge-dip tube for oxygen dispersion
17.	Bored-through tube fitting, 316 stainless steel
18.	Flange, carbon steel
19.	Vessel, 316 stainless steel, 1000 cm^3 size
20.	Coil, 2¼ inch inside diameter, 316 stainless steel
21.	Turbine, 2 ½ inch diameter, 316 stainless steel
22.	Heating mantle
23.	Safety shield
24.	Identification plate
25.	Oxygen connection, ¼ inch outside diameter tube
26.	Gland, bronze
27.	O-Ring, Viton®
28.	Packing, 3-ring set, Grafoil®
29.	O-Ring Teflon®
30.	V-Ring Teflon®
31.	Stuffing Box, 316 stainless steel

Note: Mini-Reactor, 1000-cm^3 size, Bench Scale Equipment Company, Dayton, Ohio.

iranchembook.ir/edu

Table A.8 Legend for Figures 8-10 (Continued)

Item	Description Number
A	5 ¼ inches
B	4 ¼ inches
C	15 inches
D	25 inches
E	14 inches
F	14 inches

Note: Left section of vessel illustrates the 316 stainless steel version and the right section illustrates the glass version.

iranchembook.ir/edu

Table A.9 Swelling Ratio vs % Transmittance

Swelling Ratio	% Transmittance
29.15	89.0
24.74	85
11.0	75.0
6.72	70.2
6.43	64.7
5.28	50.2
35.3	35.2
2.74	6.3

iranchembook.ir/edu

Table A.10 Log Swelling Ratio vs. % Transmittance

Log Swelling Ratio	% Transmittance
1.4646	89.0
1.3934	85.0
1.0414	75.0
0.8274	70.2
0.8082	64.7
0.7226	50.2
0.5477	35.1
0.4378	6.3

Correlation coefficient = 0.90
Degrees of freedom = 6
Slope = 69.77
Intercept = -3.42

iranchembook.ir/edu

Table A.11 Particle Size vs. Reaction Time

Reaction Time, Hours	Volume Geometric Mean, Microns
2	1.830
4	1.434
6	1.004
8	0.793
9	0.754

Note: 80.0-psi oxygen pressure autoxidation of medium soya alkyd.

iranchembook.ir/edu

Table A.12 Particle Size Distribution, 2.0 Hours

Particle Size, Microns	Cumulative	Differential
0.50	100.0	10.2
0.63	89.8	8.7
0.79	81.1	7.3
1.00	73.8	9.6
1.26	64.3	10.6
1.59	53.6	10.9
2.00	42.8	7.5
2.52	35.2	8.0
3.17	27.2	7.3
4.00	20.0	6.9
5.04	13.0	6.1
6.35	6.9	4.8
8.00	2.2	1.8
10.08	0.4	0.4
12.70	0.0	0.0
16.00	0.0	0.0

Volume Geometric Mean, microns = 1.83
Population Median, microns =1.72
Population Mode, microns = 1.61
Population Standard Deviation, microns = 2.2

iranchembook.ir/edu

Table A.13 Particle Size Distribution, 4.0 Hours

Particle Size, Microns	Cumulative	Differential
0.157	100.0	0.1
0.198	99.9	1.4
0.250	98.5	2.1
0.315	96.3	3.0
0.397	93.3	4.2
0.500	89.1	5.7
0.630	83.4	7.0
0.794	76.4	7.2
1.000	69.2	9.8
1.260	59.4	12.3
1.587	47.1	13.2
2.000	33.9	9.3
2.520	24.6	8.5
3.175	16.1	6.3
4.000	9.8	4.1
5.040	5.7	3.5
6.350	2.2	1.2
8.000	1.0	1.0
10.079	0.0	0.0
12.699	0.0	0.0
16.000	0.0	0.0

Volume Geometric Mean, microns = 1.434
Volume Median, microns = 1.503
Volume Mode, microns = 1.658
Volume Standard Deviation, microns = 2.218

iranchembook.ir/edu

Table A.14 Particle Size Distribution, 6.0 Hours

Particle Size, Microns	Cumulative	Differential
0.397	100.0	15.7
0.500	84.3	14.7
0.630	69.6	14.4
0.794	55.3	9.8
1.000	45.4	10.0
1.260	35.4	9.9
1.587	25.5	9.8
2.000	15.7	5.3
2.520	10.4	4.2
3.175	6.2	3.6
4.000	2.6	1.4
5.040	1.2	1.2
6.350	0.0	0.0
8.000	0.0	0.0
10.079	0.0	0.0
12.699	0.0	0.0

Volume Geometric Mean, microns – 1.004
Volume Median, microns = 0.898
Volume Mode, microns = 0.445
Volume Standard Deviation, microns = 1.913

iranchembook.ir/edu

Table A.15 Particle Size Distribution, 8.0 Hours

Particle Size, Microns	Cumulative	Differential
0.397	100.0	22.3
0.500	77.7	16.8
0.630	60.9	17.3
0.794	43.6	12.3
1.000	31.3	11.6
1.260	19.7	10.2
1.587	9.6	5.9
2.000	3.7	1.8
2.520	1.8	0.8
3.175	1.0	0.7
4.000	0.3	0.3
5.040	0.0	0.0
6.350	0.0	0.0
8.000	0.0	0.0
10.079	0.0	0.0
12.699	0.0	0.0

Volume Geometric Mean, microns = 0.793
Volume Median, microns = 0.729
Volume Mode, microns = 0.445
Volume Standard Deviation, microns = 1.637

iranchembook.ir/edu

Table A.16 Particle Size Distribution, 9.0 Hours

Particle Size, Microns	Cumulative	Differential
0.397	100.0	24.0
0.500	76.0	22.2
0.630	53.7	16.0
0.794	37.8	11.0
1.000	26.7	10.9
1.260	15.8	7.9
1.587	8.0	3.9
2.000	4.0	1.2
2.520	2.8	1.1
3.175	1.7	0.9
4.000	0.9	0.5
5.040	0.0	0.4
6.350	0.0	0.0
8.000	0.0	0.0
10.079	0.0	0.0
12.699	0.0	0.0

Volume Geometric Mean, microns = 0.754
Volume Median, microns = 0.665
Volume Mode, microns = 0.445
Volume Standard Deviation, microns = 1.653

iranchembook.ir/edu

Table A.17 Particle Size Distribution, 2.0 Hours

Particle Size, Microns	Cumulative	Differential
0.315	118664.0	43515.0
0.397	75149.0	31048.0
0.500	44101.0	22253.0
0.630	21848.0	9903.0
0.794	11945.0	5649.0
1.000	6296.0	3164.0
1.260	3132.0	1620.0
1.587	1512.0	804.0
2.000	708.0	395.0
2.520	313.0	177.0
3.175	136.0	80.0
4.000	56.0	37.0
5.040	19.0	12.0
6.350	7.0	6.0
8.000	1.0	1.0
10.079	0.0	0.0

Population Geometric Mean, microns = 0.488
Population Median, microns = 0.446
Population Mode, microns = 0.354
Population Standard Deviation, microns = 1.445

iranchembook.ir/edu

Table A.18 Particle Size Distribution, 4.0 Hours

Particle Size, Microns	Cumulative	Differential
0.397	128304.0	52942.0
0.500	75362.0	28204.0
0.630	47158.0	17474.0
0.794	29684.0	11202.0
1.000	18482.0	7080.0
1.260	11402.0	4112.0
1.587	7290.0	2181.0
2.000	5109.0	1147.0
2.520	3962.0	2181.0
3.175	1781.0	1147.0
4.000	634.0	423.0
5.040	211.0	147.0
6.350	64.0	46.0
8.000	18.0	18.0
10.079	0.0	0.0
12.699	0.0	0.0

Population Geometric Mean, microns = 0.488
Population Median, microns = 0.446
Population Mode, microns = 0.354
Population Standard Deviation, microns = 1.445

iranchembook.ir/edu

Table A.19 Particle Size Distribution, 6.0 Hours

Particle Size, Microns	Cumulative	Differential
0.397	86932.0	46957.0
0.500	39975.0	21151.0
0.630	18824.0	10407.0
0.794	8417.0	4764.0
1.000	3650.0	2094.0
1.260	1556.0	917.0
1.587	639.0	417.0
2.000	222.0	165.0
2.520	57.0	57.0
3.175	10.0	9.0
4.000	1.0	1.0
5.040	0.0	0.0
6.350	0.0	0.0
10.079	0.0	0.0
12.699	0.0	0.0

Population Geometric Mean, microns = 0.541
Population Median, microns = 0.491
Population Mode, microns = 0.445
Popular Standard Deviation, microns = 1.322

iranchembook.ir/edu

Table A.20 Particle Size Distribution, 8.0 Hours

Particle Size, Microns	Cumulative	Differential
0.397	84691.0	28691.0
0.500	56375.0	25477.0
0.630	30898.0	16857.0
0.794	14041.0	7886.0
1.000	6155.0	3315.0
1.260	2840.0	2374.0
1.587	466.0	365.0
2.000	101.0	79.0
2.520	22.0	12.0
3.175	10.0	9.0
4.000	1.0	1.0
5.040	0.0	0.0
6.350	0.0	0.0
8.000	0.0	0.0
10.979	0.0	0.0
12.699	0.0	0.0

Population Geometric Mena, microns = 0.603
Population Median, microns = 0.568
Population Mode, microns = 0.445
Population Standard Deviation, microns = 1.359

iranchembook.ir/edu

Table A.21 Particle Size Distribution, 9.0 Hours

Particle Size, Microns	Cumulative	Differential
0.397	123174.0	65805.0
0.500	57369.0	35221.0
0.630	22148.0	12875.0
0.794	9274.0	5669.0
1.000	3605.0	2421.0
1.260	1184.0	874.0
1.587	310.0	245.0
2.000	65.0	47.0
2.520	18.0	13.0
3.175	5.0	2.0
4.000	3.0	2.0
5.040	1.0	0.0
6.350	0.0	0.0
8.000	0.0	0.0
10.079	0.0	0.0
12.699	0.0	0.0

Population Geometric Mean, microns = 0.531
Population Median, microns = 0.493
Population Mode, microns = 0.445
Population Standard Deviation, microns = 1.278

iranchembook.ir/edu

Table A.22 Particle Size vs. Homogenization Cycles

Homogenization Cycles	Volume Geometric Mean, Microns
1	1.128
2	1.334
3	1.190
4	1.217

iranchembook.ir/edu

Table A.23 Particle Size Distribution as a Function of Homogenization (3500 psi) Cycles, 1 Cycle

Particle Size, Microns	Cumulative	Differential
0.250	100.0	1.4
0.315	98.6	3.0
0.397	95.6	5.3
0.500	90.3	8.2
0.630	82.1	11.4
0.794	70.7	14.0
1.000	56.7	15.0
1.260	41.8	13.6
1.587	28.1	9.0
2.000	19.1	8.5
2.520	10.7	5.6
3.175	5.1	2.9
4.000	2.2	1.3
5.040	0.9	0.8
6.350	0.1	0.1
8.000	0.0	0.0

Volume Geometric Mean, microns = 1.128
Volume Median, microns = 1.109
Volume Mode, microns = 1.106
Volume Standard Deviation, microns – 1.862

iranchembook.ir/edu

Table A.24 Particle Size Distribution as a Function of Homogenization (3500 psi) Cycles, 2 Cycles

Particle Size, Microns	Cumulative	Differential
0.250	100.0	0.8
0.315	99.2	1.7
0.397	97.5	3.4
0.500	94.1	5.9
0.630	88.1	9.0
0.794	79.2	12.0
1.000	67.2	14.0
1.260	53.2	15.0
1.587	38.2	12.2
2.000	26.1	9.8
2.520	16.3	6.8
3.175	9.5	5.5
4.000	3.9	2.1
5.040	1.8	1.3
6.350	0.5	0.5
8.000	0.0	0.0

Volume Geometric Mean, microns = 1.334
Volume Median, microns = 1.324
Volume Mode, microns = 1.339
Volume Standard Deviation, microns = 1.878

iranchembook.ir/edu

Table A.25 Particle Size Distribution as a Function of Homogenization (3500 psi) Cycles, 3 Cycles

Particle Size, Microns	Cumulative	Differential
0.250	100.0	2.4
0.315	97.6	3.9
0.397	93.8	5.8
0.500	88.0	7.9
0.630	80.1	9.9
0.794	70.2	11.3
1.000	58.9	14.1
1.260	44.7	12.6
1.587	32.1	8.8
2.000	23.3	7.3
2.520	16.0	5.7
3.175	10.3	4.0
4.000	6.2	2.9
5.040	3.3	2.5
6.350	0.8	0.8
8.000	0.0	0.0

Volume Geometric Mean, microns = 1.19
Volume Median, microns = 1.156
Volume Mode, microns = 1.161
Volume Standard Deviation, microns = 2.059

iranchembook.ir/edu

Table A.26 Particle Size Distribution as a Function of Homogenization (3500 psi) Cycles, 4 Cycles

Particle Size, Microns	Cumulative	Differential
0.250	100.0	1.9
0.315	98.1	3.4
0.397	94.7	5.4
0.500	89.2	7.8
0.630	81.4	10.1
0.794	71.4	11.6
1.000	59.7	12.2
1.260	47.5	12.3
1.587	35.3	9.9
2.000	25.4	9.2
2.520	16.2	7.1
3.175	9.1	4.7
4.000	4.4	2.3
5.040	2.1	1.5
6.350	0.6	0.6
8.000	0.0	0.0

Volume Geometric Mean, microns = 1.217
Volume Median, microns = 1.203
Volume Mode, microns = 1.27
Volume Standard Deviation, microns = 2.009

iranchembook.ir/edu

Table A.27 Particle Size Distribution as a Function of Homogenization (3500 psi) Cycles, 1 Cycle

Particle Size, Microns	Cumulative	Differential
0.397	40702.0	10484.0
0.5	30218.0	9694.0
0.63	20524.0	6875.0
0.794	13649.0	6620.0
1.0	7029.0	3914.0
1.26	3115.0	1917.0
1.587	1198.0	724.0
2.0	474.0	305.0
2.52	169.0	113.0
3.175	56.0	34.0
4.0	22.0	13.0
5.04	9.0	8.0
6.35	1.0	1.0
8.0	0.0	0.0
10.079	0.0	0.0
12.699	0.0	0.0

Population Geometric Mean, microns = 0.688
Population Median, microns = 0.634
Population Mode, microns = 0.445
Population Standard Deviation, microns = 1.48

iranchembook.ir/edu

Table A.28 Particle Size Distribution as a Function of Homogenization (3500 psi) Cycles, 2 Cycles

Particle Size, Microns	Cumulative	Differential
0.397	40702.0	10484.0
0.5	30218.0	9694.0
0.63	20524.0	6875.0
0.794	13649.0	6620.0
1.0	7029.0	3914.0
1.26	3115.0	1917.0
1.587	1198.0	724.0
2.0	474.0	305.0
2.52	169.0	113.0
3.175	56.0	34.0
4.0	22.0	13.0
5.04	9.0	8.0
6.35	1.0	1.0
8.0	0.0	0.0
10.079	0.0	0.0
12.699	0.0	0.0

Population Geometric Mean, microns = 0.691
Population Median, microns = 0.626
Population Mode, microns = 0.445
Population Standard Deviation, microns = 1.511

iranchembook.ir/edu

Table A.29 Particle Size Distribution as a Function of Homogenization (3500 psi) Cycles, 3 Cycles

Particle Size, microns	Cumulative	Differential
0.397	189528.0	48811.0
0.500	140717.0	46634.0
0.630	94083.0	33546.0
0.794	60437.0	30561.0
1.000	29976.0	17026.0
1.260	12950.0	7996.0
1.587	4954.0	2892.0
2.000	2062.0	1320.0
2.520	742.0	478.0
3.175	264.0	168.0
4.000	96.0	62.0
5.040	34.0	29.0
6.350	5.0	5.0
8.000	0.0	0.0
10.079	0.0	0.0
12.699	0.0	0.0

Population Geometric Mean, microns = 0.68
Population Median, microns = 0.628
Population Mode, microns = 0.445
Population Standard Deviation, microns 1.465

iranchembook.ir/edu

Table A.30 Particle Size Distribution as a Function of Homogenization (3500 psi) Cycles, 4 Cycles

Particle Size, microns	Cumulative	Differential
0.397	128451.0	35533.0
0.500	92918.0	34119.0
0.630	61469.0	20900.0
0.794	40569.0	18863.0
1.000	21706.0	11221.0
1.260	10485.0	5978.0
1.587	4507.0	2575.0
2.000	1932.0	1275.0
2.520	657.0	449.0
3.175	208.0	152.0
4.000	56.0	38.0
5.040	18.0	15.0
6.350	3.0	3.0
8.000	0.0	0.0
10.079	0.0	0.0
12.699	0.0	0.0

Population Geometric Mean, microns – 0.679
Population Median, microns = 0.617
Population Mode, microns = 0.445
Population Standard Deviation, microns = 1.494

iranchembook.ir/edu

Table A.31 Particle Size Distribution of Autoxidized Emulsion, after One Day

Particle Size, Microns	Cumulative	Differential
0.16	100.0	48.8
0.18	51.2	24.0
1.01	27.2	13.0
1.02	14.2	7.0
1.06	7.2	3.2
1.20	4.0	1.8
1.25	2.2	1.4
1.34	0.8	0.7
1.40	0.1	0.1

Volume Geometric Mean, microns = 0.41
Volume Median, microns = 0.38
Volume Mode, microns = 0.32
Volume Standard Deviation, microns = 0.75

iranchembook.ir/edu

Table A.32 Particle Size Distribution of Autoxidized Emulsion, after One Year

Particle Size, Microns	Cumulative	Differential
0.397	100.0	19.0
0.500	81.0	18.6
0.630	62.4	14.4
0.794	48.0	16.8
1.000	31.2	12.4
1.260	18.8	8.5
1.587	10.4	4.7
2.000	5.7	3.2
2.520	2.4	1.5
3.175	0.9	0.9
4.000	0.0	0.0
5.040	0.0	0.0
6.350	0.0	0.0
8.000	0.0	0.0
10.079	0.0	0.0
12.699	0.0	0.0

Volume Geometric Mean, microns = 0.814
Volume Median, microns = 0.769
Volume Mode, microns = 0.445
Volume Standard Deviation, microns = 1.637

iranchembook.ir/edu

REFERENCES

(1) *American Paint Journal,* May 1969 and May 1970.

(2) *American Society of Testing Materials,* "ASTM D 1849-1987," ASTM Publication, Philadelphia, PA, 1973.

(3) Atwood, D., Jagielksi, C. E., McDonald, C., and Wilkinson, A. E., The solution of some nonionic surface-active agents in non-aqueous solvents, *Colloid Polym. Sci.,* 1974, 252, 991.

(4) Auer, L., 1945, U.S. Patent 2,332,533.

(5) Austin, R. O., and Zetterberg, R.S.,*Official Digest,* May 1963, 487.

(6) Barrow, G. M., *Physical Chemistry,* McGraw-Hill Book Chemistry," McGraw-Hill Book Company, New York, 1973, p. 568, 742-744.

(7) Barton, A. F. M., *Handbook of Solubility Parameters and Other Cohesion Parameters,* CRC Press, Inc., Baca Raton, Florida, 1983, pp. 7-19, 141-165, 443-447.

(8) Beerbower A., and Hill, M.W., *McCutcheon's Detergent and Emulsifiers,* McCutcheon Division, MC Publishing Co., Glen Rock, NJ, 1971, pp. 223-236.

(9) Beerbower, A. and Hill, M.W., Application of the cohesive energy ratio (CER) concept to anionic emulsifier., *Am. Cosmet. Perfum.,* 87(6), 85, 1972.

(10) Becher, P., *Emulsions: Theory and Practice,* Reinhold Publishing Company, New York, NY, 1965, p. 107.

(11) Billmeyer, F. W., et al., "Experiments in Polymer Science," John Wiley and Sons, New York, 1973, pp. 147-152.

(12) Bourne, T., May *The Development of Novel Thermosetting Emulsions Containing Various Silicon, 1978.*

(13) Bufkin, B. G., and Grawe, J. R., *J. of Coatings Technology,* 1978, 50, No. 647,000.

(14) Carraher, Jr., C.E. and Sperling, L.H., *Polymer Applications of Renewable Resoure Materials,* Plenum, New York, 1983, pp. 2-24.

(15) Cowan, *Applied Polymer Science,* edited by J.K. Craver and T.W. Tess, Organic Coatings & Plastics Chemistry, Division of the American Chemical Society, Washington, D.C., 1975, p. 513.

(16) Cragg and J.A. Manson, J. Polym. Sci., 1951, 9, 3, 265.

iranchembook.ir/edu

(17) Crews, G.C. Wildman, and B.G. Bufkin, November paper presented at the Federation of Societies for Coatings Technology meeting, Houston, Texas, 1977.

(18) Dong, H., Gooch, J.W., Schork, F.J., Poehlein, G.W., Wang, S.T., Wu,, X., 2001.

(19) Flory, P.J., "Principles of Polymer Chemistry," Cornell University Press, Ithaca, 1953, p. 576.

(20) Guth, E., Gold, O. and Simha, P., 1949, *Kolloid*-2, 74, 266 (1936).

(21) Kraft, W. M., 1965,U.S. Patent 3,223,658.

(22) Collins, E. A., Bares, J., and Billmeyer, F. W., Jr., *Experiments in Polymer Science,* John Wiley and Sons, New York, 1973, pp. 149-152, 394-397.

(23) Coulter Electronics, Inc., Technical Bulletin-Coulter Counter Model TA II, Hialeah, FL March 1978.

(24) Cummings, 1966, U.S. Patent 3,266,922.

(25) Curtis, 1965, U.S Patent 3,223,659.

(26) El-Aasser, M. S., Hoffman, J. D., Kiefer, C., Leifheiser, H., Jr., Manson, G. W., Poehlein, G. W., Stoisits, R., and Vanderhoff, J. W., "Water-Base Coatings," Technical Report AFML-TR-74-208, Part I, Air Force Materials Laboratory, Air Force Systems Command, Wright–Patterson Air Force Base, Ohio, November 1974.

(27) Gooch, J. W., Bufkin, B. G, Wildman, G. C., 1983, A Process of Generating Coatings by Autoxidatively Polymerizing Emulsified Oils and Alkyds," U.S. Patent 4,419,139

(28) Gooch, J. W., "Development of Water Borne Systems for Can Coatings," GIT Project No. A4496-100, Final Report prepared for Sam Sung Specialty Paint & Ink Co., Ltd., Seoul, Republic of Korea, November 1986.

(29) Gooch, J.W., Dong, H. and Schork, F.J., "Waterborne Oil-Modified Polyurethane Coatings via Hybrid Miniemulsion Polymerization," *Journal of Applied Polymer Science,* Vol. 76, 2000, 105-114.

(30) Gooch, J.W. and Hofland, A., "Low VOC Surfactantless Alkyd Coatings," in *Proceeding of the Eighteenth Water-Borne, Higher-Solids, and Powder Coatings Symposium,* 6-8 February 1991,

(31) Griffin, W.C., Classification of surface-active agents by "HLB", *J. Soc. Of Cosmet. Chem.,* 1, 311.

(32) Hannesson, R., *Petroleum Economics: Issues and Strategies of Oil and Natural Gas Production,* Quorum Books, Westport, CT, 1998.

(33) Hansen, C.M., and Skaarup, K., The three-dimensional solubility parameter-key to paint component affinities, III. Independent calcuation of the parmeter components, *J. Paint Technol.* 1967, 39, 511.

iranchembook.ir/edu

(34) Heflin, E., Block Ccopolymers, polymer-polymer interfaces, and the theory of inhomogeneous polymers, *Acc. Chem. Res*., 8, 1975, 295.

(35) Heflin, E. and Wasserman, Z., Statisical thermodynamics of microdomain structures in block copolymer systems, *Polym. Eng. Sci.,* 17, 1799, 582.

(36) Lenz, R. W., *Organic Chemistry of Synthetic High Polymers,* Interscience Publishers, New York,1967, p. 765.

(37) Levenspiel, O., *Chemical Reaction Engineering,* John Wiley & Sons, New York, 1972, pp. 41-52.

(38) Little, R.C., Micelle size bariuim dinonylnaphthalenesulfonate in low polarity solvents by vapor phase osmometry, *J. Phys. Chem.,* 74, 1970, 1817.

(39) Long, J. S., and Ball, B. L., Jr., 1950, U.S. Patent 2,059,259.

(40) Lundberg, W.O., *Official Digest,* 1950, 302, 199.

(41) Martens, C. R., *Technology of Paints, Varnishes and Lacquers,* R.E. Krieger Publishing Co., Huntington, NY, 1974, pp.24-27.

(42) Marszall, L., Further approach to the energy balance of nonionic surfactants, *Colloid Polym. Sci.,* 1976, 254.

(43) Mattiello, J.J., *Protective and Decorative Coatings,* U.S. Government Printing Offices, 1945, p. 10.

(44) McCarthy, J. A., "The Future of Hydrocarbon Emission Regulations," an oral presentation at the Water-Borne and Higher Solids Coatings Symposium, co-sponsored by USM and the SSCT, 1979.

(45) *McCutcheon's Detergents and Emulsifiers,* McCutcheon Division, MC Publishing Co., Glen Rock, NJ, 1977.

(46) *McCutcheon's Detergents and Emulsifiers,* McCutcheon Division, MC Publishing Co., Glen Rock, NJ, 1999.

(47) Muizebelt, W. J., Donkerbroek, M.W.F., Nielen, J.B., Hussem and Biemond, M.E.F., "Oxidative crosslinking of alkyd resins studied with mass spectroscopy and NMR using model compounds", *Journal of Coatings Technology,* Vol. 70, No. 876, 1998, pp.83-92.

(48) Naburs, T., *Alkyd-Acrylic Composite Emulsions,* Thesis, Eindhoven Technical University, Eindhoven, Netherlands, 1997.

(49) Novak, I. J., 1934, U.S. Patent 2,178,604

(50) "Novel Water-Borne Coatings via Hybrid Miniemulsion Polymerization," American Chemical Society Symposium Series No. 766, P.T. Anastas, L.G., Heine and T.C. Williamson, Eds. ACS, Washington.

iranchembook.ir/edu

(51) Odian, G., "Principles of Polymerization," McGraw-Hill Book Company, New York, 1970, p. 198.

(52) Overbeek, J. Th. G., Colloid Science, Elsevier, New York, 1952, 1, 80

(53) Patton, T. C., "Alkyd Resin Technology," Interscience Publishers, New York, NY, 1962, pp. 41-87.

(54) Princen, L. H., J. Coatings Technology, 1977, 49, 88

(55) Sward, G. G., Ed., Paint Testing Manual, The American Society for Testing and Materials, Philadelphia, 1972, p.286.

(56) Taylor, W. L., J. of Am. Oil Chemists Soc., 1950, 2, 472.

(57) *The Chemical Marketing Reporter,* Chemical Prices, Schnell Publishing Company, Inc., April 2, 1990 and November 20, 1999-2000, (258, 21).

(58) The Freedonia Group, Inc., Fatty Acids to 2002, 2000, 767 Beta Drive, Cleveland, OH 44143, USA, tel: (440) 684-0484, December.

(59) Wang, S. T., F. J. Schork and Gooch, J.W., "Emulsion and Miniemulsion Copolymerization of Acrylic Monomers in the Presence of Alkyd Resin", *Journal of Applied Polymer Science,* Vol. 60, 1996, 2069-2076.

(60) Winsor, P.A., *Solvent Properties of Amphiphilic Compounds,* Butterworths, London, 1954.

(61) Vanderhoff, J. W., Brit. Polym. J., 2, 1970, 161.

(62) Vanderhoff, J. W., Tarkowski, H. L., Jenkins, M. C., and Bradford, E. B., J. Macromol. Chem., 1966, 1, 361.

(63) Vanderhoff, J. W., Bradfor, E. B., and Carrington, W. K., *J. Polym. Sci.:* Symp. No. 41, 1973, 155 .

(64) Vanderhoff, J.W., Vanderhul, J.H., Tausk, R.J.M. and Overbeek, J. Th. G., "Well-Characterized Monodisperse Latexes, in Clean Surfaces: Their Preparation and Characterization for Interfacial Studies," G. Goldfinger, ed., Marcel Dekker, New York, 1970, p. 15.

iranchembook.ir/edu

INDEX

Absolute viscosity, 85-87
Accelerated shelf stability test, 67, 142
Acetone, 40, 44, 48, 87-88, 95-96, 104, 108
Acid value, 9-12, 32, 36, 95-96
Acids, 2, 3, 9-14, 31, 36-37, 67, 137-138, 147
Acrylic, 1, 3, 6, 15, 20, 142, 144-145, 148, 150
Agglomeration, 9, 28
Agitation rate effect, 123
Aldehydes , 13-14
Alkali refined (AR) soya, 69, 72
Alkyd
  coatings, 16, 146, 150
  resins, 1-3, 9, 13-15, 67, 73, 125, 142, 144-146, 148-149
Alkyd emulsions, 1, 34, 64, 74, 136, 134-135, 144, 146
Alkyd/mineral spirits, 77
Alkyd/xylene solution, 67
Alkyd-acrylic composite emulsions, 144, 150
American Optical Company, 38
American Paint Journal, 71, 147
AMR scanning electron microscope, 43
Anionic, 58, 63
  emulsifiers, 51, 149
Arab oil embargo of 1973-74, 4
Arizona Chemical, 3
Arolon X801, 15
Ashland, 3, 15
ASTM D 1849-1987, 43, 149
ASTM D 2243-90, 43
Autoxidation reaction, 9, 23, 28, 35, 37, 47, 49, 67-70, 73-75, 77, 81, 87, 92, 95, 103, 107-108, 110, 113, 115, 119, 121, 124, 132, 137, 141-142, 144
Autoxidative polymerization, 1, 9, 15, 125, 144-147
Autoxidize, 9, 36, 48, 64, 72, 75-80, 84-85, 88, 90, 92-93
Autoxidized emulsion, 48, 72, 77-78, 85, 90, 92, 93, 95, 96, 100, 101, 104, 143
Barrett trap, 32
Bausch and Lomb Spectronic 710 Spectrophotometer, 42
Bench Scale pressure reactor, 103
Bench Scale pressure vessel, 107, 108
Blowing process, 9, 76
Bransonic® Ultrasonic Vibrator, 32
Brookfield Viscometer, 43
Butoxyethanol (2-butoxyethanol), 36
Cannon-Fenske Viscometer, 43-45
Capillary viscometer, capillary tube, 16, 86
Cationic emulsifiers, 51
Centipoise viscosity, 46, 87, 91, 92
Centrifuged, 45
  Cetyl alcohol, 14
Chain transfer, 14, 145
Chlorinated polypropylene
  Parlon® P10 (Hercules, Inc.), 21

iranchembook.ir/edu

Cleavage, 13, 14
Coalescence, 1, 15, 27, 28, 97, 145
Cobalt naphthenate, 62, 63, 77, 80-84, 92, 94, 96, 97, 100, 118, 119
Cohesion parameters, 18-21, 148
Cohesive energies, 19
Colloidal dispersions, 18
Comonomers, 15, 145, 146
Conjugated, 13, 14, 36, 37, 137, 139
Conjugated-bonds, 14
Conjugation study, 36, 132
Copolymer, 15, 16, 18, 21, 145, 146, 148
Cosmetic, 3
Cannon Fenske Viscometry
Coulter-Counter^{R} measurements, 42
Crosslink density, 1, 14, 28, 47, 87, 88, 142
Crosslinked
polymers
Crosslinking emulsions, 14
Cumulative curves
Cymel, 15
Defoaming, 21
Degree of branching, 16
Degree of crosslinking, 47, 73, 103, 114, 115, 142
Density, 1, 14, 19, 27, 28, 44-47, 66, 67, 87, 88, 142
Detergents, 3, 18, 20, 21, 51, 148, 150
Differential curves, 42, 128
Diffusion constant, D, 22
Diffusional degradation (Ostwald ripening), 15, 145
Dimmer, 14
Disproportionation, 14
Double bond, 9, 13, 14
Drying oils, 14
Dupanol C (dodecyl sodium sulfate), 52, 58, 63
Dupanol C, 52, 58, 63
Eastman Corporation, 36
Einstein's equation, 25
Electrospray ionization (EPI), 13
Emulsified particles, 14, 35, 64, 87
Emulsifiers17, 18, 20, 32, 51, 52, 62-64, 101, 103, 148, 150
Emulsifying agent, 9, 28, 32, 51, 102, 142, 144
Emulsion
particles, 28, 47, 48, 119, 126
characterization, 43, 85, 90, 92, 94
polymerization28, 47, 48, 119, 126
science, 14, 1, 9, 14, 15, 18, 20, 27, 28, 34, 36, 43, 514, 52, 61, 62-65, 67, 72, 7-77, 87, 92, 101, 108, 126, 134-137, 139, 141, 146, 148, 150
Environmental Protection Agency (EPA), 4
Epoxide, 13, 14
Epoxy-resin Epikote® 1001 (Shell Chemicals), 21
Ether-crosslinks, 13, 14
Ethylene glycol monobutyl ether (butyl cellosolve), 65
Exotherm, 9
Fats, 1, 2
Fatty acids, 2, 3, 9, 13, 36, 37, 37, 137, 138, 147
Fick's Law, 21, 113
Foaming, 21, 67
Food, 3
Freeze-thaw stability, 37, 43, 52, 62, 89, 93, 135, 137, 142
Gafac, 52, 62-64, 92-94, 101
Gaulin Sub-Micron Disperser and Homoginizer, 32, 130

iranchembook.ir/edu

Gel permeation chromatography (GPC), 125, 126
Gel, 24, 25, 125
gel-state, 9
gel-phase, 23
Georgia Institute of Technology, 16, 146
Georgia-Pacific, 3GPC (gel peremation chromatography), 125, 126
Gradient Polymer Elution Chromatography, 145
Graft copolymer, 16, 18, 146
Green technology, 4, 146
Hansen parameters, 19
Henkel, 3
Henry's Law, 22, 23
Constants, 23
Hercules Corporation, 36, 37, 137
Hilderbrand parameter, 19
HLB values, 21
Hydrodynamic measurements, 25
Hydroperoxide, catalyst, 13, 70, 71
Hydrophile, 17-20, 51, 52, 61, 62, 102
Hydrophile-Lipophile Balance (HLB), 17, 19, 20, 51, 52, 61, 62
Hydrophobes, 15, 145, 146
Ideal gas constant, 22
Igepal (surfactants), 52, 58, 62, 63, 81, 86, 101, 134
Induction period, 9, 109, 110, 113, 114
Inherent viscosity, 16
Intrinsic viscosity, 16, 17, 44, 69-76, 86, 113, 114, 133, 134, 141, 142
Inverse-phase emulsification, 144
Inversion of phases, 9
Ionic surfactants, 18, 149
Kinetic study, 103
Land use, 5, 6
Latex, 1-4, 14, 15, 25, 27, 28, 44, 46, 47, 145, 146, 149
coatings, 1-4, 6, 9-16, 26, 27, 144-148, 150
dispersions, 15, 18, 20, 145
Linoleic fatty acid, 10-14
Liquid suspensions, 18
Los Angeles Rule 66, 4
Lubricants, 1
Macroemulsion, 15, 16, 145, 146
Macromers, 15, 146
Mark-Houwink Equation, 114, 125
Mass spectroscopy, 14, 148
McCutheon's Detergents & Emulsifiers, 18, 51
McWhorter Technologies, 46
Medium soya/linseed emulsion, 32
Methylanthraquinone (2-methylanthraquinone), 71
Methylene group, 14
Microdomains, 18
Microscopic measurement, 38
Mineral spirits, 8, 33, 36, 52, 61, 62, 65, 77, 82, 83, 85, 86, 100
Miniemulsion, 15, 16, 145, 146, 148, 150
Miscelle, 18
Molar volume, 24
Monomer droplets, 15, 145
Network junctions, 24
New York Times, 4
Nitrogen inlet, 32
Nonionic surfactants, 149
Nonylphenoxypoly (ethyleneoxy)$_4$ alcohols, 33, 58, 60, 63, 81, 137
Nuclear magnetic resonance (NMR) spectroscopy, 13

iranchembook.ir/edu

Oil Producing and Exporting Countries (OPEC), 4
Oils, 1-12, 14, 15, 26, 28, 31, 32, 36, 37, 51,70, 141, 145, 150
Oil alkyds
Extra-long, 31
Long, 31
Medium, 139
Olefinic unsaturation, 137
Oleic
acid, 13, 14, 17, 18, 37, 137
fatty acids, 9
Oligomers, 14, 145
Optical microscopy, 28
Ostwald ripening, 15, 145
Oxygen concentration, 22, 48, 49, 96, 103, 107-109, 111, 114, 115, 118, 143
Oxygen pressure, 22, 47, 95-97, 101, 103, 107-109, 112, 118, 121, 123, 142
Paint Testing Manual, 43, 149
Paints, 3-5, 20
Pamolyn R fatty acids, 37, 137
Pentadienyl radical, 13
Percent
elongation, 43, 62, 72, 81, 96
transmittance, 38, 40, 87, 95, 96, 103, 104, 108, 109, 123
Peroxide, 9, 13, 14, 70, 71, 76
Peroxy-crosslinks, 13, 14
Persian Gulf War, 4
Petroleum, products, 1, 2, 6
pH, 21, 28, 52, 62, 85-87, 90-93, 95
Plastics3, 147
Polydispersity, 15, 146
Polymer-solvent interactions, 48
Polyol, 31, 32, 34
Polyurethane resins, 15, 145
Potassium oleate, 17, 18
Pressure regulator, 34, 35, 49, 107
Radicals, 13, 14, 71, 76, 81, 110, 113, 139
Recinoate, 14
Relative viscosity, 16, 43, 86, 87, 91, 92
Raw materials, 1, 67
Resins, 1-3, 6, 7, 9, 13-15, 21, 26, 27, 67, 73, 125, 144-146, 148
Resins kettle, 31, 68, 69, 70, 74
Rubber, 3, 23, 24, 72
Sakurods, 16
Scanning electron microscopy (SEM), 28, 43, 97
Scission, 13, 14
Secondary ion mass spectrometry (SMS), 13, 14
Shear modulus, 28
Shear stability, 15, 145
Sodium lauryl sulfate, 14, 31, 94, 96, 97, 100
Sol phase, 23
Solubility parameter, 21, 23, 51, 148, 149
Solution viscosity, 16, 44
Solvents, 4, 6-8, 18, 21, 23, 36, 48, 148, 149
Soya
alkyds, 133, 138, 139
urethane alkyd, 132-134, 138, 139
Specific volume, 24
Spectrophotometer, 42, 48, 104
Staudinger's equation, 16
Steam jacketed condenser, 32
Stoke's Law, 27
Stress-strain relationship, 77
Surfactants, 3, 18, 21, 101, 149
Sward Hardness Rocker Tester, 43
Sward Hardness Test, 81, 84
Swelling ratio, 14, 23-25, 44, 46-48, 87, 88, 103, 104, 106-108, 115, 138, 142

iranchembook.ir/edu

Sylfat R , 37
Sylvachem Corporation, 36, 37, 137
T-Det, 62-65, 96, 97, 101, 108, 123
Tensile strength, 43, 62, 72, 77, 78, 80, 81, 83, 89-92, 96, 97, 101, 133, 138, 139, 141-143
Thermometer, 32
T-Mulz, 62, 63
Toiletries, 3
Toluene diisocyanate, 31
Transmittance (percent), 2, 38, 48, 87, 95, 96, 103, 104, 108, 109, 123
Turbidimetric measurement (turbidity), 47
Turbidimetric method, 96, 104, 108, 115
Twin Rivers Technologies, 3
Tyndal Effect, 44
Ultrasonic vibration, 14, 64
Ultra-violet (UV) light, 71
Unichem North America (ICI), 3
Union Camp, 3
Unsaturation, 9, 137, 139
Urethane alkyd (resin), 31, 41, 42, 132-134, 138, 139, 143
Vegetable oil-based coatings, 2
Vegetable oils, 1, 2, 4-9, 15, 26, 31, 36, 51, 70, 141, 145
Vinyl, 1
Viscosity, 10-12, 16, 17, 22, 25, 27, 43-46, 69-72, 75, 76, 85-89, 91-93, 113, 114, 126, 133, 134, 141, 142, 144
Viscosity-average molecular weight16, 72, 75
Volatile organic compounds(VOC), 16, 146, 150
Volume fraction, 24-26, 45, 46
Washability, 87
Water cooled condenser, 32
Water dispersible, 4
Water reducible, 4
Water soluble, 4
Water vapor, 26
Water-phase retarder, 15, 145
Weight fraction, 17
Westvaco, 3
Witco, 3
Xylene, 8, 32, 36, 39, 65-67, 88-92, 108
Zirconium naphthenate, 121